THE UNIVERSITY OF CHICAGO

DISCOVERY AND VALIDATION OF METHACRYLLYSINE MODIFICATION ON HISTONE PROTEINS

A DISSERTATION SUBMITTED TO

THE FACULTY OF THE DIVISION OF THE BIOLOGICAL SCIENCES

AND THE PRITZKER SCHOOL OF MEDICINE

IN CANDIDACY FOR THE DEGREE OF

DOCTOR OF PHILOSOPHY

COMMITTEE ON CANCER BIOLOGY

BY

KYLE DELANEY

CHICAGO, ILLINOIS

JUNE 2020

Table of Contents

LIST OF FIGURES

LIST OF TABLES

ACKNOWLEDGEMENTS

While this bears the name of a single author, the work contained within could not have been possible without the support of many individuals. I would like to begin by thanking my advisor, Dr. Yingming Zhao. Before I applied to graduate school, I was reading scientific papers on a broad variety of subjects to determine what topic I would like to study. During this process, I came across the works of the Zhao laboratory. Already having an interest in protein posttranslational modifications, I was truly excited by the prospect of research that could uncover and explore new mechanisms for biological functions. I wanted to venture boldly into this area with the hope that we would learn something new and exciting about biology. I thank Yingming for giving me the opportunity to pursue my passion for this research. Thank you also for trusting me with this project and giving me the independence to forge my own path, even when it meant stumbling. Yingming's influence has been critical in shaping the scientist that I've become. He has guided me at every step of the way in navigating the academic research world. I thank him for the lessons that he has taught me.

I also want to thank my committee members Dr. Xiaoyang Wu, Dr. Lev Becker, and Dr. Navdeep Chandel. They have provided critical feedback and a listening ear throughout this process. I want to thank the chairs of the Committee on Cancer Biology during my tenure, Dr. Kay Macleod and Dr. Stephen Kron. Thank you Kay for believing in me and giving me the opportunity to come to the University of Chicago. Thank you Steve for giving me helpful advice when I first arrived as a first year student. I also thank Steve for his guidance in helping me to complete my graduate work while the world wrestles with the COVID-19 pandemic. I thank Dr. Nancy Schwartz, Dr. Louis Phillipson, and Dr. Richard

Kraig for guiding me through the HHMI Med-Into-Grad masters program. I thank Dr. James Labelle for serving as my clinical mentor during said masters program. I want to thank those in administrative positions including Judy Sun, Emily Traw, Nadja Otikor, Helen Polansky, Dr. Lisa Abston-Leftridge, Laurie Risner, and Laura Negrete. Special thanks to Judy for helping me to compile and submit my F31 application.

The original research contained herein would not have been possible without the experimental contributions of a number of people. I thank Dr. Minjia Tan for his critical contributions to this project. I thank Dr. Sunjoo Kim, Dr. Yejing Weng, Dr. Jun Ding, and Dr. Lu Yang for their critical efforts in operating the LC-MS/MS machines for processing the samples that I prepared. I thank our collaborators Dr. Y. George Zheng and Zhesi Zhu for their contributions on the *in vitro* enzymatic work for HAT1. I thank Dr. Saadi Khochbin for his expertise and efforts during this project. I thank Dr. Mark Parthun for providing the knockout MEF cells required for our experiments.

I want to thank the senior postdocs that taught me so much during my time in the laboratory, Dr. Di Zhang and Dr. He Huang. Di trained me to perform the majority of the protocols that I undertook during my time in graduate school. He has always been very patient and willing to answer all of the many questions that I have asked him over the years. I have relied greatly upon Di's insight and composure to help me navigate the difficulties inherent in working in this laboratory. He is a tremendously gifted scientist and I wish him all the best in his future endeavors. I want to thank He Huang for teaching so much of what I know about the technical intricacies of mass spectrometry. He was critical in helping me to understand how to interpret MS/MS spectra quality. I was so happy for

him and his family when he had the opportunity to return to China to continue his career. I wish him all the best.

I want to thank Mat Perez-Neut. Mat is one year below me in the CCB program. He has been a crucial friend, confidant, and colleague during this process. It has been a joy to watch him grow as a scientist during his time with our lab. I wish Mat all the best in his current and future efforts. I thank Dr. Jianfeng Du for always being so friendly and helpful. I wish all the best for Wenchao Liu as she navigates the road ahead. I want to thank all the members of our laboratory that I have worked with. This includes the members with whom I wish I had interacted with more including Dr. Gozde Colak, Dr. Jingfang Liu, Dr. Junfung Huang, Dr. Xiaoling Zang, Dr. Okwang Kwon, and Dr. Jinjun Gao.

I want to thank the friends that I've made in graduate school. Thank you to Dr. Alex Ling, Dr. Sriram Sundaravel, and Logan Poole for their support and friendship as the other members of my incoming year. Thank you to the rest of our group Jasmine, Dr. Matt Krause, Sophia Krause, Dr. Rashi Rangaraj, and Anastasia Hains for their friendship. Thank you to Ryan Duncombe, Jess Fessler, Chris Stamper, Shan Kasal, Jaime Chao, Sean Wallace, and Steven Erikson for their friendship. Thank you to all of the members of CCB.

Finally, I would like to thank my family for their support. I thank my mother for always being extremely supportive and a great listener. I thank my father for showing an interest in what I do and expressing enthusiasm when I tell him about my work. I thank my brother for his friendship and support over the years.

ABBREVIATIONS

ACAD8	acyl-CoA dehydrogenase family member 8
BCAA	branched-chain amino acid
BCAT	branched-chain amino acid transferase
BCKDC	branched-chain α-ketoacid dehydrogenase complex
ECHS1	enoyl-CoA hydratase short chain 1
HAT	histone acetyltransferase
HDAC	histone deacetylase
HIBADH	3-hydroxyisobutyrate dehydrogenase
HIBCH	3-hydroxyisobutyryl-CoA hydrolase
Kac	acetyllysine
KAT	lysine acetyltransferase
Kbhb	β-hydroxybutyryllysine
Kbu	butyryllysine
Kbz	benzoyllysine
Kcr	crotonyllysine
Kglu	glutaryllysine
Khib	2-hyrdroxyisobutyryllysine
Khmg	3-hydroxy-3-methylglutaryllysine
Klac	lactyllysine
Klip	lipoyllysine
Kmal	malonyllysine
Kmea	methacryllysine
Kmg	3-methylglutaryllysine
Kmgc	3-methylglutaconyllysine
Kmyr	myristoyllysine
Kpr	propionyllysine
Ksuc	succinyllysine
PTM	posttranslational modification

CHAPTER 1

INTRODUCTION

1.1 Protein posttranslational modifications

1.1.1 Significance

The central dogma of biology is that the flow of genetic information proceeds from DNA to RNA to protein. Proteins are the main functional macromolecular components of living beings. It is estimated that there are approximately 19,000 nuclear protein coding genes in the human genome.[1] However, the number of unique proteins (aka proteoforms) is not as simple as a one to one ratio with gene number. One of the main systems for diversifying proteins is through posttranslational modifications (PTMs).

PTMs broadly refer to covalent attachment of chemical groups to protein backbone or side chains or the cleavage of proteins at specific residues after translation by the ribosome.[2] Over 450 unique types of posttranslational modifications are recorded on in the UniProt database.[3] The proteoforms that result from combinations of posttranslational modifications, alternative gene splicing, and coding mutations create a proteome that is multiple orders of magnitude more complex than that represented by gene number alone.[4] Understanding biology requires functional characterization of not only genes and proteins but also the regulatory mechanisms that dictate activity of proteins

Protein structure dictates function. Thus, the ability of proteins to be posttranslationally modified creates one of the central paradigms for altering of protein structural conformation and therefore function. For example, protein phosphorylation involves the addition of a negatively charged group to serine, threonine, or tyrosine side chains. This leads to a conformational change that affects enzymatic activity of multiple types of proteins including kinases.[2] From this system

of adding onto protein structure with chemical moieties, cells are able to carry out a number of cell signaling processes PTMs can also positively or negatively impact the ability for protein-protein interactions to occur. Phosphorylation signaling cascades are foundational in cell signaling. Reactive oxygen species mediate key signals in modulating cellular stress response. . The addition of hydrophobic lipid modifications provides a mechanism for attachment and localization of proteins to lipid membranes. Ubiquitination of proteins marks them for degradation by the proteasome. Lysine methylation of histones is associated with the activation or repression of gene transcription. These are but a few of the many examples of ways that PTMs function in physiology.

PTMs are also critically important to our understanding of diseases. The regulation of PTMs are central to many of the hallmarks of cancer.[5] Regulators of phosphorylation including kinases and phosphatases are some of the most commonly disrupted oncogenes in cancer.[6] Likewise, many genes that regulate the epigenome are also disrupted in cancer and represent key therapeutic targets.[7] For example, the histone methyltransferse EZH2 is frequently altered in a variety of cancers including breast, prostate, and lymphoid.[8] An EZH2 inhibitor has also recently been FDA approved for the treatment of epithelioid sarcoma.[9] In another example, multiple histone deacetylase (HDAC) inhibitors have been FDA approved for the treatment of cutaneous or peripheral T cell lymphomas.[7] There are also oncogenic mutations in histone proteins themselves at residues that disrupt their epigenetic patterns.[10] As demonstrated, PTMs represent a crucial factor in pathology and understanding their regulation has therapeutic implications for diseases such as cancer.

The list of important PTMs and their associations with disease go on. Thus, it would not be possible to succinctly and comprehensively cover all of the work that has been done on

PTMs. In the interest of brevity, this work will use the epigenetic regulation of gene expression by histone lysine acetylation (Kac) as an example of the effects of PTMs. We selected to focus on lysine acetylation as its history is highly relevant to the original work contained herein.

1.1.2 Lysine acetylation of histones and epigenetic regulation

The acetylation of amino acids was first discovered in the late 1940s.[11] In the early 1960s, it was discovered that histones were heavily acetylated using extracts from calf thymus.[12] Shortly thereafter, Allfrey and colleagues showed that isotopic acetate could be incorporated into histones independent of protein synthesis inhibition suggesting that it occurred posttranslationally.[13] Allfrey and colleagues further proposed that the acetylation of histones could serve as a mechanism regulating transcription.[13] Since these initial experiments, acetylation of histones has emerged as a key factor in the epigenetic regulation of gene expression. The term "epigenetics" refers to mechanisms that modulate gene expression without directly impacting the underlying genetic code. Two of the most studied types of epigenetic histone modifications are acetyllysine and methyllysine (**Figure 1.1**). The history of the acetylation of histones provides key insight into the process by which a PTM is confirmed to be an epigenetic regulator and will be discussed presently.

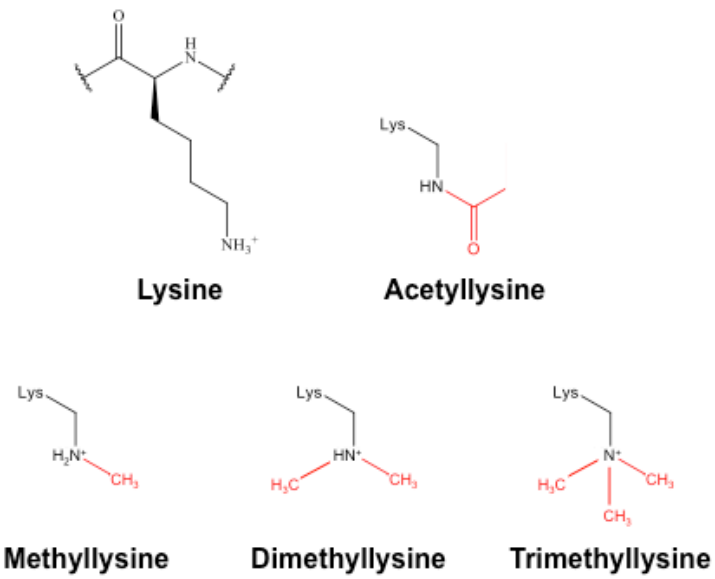

Figure 1. 1 Structures of acetyllysine and methyllysine.
The structures of lysine, acetyllysine, methyllysine, dimethyllysine, and trimethyllysine are shown as indicated.

The first direct evidence of a connection between histone acetylation and gene expression was published in the late 1980s and early 1990s. Crane-Robinson and colleagues found that chromatin around the alpha D globin gene in chicken embryo erythrocytes was strongly acetylated relative to input controls.[14] Around this time, multiple groups reported that mutations of specific histone lysine residues in yeast affected telomeric gene silencing and expression of the mating locus.[15–18] In 1996, the major discoveries of enzymes that either added or removed Kac from histones demonstrated that this was a directed cellular process and not simply the result of chemical reactions.[19,20] This represented a critical turning point in the understanding of Kac on histones and was followed by a tremendous expansion in the field as visualized by the dramatic output in the number of publications in the following years up until present day.[21]

Jenuwein and Allis proposed that the epigenetic modification of histones provided a type of code that dictated chromatin related processes.[22] The primary regulatory proteins to add, interpret, and remove histone modifications are referred to as writers, readers, and erasers, respectively (**Figure 1.2**). Much work has been done to study histone marks in efforts to decode their effects on these processes. For purposes of brevity, this work will cover a few milestones in this field. Ming-Ming Zhou and colleagues reported that Kac was bound by the bromodomain of PCAF, thus identifying the first reader protein.[23] This and the further study of reader proteins demonstrated that proteins could recognize Kac sites and effectively served to interpret the signal generated by patterns of histone marks. In 2007, chromatin immunoprecipitation coupled with next generation sequencing (ChIP-Seq) was developed.[24–27] ChIP-Seq has since become the dominant technology in understanding the correlations with histone marks and transcriptional processes. The attempts to decode the functions of specific Kac histone marks are still an area of active research.

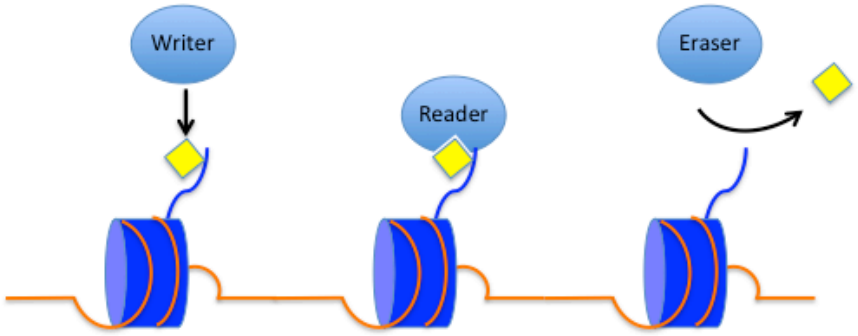

Figure 1. 2 Schematic of writers, readers, and erasers.
There are three main classes of regulatory proteins relevant to histone marks. Writer proteins (shown on left) catalyze the addition of the PTM to the histone protein. Readers (middle) are proteins with binding pockets that are capable of interacting with the PTM modified form of the histone. Erasers (right) catalyze the removal of the PTM moiety from histones. The diagram depicts three nucleosome complexes with protruding N-terminal histone tails represented by blue cylinders. The orange line indicates the DNA that surrounds the histone octamers. A yellow diamond represents the PTM moiety.

While the discussion thus far has been on histone acetylation, Kac is found a variety of different proteins. The acetylation of tubulin was first reported in 1983.[28] Outside of tubulin and histones, only a handful of Kac substrates were known for a long time. For example, lysine acetylation was identified to activate p53.[29,30] However, it wasn't until our laboratory published the first proteome wide study of Kac sites that the true scope of Kac substrates was appreciated.[31] In particular, it was discovered that mitochondrial proteins were heavily acetylated to an extent that had not been previously appreciated. Later work further confirmed that mitochondrial proteins were heavily acetylated and impacted cellular metabolism.[32,33] Thus, Kac serves as a key regulatory mechanism across the proteome.

1.1.3 Open questions

The discovery of previous PTMs revolutionized our knowledge of cell signaling and biology. What would modern biology look like without protein phosphorylation? What if the field had never identified histone lysine acetylation or methylation? Where would this put us in our ability to understand cell-signaling mechanisms? The identification of previous posttranslational modifications has had far reaching implications across many fields.

A driving goal of our laboratory is to discover new types of PTMs that have important biological functions. We argue that true understanding of cell signaling mechanisms requires proper identification of all of the chemical moieties that are involved. It is unclear how many types of PTMs that have roles in cell signaling are still yet to be discovered. The following sections will provide a historical look at the discovery and validation of PTMs to provide a background for understanding the methods for discovering new modifications. This includes understanding the rational for the discovery of a new PTM, lysine methacrylation (Kmea), which is the focus of the experimental work contained herein.

1.2 Acyl-CoAs as sources of posttranslational modifications

1.2.1 Metabolic origins of PTMs

The chemical moieties that constitute PTMs need to be derived from a reaction donor. High energy metabolites serve as precursors for enzymatic PTMs. Kinases use ATP to add a phosphate moiety to hydroxyl group on serine, threonine, or tyrosine residues.[34] Methyltransferases use S-adenyl-methionine to add methyl groups to the side chains of lysine, arginine, and histidine residues.[35] Acetyltransferases add acetyl groups to lysine using the cofactor acetyl-CoA.[19] The list of enzymatically catalyzed modification types goes on and includes the likes ubiquitination and glycosylation among others.[2] It is thus evident that organisms have evolved to utilize a variety of metabolic precursors to serve signaling functions at the molecular level.

In addition to enzymatically-regulated modifications, the existence of reactive molecules can also lead to non-enzymatic protein modifications. Reactive oxygen species such as hydrogen peroxide are highly reactive for the thiol group of the cysteine side chain.[36] Aldehydes are highly reactive chemical species that are produced as byproducts of metabolism or by the oxidation of lipids.[37,38] Acyl-CoAs can react with free lysines, especially at pH representative of the inner mitochondrial matrix.[39] These are a few of the many types of reactive metabolites that are able to modify proteins.

In summary, it is well established that a host of reactive metabolic species are involved in chemical reactions whether enzymatically catalyzed or not. The scope of this work is focused on the acyl-CoA species. For this purpose, the chemistry of acetyl-CoA with relation to its role connecting metabolism and signaling will be discussed. Following that example, more general observations regarding the acyl-CoAs will be explored. Finally, the background of metabolite

methacrylyl-CoA will be examined due to its central importance to the experiments presented in this work.

1.2.2 Lysine acetylation is derived from acetyl-CoA

Coenzyme A (CoA) and Acetyl-CoA were discovered in the late 1940s.[40,41] The coupling of acetate to CoA was referred to as activated acetate. It was around this time that protein acetylation was first discovered.[11] Bloch, Lipmann, and Lynen would later win the Nobel Prize for these discoveries. This work established that acetyl-CoA was a chemically reactive molecule that modified proteins.

Acetyl-CoA is generated from the catabolism of pyruvate, fatty acids, or amino acids within mitochondria.[42] Since acyl-CoAs cannot cross the mitochondrial membrane, the metabolism of citrate by ATP citrate lyase serves as the primary source for nucleocytosolic acetyl-CoA.[43] Acyl-groups can be transported out of mitochondria through the carnitine shuttle pathway.[44] It has been proposed that acetyl-carnitine from the mitochondria can be converted into nuclear acetyl-CoA.[45] Free acetate can also be converted into acetyl-CoA by short chain acyl-CoA synthetases like ACSS2.[46] Hypoxic cancer cells and some tumors are highly dependent on acetate for the generation of their acetyl-CoA pools.[47,48] The pyruvate dehydrogenase complex is also reported to partially localize to the nucleus to produce acetyl-CoA.[49]

Acetyl-CoA concentrations in cells range from approximately 2-13 μmol in cultured cells depending on the glucose concentration in the media.[50] Varying concentrations between subcellular compartments are thought to be important, but at the time of the writing of this document the technology for isolating and measuring those pools are still in early development.[43] There is however evidence that certain biological circumstances require acetyl-CoA production in the proximity of chromatin. Chromatin bound ACSS2 is hypothesized to provide local high

concentration microenvironments of acetyl-CoA for histone acetylation under certain conditions.[51,52] Mice with attenuated hippocampal ACSS2 have decreased transcription of genes where wild type ACSS2 localizes and have impaired long term spatial memory.[51] Under conditions of nutrient starvation, ACSS2 localizes to lysosomal and autophagic genes to promote their expression.[52] The pyruvate dehydrogenase complex has also been reported to associate with p300 on chromatin to provide local acetyl-CoA production for acetylating histones at enhancers.[53] It is not clear to what extent local generation of acetyl-CoA species is needed for histone acetylation instead of generalized availability of diffuse nuclear acetyl-CoA. In summary, acetyl-CoA levels are metabolized in various compartments of the cell in part to serve as the precursors for Kac across the proteome.

1.2.3 Acyl-CoAs

The human metabolome database (HMDB) lists over 300 types of acyl-CoA species. Only a small fraction of these have been associated with posttranslational protein modifications. Acyl-CoAs are reactive thioester metabolites. Acetyl-CoA and succinyl-CoA non-enzymatically modify proteins *in vitro* at physiological pH levels.[39] The reaction increases with increasing pH that is consistent with the environment of the mitochondrial matrix. Negatively charged dicarboxyl-acyl-CoAs like succinyl-CoA reportedly can form anhydride intermediates that are highly reactive with lysines.[54] Levels of acyl-CoA species correlate to the levels of histone acylations.[55] Kcr is an exception to this trend as it does not correlate as closely with crotonyl-CoA.[55] If the nonenzymatic transfer is a general property of acyl-thioesters, then it is likely that many more if not all acyl-CoA species can produce lysine modifications at some frequency. The challenge to the field will be to determine those species that are the most relevant to biological

function. One way to prioritize those likely to have impacts in cell signaling processes is to focus on those acyl-CoA species that yield enzymatic regulated PTMs.

1.2.4 Methacrylyl-CoA

Methacrylyl-CoA is an endogenous intermediate involved in the catabolism of valine.[56] A diagram illustrating the pathway for valine catabolism is shown in **Figure 1.3**. Valine is one of the branched chain amino acids (BCAAs) along with leucine and isoleucine. Unlike other amino acids, the branched chain amino acids typically avoid first pass metabolism in the liver due to the low levels in liver BCKDC.[57] Skeletal muscle and to a lesser extent adipose contribute the most to the initial breakdown of branched chain amino acids. Though it confirmed the metabolic importance of skeletal muscle, a recent isotopic tracer study in mice demonstrates that most bodily tissues rapidly catabolize branched chain amino acids into the TCA cycle *in vivo*.[58]

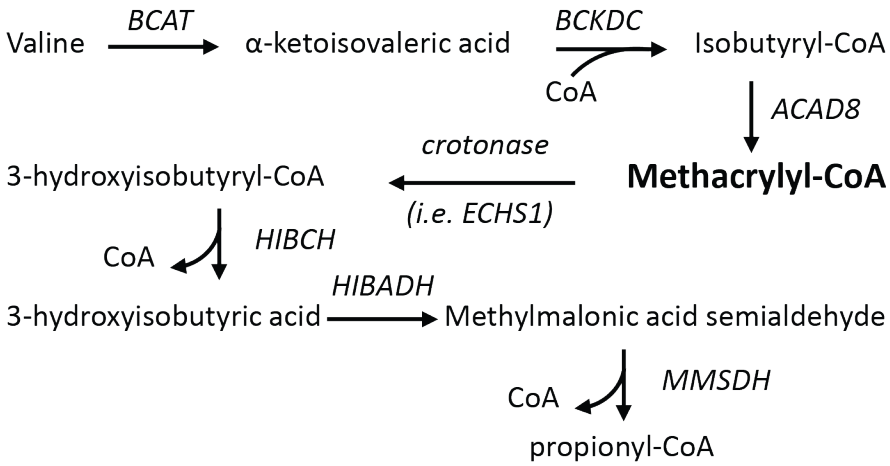

Figure 1. 3 Valine catabolic pathway.
The mitochondrial metabolic pathway for valine catabolism is shown with the names of the metabolic intermediates and abbreviations for key enzymes. Note that while this pathway is drawn with regards to the direction of complete catabolism, certain steps in the pathway are bidirectional such as the conversion of methacrylyl-CoA to 3-hydroxyisobutyryl-CoA. The abbreviations used in this figure stand for the following enzymes or enzyme complexes: *BCAT*, branched-chain amino acid transferase; *BCKDC*, branched-chain α-ketoacid dehydrogenase complex; *ACAD8*, acyl-CoA dehydrogenase family member 8 (aka isobutyryl-CoA dehydrogenase); *crotonase* (aka enoyl-CoA hydratase), multiple members of the crotonase family have been implicated in this interaction including ECHS1; *ECHS1*, enoyl-CoA hydratase short chain 1; *HIBCH*, 3-hydroxyisobutyryl-CoA hydrolase; *HIBADH*, 3-hydroxyisobutyrate dehydrogenase; *MMSDH*, methylmalonate-semialdehyde dehydrogenase.

Beyond understanding the pathway, how can we understand if methacrylyl-CoA itself has a role in pathophysiology? One possibility is to examine diseases where methacrylyl-CoA and BCAA metabolism are disrupted. For this purpose, we will examine three disease areas that may be informative: leigh syndrome, cancer, and diabetes

The potential relevance for methacrylyl-CoA in diseases is perhaps most obviously associated with leigh syndrome. Leigh and leigh like syndromes are the most common form of in-born error of metabolism and can result from monogenic mutations in over 75 different genes.[59] While the majority of mutations are associated with mutations in the electron transport chain, there is a subset of individuals with the diseases that have disrupted valine catabolism. Multiple cases have been reported of Leigh syndrome patients with mutations in either ECHS1 or HIBCH, two enzymes downstream of methacrylyl-CoA.[60–70] For patients with these mutations, the accumulation of methacrylyl-CoA is hypothesized to be a causal factor due to its capacity to alkylate cysteines.[60] Elevated levels of the alkylated cysteine products S-2-carboxypropyl-cysteine and S-2-carboxypropyl-cysteamine are detectable in the urine of patients with HIBCH and ECHS1 mutations.[60,71] Supporting the possibility for toxicity, the enzymes directly downstream of methacrylyl-CoA production have been speculated to be expressed at high levels under healthy physiological conditions in order to prevent the accumulation of methacrylyl-CoA.[72–75] It is still unknown which proteins are the critical targets of alkylation by methacrylyl-CoA. Deficiencies in respiratory chain proteins and pyruvate dehydrogenase have been reported in these patients suggesting that they may be potential alkylation targets.[65,66,69] However, the exact pathologically relevant protein cysteine residues that are alkylated have yet to be reported. There are efforts by physicians to neutralize the effects of methacrylyl-CoA through dietary restriction of valine and treatment with nucleophile N-acetylcysteine.[62]

Another area where methacrylyl-CoA may be relevant is in cancer. Disruption of BCAA metabolism has also been associated with a variety of forms of cancer. Patients that develop pancreatic ductal adenocarcinoma have elevated plasma BCAA levels between 2 to 5 years prior to diagnosis.[76] This appears to due to reduce uptake of BCAAs in pancreatic ductal adenocarcinoma tumors relative to normal tissue.[77] In hepatocellular carcinoma, elevated BCAA levels resulting from reduced catabolism supports carcinogenesis through activation of mTORC1.[78] The role of BCAAs in cancer appears to be tissue dependent as non-small cell lung cancer tumor models with the same causal mutations as pancreatic ductal adenocarcinoma tumors instead increase uptake of BCAAs to use as a source of nitrogen to support their metabolic requirements.[77] Glioblastoma tumors upregulate BCAT1 to increase BCAA catabolism.[79] While it is evident that BCAA metabolism is disrupted in a variety of cancers, there is limited evidence for a role of methacrylyl-CoA in the pathology. Ishigure and colleagues found that hepatocellular carcinoma tumors have reduced expression of catabolic enzymes and thus would be expected to be associated with higher levels of methacrylyl-CoA.[75] However, methacrylyl-CoA levels were not measured directly in this work. Thus, further research is needed to determine if methacrylyl-CoA levels have pathological relevance to cancer.

A final potential condition of pathological relevance for methacrylyl-CoA is that of obesity and diabetes. It has been known for 50 years that there is a connection between increased blood levels of BCAAs and obesity.[80,81] This connection was given renewed attention in 2009 when Newgard and colleagues found that blood BCAA levels strongly correlated with insulin resistance in patients.[82] Furthermore, they found that high fat diet when combined with high dietary levels of BCAAs led to development of insulin resistance in mice. Similarly, restriction of dietary BCAAs was associated in improved insulin sensitivity in animal models.[83,84] As such,

insulin resistance is associated with disrupted BCAA metabolism in patients and animal models. One hypothesis for the mechanism behind this phenomenon is that BCAA catabolism interferes with lipid oxidation and leads to lipid accumulation.[85] Obesity suppresses expression of BCAT and BCKDH in adipose and increases BCKDK expression in liver.[86,87] In insulin resistant mice, there is an increased burden on skeletal muscle for BCAA catabolism associated with decreased BCAA metabolism in adipose and liver.[58] Skeletal muscle catabolism of valine leads to the release of 3-hydroxyisobutyrate which stimulates trans-endothelial fatty acid transport in a paracrine manner.[88] This allows for accumulation of lipid species in muscle. Furthermore, 3-hydroxyisobutyrate levels are elevated in muscles of db/db mice and human patients with diabetes. The role of other intermediates in the catabolism of valine such as methacrylyl-CoA in this pathology is poorly understood.

1.3 Discovery of novel lysine acylations

1.3.1 Methods to discover new lysine acylations

Given the importance of PTMs in biology, it is critical that the field have an understanding of the prevalence and breadth of all biologically relevant modifications. The challenge therefore is to identify any and all PTM types that occur in biological systems. In section 1.2, we established that acyl-CoAs represent a class of metabolites that are capable of generating PTMs. The existence of over 300 types of acyl-CoAs, as reported on HMDB, presents a wide array of potential modifications that can occur on lysine residues. Our laboratory used this knowledge to explore the breadth of lysine acylations that exist. In total, we have discovered and published 10 new types of acylations as of the composition of this work (**Figure 1.4**).[89–91] Here we summarize the methods that have been utilized to discover new modifications and the knowledge gained from studying lysine acylations.

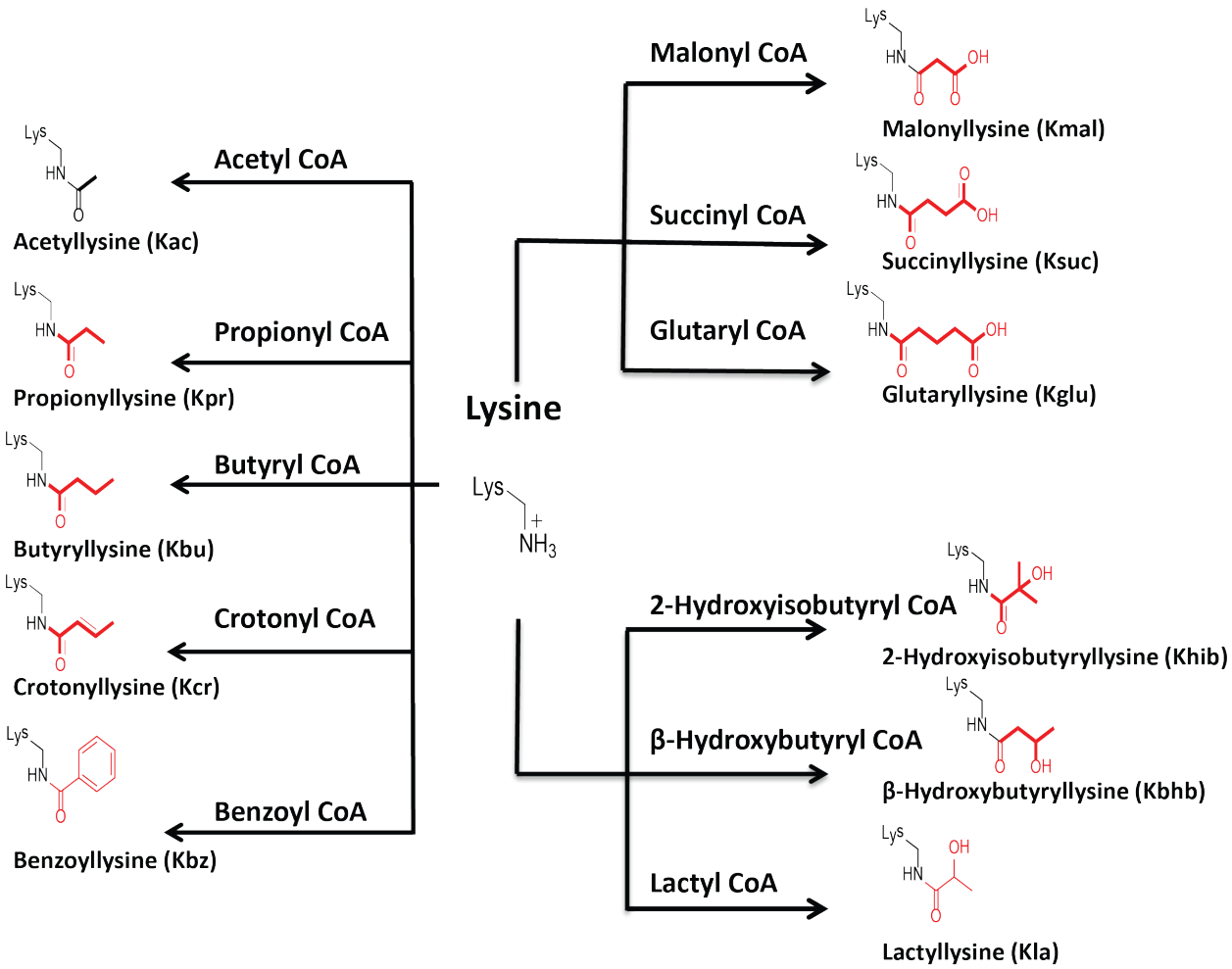

Figure 1. 4 Structures of acyllysines discovered by our lab.
Structures of the 10 published lysine acylations discovered by our laboratory are highlighted in red. The structure of acetyllysine is included for reference. All relevant acyl-CoA species that give rise to these lysine acylations are listed beside the structures. The abbreviations for each acyllysine name are included below each structure.

Where does one begin to look for undiscovered lysine acylations? Histone proteins provide an ideal substrate for the discovery of new types of posttranslational modifications for multiple reasons. First, they are known to be heavily modified by a variety of posttranslational modifications.[92] Second, they are readily purified and isolated by acid extraction.[93] Third, the unstructured nature of histone tails makes them relatively easy to mimic *in vitro* using synthetic peptide chemistry.[94] These traits have made histones a fruitful system for the detection and validation of new PTMs.

Our laboratory has employed mass spectrometric proteomics technologies to search for new modifications. Acyllysine modifications have the advantage of being relatively stable during sample preparation and analysis by mass spectrometry when compared to many other types of modifications. For example, S-acetylation of cysteine occurs more readily than N-acetylation of lysine *in vitro*, but the cysteine modification is less stable and prone to nucleophilic attack.[95] Lysine acylations are also readily enrichment by immunoprecipitation. This is in contrast to cysteine modifications like cysteine succination for which efforts of antibody enrichment have so far been unsuccessful.[96] Together these qualities allow lysine acylations to be readily enriched and detected using mass spectrometric technology.

In our lab, we have employed two major approaches to discover new types of posttranslational modifications on histones.[89] The first method relies on cross-reactivity of modification specific antibodies for modifications of similar structures. We used anti-Kac antibodies to enrich and identify histone peptides bearing propionyllysine (Kpr) and butyryllysine (Kbu) modifications, the first lysine acylations that our laboratory discovered.[97] We employed this same method for the discovery of malonyllysine (Kmal) and glutaryllysine (Kglu) given their structural and charge similarity to succinyllysine (Ksuc).[98,99] The second

major approach has been to look for novel mass shifts on proteins' specific amino acid residues. Our laboratory developed and utilized the software program PTMap to scan peptides for novel mass shifts between -100 and +200 Da in 1 Da increments among all the 20 ribosomally coded amino acid residues.[100] Other software programs that look for new posttranslational modifications continue to be developed. One such program is MSFragger, which uses a fragment-ion indexing method.[101] Once a novel mass shift is identified the possible structural isomers can be inferred under the assumption that the structure is an acylation. The detection of novel mass shifts led our laboratory to discover crotonyllysine (Kcr), 2-hyrdroxyisobutyryllysine (Khib), benzoyllysine (Kbz), and lactyllysine (Klac).[90,91,102,103] In addition, other groups have also reported on the identification of new lysine acylations on proteins using similar methodology.[54,104,105] All of the new modifications that our laboratory has discovered have been lysine acylations, with the lone exception of tyrosine hydroxylation.[102] To illustrate the knowledge gained from the discovery of these modifications, we will closely examine studies of Kcr. Kcr is one of the more highly studies modifications studied by our laboratory and highly relevant for the original research described in this work.

1.3.2 Lysine crotonylation

During a set of experiments to catalog histone marks, our laboratory discovered detected a novel mass shift of +68.0230 Da on lysine residues from HeLa histones.[102] In the same work we validated that this new mark was Kcr on the basis of MS/MS fragmentation patterns, co-elution with synthetic peptides, isotopic metabolite labeling, and pan specific Kcr antibody detection. Furthermore, we demonstrated that this modification was enriched on testis specific genes that escape X-chromosome inactivation in mouse spermatogenesis through ChIP-Seq. The sites of Kcr correlated with active gene expression and were enriched at promoters and

enhancers. This provided the first evidence that the discovery of Kcr represented the identification of a new functionally relevant epigenetic histone mark.

In the time since the initial discovery of Kcr, a number of important studies have been performed that have improved our understanding of the roles and regulation of Kcr. The transcriptional activator and acetyltransferase p300 can catalyze the addition of Kcr to histones in a way that promotes transcription using in vitro and cell culture assays.[106] Similarly, additional work established that this modification was reversible as HDAC 1-3 and SIRT 1-3 were identified to catalyze its removal.[102,107–111] These studies established that the addition and removal of Kcr could be enzymatically regulated, which is considered to be crucial requirement for modifications that serve epigenetic and signaling functions.

How does Kcr promote transcription? One way is through promotion of the open chromatin state by neutralizing the positive charge state of lysine to disrupt contact with negatively charged DNA. This is presumably the main mechanism for Kcr mediated transcription in *in vitro* transcription assays.[106] Another way that epigenetic marks function is through the interaction with reader proteins. Readers are proteins that contain structural pockets that recognize PTMs and mediate protein-protein interactions. With regards to histones, readers serve a critical function to recognize the modifications on chromatin and to bring other proteins such as transcriptional activators or repressors to key sites. In support of its ability to serve as a bona fide epigenetic mark, Kcr is recognized by multiple reader proteins. YEATS2, Af9, and Taf14 are all YEATs domain containing proteins that bind to Kcr.[112–114] Similarly, the double PHD finger containing proteins DPF2 and MOZ can also bind Kcr.[115] Collectively this work suggests that Kcr is a regulated epigenetic modification that can be detected to assist with transcriptional activation.

1.3.3 Other lysine acylations

Lysine acylations range from those with short carbon chains like Kac to longer fatty acyl chains like myristoyllysine. New lysine acylations have been discovered in recent years. In addition to Kcr, our laboratory has published the first identifications of 9 additional types of lysine acylations (**Figure 1.4**) including: Kcr,[97] Kbu,[97] Kmal,[98] Ksuc,[116] Kglu,[99] Khib,[103] β-hydroxybutyrylation (Kbhb),[117] Kbz,[90] and Kla.[91] Matthew Hirschey and colleagues reported the first identification of lysine 3-hydroxy-3-methylglutarylation (Khmg), 3-methylglutaconylation (Kmgc), and 3-methylglutarylation (Kmg).[54] The literature thus far suggests that these new types of lysine acylations play important roles cellular processes akin to the roles of Kac.

Like Kac and Kcr, many of these lysine acylations are correlated with active gene transcription. H4K8hib is associated with active gene transcription in meiotic and post-meiotic male germ cells during their differentiation.[103] H3K9bhb is enriched at active genes associated with starvation induced metabolism in fasted mice.[117] H3K79suc localizes to transcription start sites and is positively associated with tumor growth.[118] H4K91glu is positively associated with actively transcribed genes and appears to be downregulated during mitosis and in response to DNA damage.[119] Increases in H3K18la are associated with upregulation of M2-like genes including Arg1 following prolonged stimulation of macrophages with M1 stimuli.[91] While all of the aforementioned modifications have a positive association with transcription like Kac, it does not necessarily mean that they are equivalent with Kac. While Kbu is associated with active gene expression, the bromodomain reader protein Brdt does not bind at sites modified with H4K5bu in contrast to the Kac modified site.[120] Thus, there appear to be important distinctions between Kac and other acylations that still require further study.

The second way that lysine acylations have been associated with function is through regulation of enzymatic activity. The lipoylation of lysines has been known to be critical for the function of multienzyme complexes like pyruvate dehydrogenase since the 1970s.[121] Biotinylated lysines are critical for the enzymatic activity of ATP-dependent carboxylases.[122] Ksuc occurs on residues that affect enzymatic activity of isocitrate dehydrogenase, glyceraldehyde 3-phosphate dehydrogenase, and serine hydroxymethyltransferse.[116] Other enzymes proposed to be regulated by Ksuc include pyruvate dehydrogenase, succinate dehydrogenase, GAPDH, and carbamoyl-phosphate synthase 1.[123–125] The glutarylation of carbamoyl-phosphate synthase 1 also negatively affects its enzymatic activity as has been observed in mouse models of glutaric acidemia.[99] Malonylation of glycolytic enzymes including GAPDH was associated with decreased glycolytic flux.[126] Furthermore, macrophage stimulation with LPS induces malonylation of GAPDH, which disrupts its binding to TNFα and promotes translation.[127] Similarly, Khib occurs on multiple enzymes in the glycolytic pathway and in particular is associated with negative regulation of enolase 1.[128] Khmg and Kglu reduce the activity of malate dehydrogenase.[54] Khmg, Kmgc, Kmg, and Kglu block the biotinylation of K677 on methylcrotonyl-CoA carboxylase A, which results in reduced leucine catabolic flux.[104] Thus, multiple lysine acylations appear to provide a feedback mechanism for the modulation of metabolic flux.

Long chain fatty acyllysines are comparably not as well understood. The hydrophobicity of these modifications has presented technical challenges for sample preparation and analysis that is compatible with LC-MS/MS workflows. A few proteins to date have been identified that contain myristoyllysine including TNFα.[129] Work on myristoylation of K-Ras suggests that it has a role in endomembrane localization.[130] Regulation of protein-membrane interactions is observed

in other lipid modifications S-palmitoylation.[131] More work needs to be performed in this area to better catalog and understand the roles of fatty acyllysine modifications.

The field of lysine acylations has rapidly progressed in recent years and there continue to be new discoveries. Marcus Glomb and colleagues reported the identification of lysine tigylation, 2-methylbutyrylation, acetoacetylation, and isovalerylation.[105] These were all hypothesized to result from acyl-CoA species in contrast to the acylations reported by the Glomb group that are hypothesized to result from aldehyde reactions.[132,133] The functional roles of these modifications are poorly understood. Given the deluge and variety of potential modifications on proteins, it will be critical for the field to identify those that are the most physiologically relevant. One potential criterion for focusing on critical modifications is to focus on those that are enzymatically regulated. For this purpose, a more thorough review of the importance and types of enzymatic regulators is discussed in the following section.

1.4 Writers: acetyltransferases

1.4.1 Overview

The enzymatic addition of acetyl moieties to lysine residues is catalyzed by lysine acetyltrasnferases (HAT or KAT). HAT1 was the original acetyltransferase to be identified and cloned in yeast.[134] Yeast without functional HAT1 did not have a readily observable phenotype. Thus, the discovery of HAT1 did not immediately validate the hypothesis at the time that acetyltransferases regulated gene expression. Instead it was the discovery of GCN5 by Allis and colleagues in tetrahymena that provided the smoking gun for the connection between acetyltransferases and gene expression.[19] More acetyltransferases were discovered and they can broadly be classified into at least five families: HAT1, GCN5/PCAF, p300/CBP, MYST, and the fungus specific Rtt109.[135] In addition there are other subfamilies of acetyltransferases that

include ACTR, ATF-2, CLOCK, TAF250, and SRC1.[136–139] There is an alternative nomenclature for these enzymes that renames them as KAT1-KAT13D which will be used interchangeably in this work.[140] The majority of these enzymes have been associated with transcriptional activation via their ability to acetylate nucleosomal histones. HAT1 (aka KAT1) is unique from the others in multiple regards. Given the relevance of HAT1 to the work contained herein, the following section will summarize current knowledge of HAT1 in greater detail.

1.4.2 HAT1

Chicoine and colleagues were the first to report that newly synthesized H4 histones are acetylated at lysine residues 4 and 11 in tetrahymena thermophilia.[141] It was later discovered that the acetylation of analogous lysine residues of 5 and 12 was conserved in newly synthesized H4 histones in drosophila and human cell lines.[142] Chromatographic separation of drosophila melanogaster embryos yielded extract with acetyltransferase activity specific for histone H4.[143] Similarly, fractionation experiments by Lopez-Rodas and colleagues suggested the existence of multiple acetyltransferases in yeast which were classified as being type A or B.[144–146] The hallmark difference between the type A and type B histone acetyltransferases was that only the former type used nucleosomes as substrates while the latter targeted soluble histones. Their work further suggested that the type B histone preferentially targeted histone H4. Additional work in other organisms supported the existence of acetyltransferases specific for free histone H4.[147–149] Through a temperature sensitive mutant screen in yeast, HAT1 became the first acetyltransferase to ever be identified and cloned.[134] The recombinant catalytic subunit of the HAT1 complex had acetyltransferase activity for histone H4 at residues 5 and 12 *in vitro.*[150] The activity of HAT1 was consistent with it being a type B acetyltransferase. Subsequent work suggested that a type B HAT was also responsible for the H4K5 and H4K12 acetylation in human cells.[151] Collectively,

this work provided the foundation for our current understanding of HAT1 as the primary enzyme responsible for acetylation of H4K5 and H4K12 on nascent histones.

The initial work on type B HATs suggested that the enzymes were primarily localized to the cytoplasm.[143–148,150–154] However, later experiments using fractionation and immunofluorescence microscopy revealed that HAT1 is primarily localized to the nucleus.[155–158] HAT1 has been reported to be necessary for telomeric silencing in S cerevisiae in a manner that requires both its catalytic activity and nuclear localization.[159,160] A similar requirement in telomeric silencing has also been reported in S pombe.[161] Recent work has found connections between HAT1 and mitochondrial function which may involve expression of mitochondria associated genes in a cell specific manner.[162,163] Given that it does not directly acetylate chromatin bound histones, the effects of HAT1 on transcription are likely to proceed through mechanisms distinct from HATs that serve as transcriptional activators.

Despite being the first acetyltransferase gene to be identified, the exact functional roles of HAT1 continue to largely remain unclear. One of the long standing proposed functions of HAT1 is that it functions in the nuclear import of nascent histones.[164] Mutation of H4K5 and H4K12 to the unacetylatable arginine or the acetyl-mimetic glutamine were found to decrease and increase nuclear import in *Physarum polycephalum*, respectively.[165] Similarly, using glutamine mutations to mimic H4K5ac and H4K12ac also increased rates of nuclear import using an *in vitro* assay.[166] The role of these modifications in nuclear import is consistent with findings that diacetylated H4 and HAT1 have been isolated in complex with the chaperone Asf1 and karyopherin/importin proteins.[167,168] However, deletion of HAT1 in MEF cells affected the modification status but not the availability of histones for newly deposited histones.[169] Furthermore, histone H4 in MEF HAT1 knockouts still primarily localizes to the nucleus without noticeable accumulation in the

cytoplasm.[170] Similarly, stable knockdown of HAT1 does not affect HAT1 protein levels despite the fact that transient knockdown reduces histones H3 and H4 in a nutrient dependent manner.[171] Loss of HAT1 also does not prevent histone H4 nuclear import in Drosophila melanogaster.[172] As such, it appears that HAT1 and the diacetylation of H4 are either not required for nuclear import or that there are compensatory pathways for histone import into the nucleus.

Another model for HAT1 activity was related to its proposed role in histone deposition.[164] The catalytic unit Hat1p exists in the NuB4 complex paired with Hat2p and Hif1p in nuclei of yeast.[156,158] Due to its association with the protein Hif1p that is involved in histone deposition, it was hypothesized that HAT1 may also have a role in the histone deposition. In human cells, HAT1 has also been reported to interact with the human homolog of Hif1p known as NASP suggesting evolutionary conservation of this interaction.[167,173] Of note, the importance of the acetylation of H4K5 and H4K12 by HAT1 was found to not be required for chromatin assembly in yeast.[174] Indeed, the entire the H3 and H4 N-terminal histone tails are not necessary for nucleosome assembly mediated by CAF-1 *in vitro*.[175] However, more recent evidence using MEF HAT1 knockout cells suggest that not only is HAT1 not necessary for deposition, but that rates of deposition might be slightly higher in its absence.[170] As such the involvement of HAT1 and its targets of acetylation are thought to only have a limited effect on chromatin assembly at least those associated with replication.

Despite its reportedly limited impact on replication associated chromatin assembly, HAT1 still may be involved in histone deposition for certain situations. Multiple papers have indicated the involvement of HAT1 with assembly of proteins at the centromere, including being vital in the deposition of CENP-A.[176–179] HAT1 was also reported to be required for chromatin reassembly following DNA double strand break repair.[180] A screen in yeast for genes that

affected histone turnover revealed that the NuB4 complex including Hat1p affected turnover rates.[181] The role of HAT1 in histone turnover has been proposed to be associated with double strand break repair in mammalian cells.[182] Deletion of HAT1 was associated with defects in repair of double-strand breaks in various eukaryotic systems.[156,183–185] Furthermore, Hat1p localizes to sites of double stranded breaks in yeast.[186] Further supporting an important role in DNA repair, MEF HAT1 knockout cells have genomic instability and are sensitive to both double and single strand DNA damage.[169]

Another potential function is that HAT1 is necessary for maintaining the appropriate epigenetic state for newly incorporated histones.[170] Agudelo and colleagues found that bromodomain containing proteins like Brd3 were depleted at nascent chromatin in HAT1 knockout MEF cells. The effects of recruiting reader proteins are likely transient as it is known that H4K5ac and H4K12ac modifications are rapidly removed by deacetylases following incorporation into chromatin.[169,187] While engagement of reader proteins may be one function of maintaining the acetylation pattern, it is not the only proposed function. Gruber and colleagues have proposed that the acetylation of histones in the cytoplasm followed by deacetylation in the nucleus creates a way to shuttle acetate to the nucleus.[171] All together, it is evident that the functional roles of HAT1 are still an active area of study and may be more complicated than a single mechanism.

The necessity of HAT1 for viability appears to vary based on the model organism employed. In the early genetic studies of HAT1, deletion of Hat1p had no effect on viability in Saccharomyces cerevisiae.[134,150] Similarly, viability was unaffected following knockout in Saccharomyces pombe and DT40 chicken cells.[184,185] Drosophila melanogaster lines with deletion of HAT1 are also viable.[172] In contrast, mice bearing homozygous deletion HAT1 are

embryonic lethal and die in late embryogenesis.[169] Mice that are heterozygous for HAT1 have decreased survivability relative to wild type mice and show a range of phenotypes associated with early aging.[163] The functional reason that HAT1 is required for viability in mice is currently unknown. Collectively, the data suggests that HAT1 may be required for life in mice and other mammals but not in other eukaryotes.

With regards to its role in pathology, HAT1 has been associated with cancer in multiple studies. Analysis of TCGA data shows that high HAT1 expression is correlated with poor outcome relative to patients with low HAT1 expression in multiple cancer types including adrenocortical carcinoma, bladder urothelial carcinoma, kidney chromophobe, lower-grade glioma, hepatocellular carcinoma, and lung adenocarcinoma.[171] Osteosarcoma patients had higher expression of HAT1 by IHC than control bone samples from amputee patients.[188] The authors proposed that low expression of microRNA miR-377 in osteosarcomas led to increased HAT1 and reduced apoptosis. In contrast, another group reported that degradation of HAT1 promoted osteosarcoma growth in cells expressing oncogenic RAS mutations.[189] In pancreatic ductal adenocarcinoma, HAT1 negatively regulates PD-L1 expression and knockdown of HAT1 in xenograft tumors improved response to PD-1 checkpoint blockade inhibitors *in vivo*.[190] HAT1 downregulates BCL2L12 to protect cells against apoptosis in nasopharyngeal cancer.[191] HAT1 had a proapoptotic effect in lung cancer cells in which it was overexpressed through upregulation of FAS.[192] HAT1 is reported to promote proliferation and confer cisplatin resistance in hepatocellular carcinoma.[193] HAT1 levels are elevated in rat hepatocellular carcinoma induced by methyl deficient diet.[194] HAT1 mRNA transcripts were found to be higher in primary and metastatic colorectal cancer when compared to normal tissue.[195] Together this data suggests that HAT1 may have multiple roles depending on the type of cancer.

1.4.3 Activity for other acylations

The work of our laboratory and others has found that a variety of previously classified acetyltransferases can catalyze the activity of other modifications. Of the acyltransferases identified thus far, p300 has the greatest promiscuity of substrate utilization. The enzyme p300 serves as a writer for Kpr,[97,196] Kbu,[97,120] Kcr,[106] Khib,[128] Kbhb,[197] and Klac.[91] CBP is a close family member of p300 and the two are often referred to in combination as CBP/p300 in the literature. Based on kinetic analysis, p300 activity decreases as a factor of increasing acyl-CoA chain length.[55,197] The ability to accommodate a wide variety of cofactors is likely due to the fact that p300 contains deep aliphatic pocket in its active site.[197] Importantly, p300 catalyzed acylations are able to activate *in vitro* transcription providing direct evidence of a functional relevance for the new types of histone marks.[91,106,120,128] Interestingly, the detected Khib substrates of p300 regulation have minimal overlap with its Kac substrates.[128] Furthermore, Khib modifications on glycolytic enzymes like ENO1 are associated the regulatory effects of p300 on glycolysis.[128] As such, the evidence suggests that p300 is able to utilize acyl-CoAs for activities equivalent and distinct from those mediated by its Kac substrates.

Others previously classified acetyltransferases besides p300 also act as writers for acylations. In vitro, Kpr and Kbu are catalyzed by KAT2A and KAT2B.[198,199] Kpr is also catalyzed by KAT5, KAT6A, KAT7, and KAT8 *in vitro*.[199,200] KAT6A is notable in that it can catalyze Kac, Kpr, Kbu, and Kcr on H3K23.[201] The loss of its binding partner BRPF1 results in loss of H3K23 acylations and is associated with various pathologies including intellectual disability and cancer.[201] KAT2A in complex with nuclear succinyl-CoA producer α-KGDH are responsible for H3K79suc at transcription start sites.[118] KAT2A has also been reported to correlate with active gene expression through the enzymatic addition of H4K91glu.[119] Tip60 (aka

KAT5) is a writer for Khib.[202] As such there are a variety of acetyltransferases that can utilize a variety of acyl-CoA substrates.

The aforementioned results highlight that acetyltransferases represent an ideal candidate pool for finding enzymatic writers for any newly discovered acylations. However, it cannot be said that any of these enzymes are unique for any of the new acylations as all of these enzymes also possess activity for Kac. Additional approaches such as fractionation can be used to look for specific acyltransferases. This approach was used in finding that p300 has activity for Kcr.[106] However, no non-acetyl specific writers have been reported to date. It is worth noting that CPT1A, which is not an lysine acetyltransferase, has been reported to function as a lysine succinyltransferase.[203] Whether enzymes similar to this exist should be the subject of future research.

Not all HATs have reported promiscuity for other acyl-CoA species. Therefore it is still the subject of ongoing research to determine how many of them can utilize alternative substrates. HAT1 is an acetyltransferase for which acetyl-CoA has been the only reported cofactor. Indeed, Levy and colleagues recently reported that butyryl-CoA and crotonyl-CoA were not strong binding competitors for HAT1 binding relative to immobilized CoA.[204] However, other many other acyl-CoA species that yield modifications were not tested by this assay. In summary, acetyltransferases are known to catalyze a variety of acyllysine modifications and are still the subject of ongoing investigations. The acetyltransferases that are capable of catalyzing non-acetyl lysine acylations are summarized in **Table 1.1**.

KAT ID	Alternative Name	Acylations
KAT2A	GCN5	Kbu, Kglu, Kpr, Ksuc
KAT2B	PCAF	Kbu, Kpr
KAT3A/B	CBP/p300	Kbhb, Kbu, Kcr, Khib, Klac, Kpr
KAT5	Tip60	Khib, Kpr
KAT6A	MOZ	Kbu, Kcr, Kpr
KAT7	HBO1	Kpr
KAT8	MOF	Kpr

Table 1. 1 List of acetyltransferases that catalyze lysine acylations in addition to Kac.
The lysine acetyltransferases that can catalyze acylations in addition to Kac are listed here. Both KAT and HAT nomenclature is given for each listed enzyme. Also listed are the corresponding acylations that are catalyzed by each enzyme. The acylation are abbreviated as follows: Kbhb, β-hydroxybutyryllysine; Kbu, butyryllysine; Kcr, crotonyllysine; Kglu, glutaryllysine; Khib, 2-hyrdroxyisobutyryllysine; Klac, lactyllysine; Kpr, propionyllysine; and Ksuc, succinyllysine.

1.5 Erasers: deacylases

1.5.1 Overview

There are a total of 18 mammalian deacetylase genes. They are divided into five classes: I, IIa, IIb, III, and IV. One of the main distinctions is with regard to the mechanism of catalysis.[205] Classes I, II, and IV catalyze the removal of Kac modifications in a zinc dependent manner. In contrast, the class III enzymes (aka sirtuins) utilize NAD+ as a cofactor. The following sections provide the background for these genes separating them by the mechanism of catalysis.

1.5.2 HDAC 1-11: zinc dependent deacylases

Part of the initial indication that histone acetylation was enzymatically regulated came from the observation that butyrate treatment of Friend erythroleukemic cells led to increased acetylation and cell differentiation.[206] Shorty thereafter it was discovered that butyrate acts through inhibiting deacetylation of histones in cell extracts.[207,208] Additional naturally occurring small molecule HDAC inhibitors including Trichostatin A and Trapoxin were discovered approximately 20 year later.[209,210]

HDAC inhibitor compounds were critical to the initial identification of the relevant proteins. Schreiber and colleagues used an affinity matrix based on Trapoxin to identify HDAC1.[20] Mammalian HDAC1 was a homolog of yeast Rpd3, which had been previously reported to be involved in repression of transcription.[211] Shortly thereafter, HDAC2 was discovered as a mammalian homolog to Rpd3 and confirmed to have deacetylase activity.[212–215] HDAC3 was also discovered based on its homology to Rpd3.[216,217] Thus these studies established that histone acetylation was an enzymatically reversible modification.

However other enzymes were also annotated as "HDACs" largely due to their homology with these and related proteins. HDAC 4-6 were discovered based on their homology to the Rpd3 related protein Hda1p.[218] HDAC7 was identified as a SMRT interacting protein in a yeast two-hybrid screen.[219] HDAC8 was revealed by searching GenBank for genes with homology to a conserved domain of HDAC1 and HDAC3.[220] The splice variants of HDAC9 were reported by multiple groups based on the similarity of these transcripts to HDACs 4 and 5.[221–225] Four different groups independently discovered HDAC10.[226–229] HDAC11 was identified in a GenBank search for genes homologous to the yeast protein HOS3.[230] As such, these enzymes were classified as histone deacetylases largely on the basis of homology. With the exception of HDAC6, none of these enzymes possess strong lysine deacetylation activity. The study of HDAC 1-11 for other acyllysines has provided additional insight into their regulatory roles.

Of the lysine acylations discovered by our group, Kcr has been the one most studied with regards to its potential regulation by HDAC1-11. In our lab's original publication on the discovery of Kcr, we reported that none of HDAC1-11 had significant activity for Kcr.[102] Shortly thereafter, Christian Olsen's group reported that HDAC3 was the only zinc dependent deacetylase to remove Kcr *in vitro.*[231] However, a later screen by members of the same group demonstrated that HDAC1, HDAC2, and HDAC3 are *in vitro* decrotonylases.[110] HDAC1-3 and HDAC8 were also reported to regulate Kcr in culture as assessed by overexpression and knockdown experiments.[108] Similarly, HDAC1-3 were able to catalyze the removal of Kcr groups from modified recombinant histones *in vitro.*[232] However, knockout of HDAC1 and HDAC2 but not HDAC3 was associated with increased Kcr in mouse embryonic stem cell.[111] Thus, the majority of evidence to date ascribes decrotonylase activity to HDAC1-3 with the

caveat there may be cell type or assay associated differences that explain the inconsistencies in the published results.

HDAC1-3 can also regulate some of the other acylations discovered by our group. Specifically, HDAC1-3 catalyzes the removal of Kbu[232] and Khib[202] *in vitro.* Haitao Li and colleagues were the first to report that HDAC3 catalyzes the removal of the S form of Kbhb.[233] This combined with the aforementioned Kcr data demonstrate that HDAC1-3 are the most promiscuous of this class of enzymes for short-chain and hydroxylated acylations.

Despite being referred to as "deacetylases", there are members of the zinc dependent deacetylase family that are incapable of catalyzing the removal of Kac. The class IIa HDACs 4, 5, 7 and 9 do not remove any known naturally occurring substrate though they do catalyze the removal of trifluoroacetyllysine *in vitro.*[234] HDAC8 possesses weak deacetylation activity but can remove longer acyl-chains.[235] Similarly, HDAC11 also has higher activity for fatty acylations like myristoylation.[110,236] While HDAC10 is reported to deacetylate a few cytosolic Kac substrates,[237,238] it has recently been identified as a polyamine deacetylase.[239] Thus, several of the previously classified acetyltransferases are now better understood to regulate substrates other than Kac. It is still to be determined whether there are additional substrates to be uncovered for enzymes HDAC1-11.

1.5.3 SIRT 1-7: NAD+ dependent deacylases

The other category of HDACs corresponds to those that use NAD+ as a cofactor. These are the class III HDACs, otherwise known as sirtuins. "Silent information regulator" or Sir proteins including Sir2 were found to be associated with repression of transcription in yeast.[240,241] The initial biochemical analyses suggested that the activity of Sir2 was that of an ADP-ribosyltransferase.[242,243] Within the following year, Sir2 was identified to catalyze the

removal of Kac from histones.[244–247] In humans, there are 7 members in the sirtuin family so named for their similarity to the yeast Sir2 protein.[248] The sirtuins have a unique mechanism of catalysis among the HDAC family of proteins. The sirtuin catalytic reaction involves transfer the acetyl group to an NAD+ cofactor yielding the products of 2'-O-acetyl-ADP-ribose and nicotinamide.[244,249] The activities of sirtuins have since been implicated in a wide variety of biological functions including regulation of transcription and metabolism, and extending life span to name a few.[250–252]

It was recognized early on that not all of the human sirtuin enzymes demonstrated deacetylation activity.[248] The breadth of modifications that are targeted by sirtuins began to become clear as new types of acyl modifications were discovered. As new types of acyl modifications continue to be discovered, the substrate diversity of sirtuins continues to be an expanding field.

Much like HDAC 1-3, SIRT1-3 are bona fide deacetylases that are able to catalyze the removal of other types of acylations.[109] SIRT1 and SIRT2 in particular are able to catalyze the removal of Kpr, Kbu, and Kcr *in vitro*.[109] Knockdown SIRT3 was also observed to increase histone Kcr levels.[107] This observation is interesting given that canonically SIRT3 is considered a mitochondrial protein. SIRT3 is also a reported eraser for Kbhb, though specifically the S-form of the modification rather than the R-form that our laboratory hypothesized to be the dominant one.[233] Overexpression of SIRT1 is also reported to decreased levels of multiple site specific Kcr signals including the canonical target H3K9 as well as noncanonical substrates H3K4, H3K18, and H4K8.[108] Of the aforementioned sirtuins, SIRT2 is notable for the diversity of structures that it can reportedly remove. SIRT2 can remove the comparably bulky lysine benzoylation moiety from histones.[90] SIRT2 is also reported to remove fatty acyl groups from RAS proteins.[130]

Through initially identified for their deacetylase activity, it is now apparent that SIRT1-3 are capable of regulating diverse types of acyl modifications.

The aforementioned examples were cases where deacetylases had other targets besides Kac. Given the defined role of these enzymes on Kac, the other members of the sirtuin family were also designated as deacetylases. However, SIRT5 is a clear example of a case where the classification of "deacetylase" has turned out to be a misnomer. In contrast to its weak affinity to Kac, SIRT5 has strong deacylase activity for the negatively charged lysine acylations Ksuc, Kmal, and Kglu.[98,99,123] Our lab's characterization of the SIRT5 knockout mouse succinylome identified effects on respiration associated with succinylation of pyruvate dehydrogenase complex and succinate dehydrogenase.[124] Another laboratory also found that succinylation of HMGCS2 has negative effects on ketogenesis.[125] The effects of Ksuc accumulation following SIRT5 deletion were particularly pronounced in heart tissue and associated with cardiac hypertrophy.[253] The proteome wide profile for malonylated substrates differed from the succinylated sites through it also occurred on multiple enzymes involved in metabolic processes like glycolysis.[126,254] Collectively this demonstrates that SIRT5 is an enzyme that is a specific regulator of negatively charged acylations that has important roles in regulating metabolic enzyme activity.

The remaining sirtuins SIRT4, SIRT6 and SIRT7 all have reported activity for targets other than Kac. SIRT7 is a desuccinylase for H3K122suc as part of DNA damage response.[255] SIRT4 can catalyze the removal of the negatively charged acylations Ksuc, Kglu, Khmg, and Kmg.[104] In the case of SIRT4, this enzyme does not appear to be specific for negatively charged modifications as it also catalyzes the removal of lipoyllysine (Klip).[256] SIRT6 removes long chain acylations like lysine myristoyllysine.[109,257] The catalytic efficiency of SIRT6 is 300 fold

greater for peptides myristoyllysine than acetyllysine.[257] However, the presence of micromolar concentrations of long chain free fatty acids increase the deacetylase activity of SIRT6 while simultaneously decreasing its affinity for myristoylated peptides.[109] It should also be noted that the *in vitro* activity for SIRT6 is increased if nucleosomes are used as substrate rather than peptides or free histone.[258] Taken together, the evidence suggests multiple HDAC enzymes have evolved with the capacity to regulate a wide range of acyl modifications. The lysine acylations that are the reported substrates of HDACs are summarized in **Table 1.2**.

HDAC ID	Acylations
HDAC1	Kac, Kbu, Kcr, Khib
HDAC2	Kac, Kbu, Kcr, Khib
HDAC3	Kac, Kbhb, Kbu, Kcr, Khib
HDAC4	N/A
HDAC5	N/A
HDAC6	Kac
HDAC7	N/A
HDAC8	Kac*, Kmyr
HDAC9	N/A
HDAC10	Kac*
HDAC11	Kmyr
SIRT1	Kac, Kbu, Kcr, Kpr
SIRT2	Kac, Kbu, Kbz, Kcr, Kpr
SIRT3	Kac, Kbu, Kcr, Kpr
SIRT4	Kglu, Khmg, Kmg, Ksuc
SIRT5	Kglu, Kmal, Ksuc
SIRT6	Kac*†, Kmyr
SIRT7	Kac*, Ksuc

Table 1. 2 List of HDAC lysine acylation substrates.
The reported lysine acylations for all 18 HDACs are listed. The abbreviations for the acylations are as follows: Kac, acetyllysine; Kbhb, β-hydroxybutyryllysine, Kbu, butyryllysine; Kbz, benzoyllysine; Kcr, crotonyllysine; Kglu, glutaryllysine; Khib, 2-hyrdroxyisobutyryllysine; Khmg, 3-hydroxy-3-methylglutaryllysine; Klac, lactyllysine; Kmal, malonyllysine; Kmg, 3-methylglutaryllysine; Kmyr, myristoyllysine; Kpr, propionyllysine; and Ksuc, succinyllysine. (*) denotes enzymes that are reported to weakly catalyze removal of Kac. (†) SIRT6 weakly catalyzes Kac removal of peptides *in vitro*, but is reported to have higher activity for nucleosomes and in the presence of long chain free fatty acids.[109,258]

CHAPTER 2

DISCOVERY OF METHACRYLLYSINE

2.1 Introduction

As discussed in the preceding sections, the discovery of new modifications in recent years has expanded the field's understanding of the cell signaling mechanisms. In particular, lysine crotonylation has emerged as an enzymatically regulated epigenetic modification associated with active gene expression.[102,106] While it is known that there are multitudes of acyl-CoA metabolite species involved in cell metabolism, it is poorly understood to what extent other acyl-CoA metabolites are used in enzymatically regulated processes.

The identification of PTM identity by mass shift has important caveats. Comparison of MS/MS fragmentation of synthetic peptides to *in vivo* samples is insufficient for correct identification of PTMs.[259] One reason for this is that structural isomers of the same modification will often yield the same MS/MS fragmentation pattern. For example, Khib and Kbhb are structural isomers that derive from distinct acyl-CoAs.[103,117] Methacrylyl-CoA is a known metabolite that is a structural isomer of crotonyl-CoA.[56] We thus hypothesized that methacrylyl-CoA could serve as a precursor to PTMs similar to the role of crotonyl-CoA in Kcr

In the following section, we report the identification of a new type of histone posttranslational modification, methacryllysine (Kmea). Kmea is a structural isomer of Kcr. We validated the identity of Kmea as being separate from Kcr using synthetic peptides for MS/MS fragmentation, HPLC co-elution, and ozonolysis. We also validated the existence of this PTM in cells using a pan specific Kmea antibody for western blot and IP enrichment. Furthermore, we confirmed that treatment of cells with methacrylate led to direct incorporation into this

modification using isotopic labeling. In total, we identified 25 Kmea modified histone sites in HeLa cells. This work establishes Kmea as a new type of histone mark.

2.2 Results

2.2.1 Discovery and validation of methacryllysine (Kmea)

Based on the ability of other CoA species to form lysine acylations, we hypothesized that the endogenous metabolite methacrylyl-CoA would lead to the formation of the modification methacryllysine (Kmea) (**Fig 2.1**). Kmea is a structural isomer of another modification that we previously discovered, crotonyllysine (Kcr).[102] Due to the structural similarity, we hypothesized that we could enrich Kmea modified sites using a Kcr pan antibody. To narrow our search for potential Kmea sites, we focused on sites detected in HeLa cells by IP-MS/MS that were not detected by isotopic crotonate labeling in our previous work.[102] This provided us with seven candidates for which we generated synthetic peptides including: H2AK95, H3K122, H4K59, H4K31, H4K59, H4K77, and H4K79.

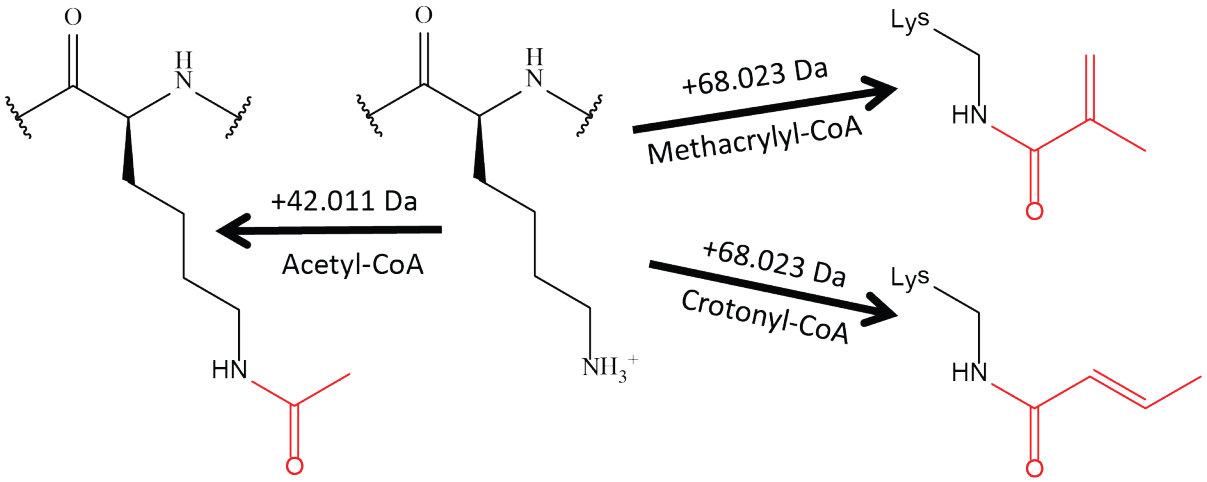

Figure 2. 1 Structure of methacryllysine and comparison to other acylations.
Lysine (center) is capable of being modified with multiple different PTMs depending on which acyl-CoA is involved in the reaction. The appropriate acyl-CoAs as well as the associated additional mass added to lysine is indicated for acetyllysine (left), methacryllysine (upper right), and crotonyllysine (lower right).

We performed immunoenrichment on trypsin digested histone extracts from HeLa cells using a pan Kcr antibody. These enriched samples were submitted to LC-MS/MS for analysis. We compared the fragmentation patterns for histones with +68.023 Da mass shifts on H4K91 from HeLa histones to synthetic peptides with either the Kcr or Kmea modifications (**Fig 2.2A**). The fragmentation patterns obtained by LC-MS/MS were identical for all three sets of peptides (**Fig 2.2A**). To validate the identity of the peptide from HeLa histones, we performed co-elution experiments. In co-elution, any peptides that can be separated by chromatography are confirmed to have distinct chemical structures. We found that the synthetic H4K91cr peptide eluted in a different peak than the H4K91+68.023 peptide isolated from HeLa cells (**Fig 2.2B**), confirming that the peptide isolated from cells was not modified with Kcr. In contrast, we found that the H4K91+68.023 Da peptide from HeLa cells co-eluted with the synthetic H4K91mea peptide (**Fig. 2.2C**), supporting its identification as a Kmea peptide. We validated H4K31mea using the same approach (**Figure 2.3**). These results provide the first evidence for the existence of Kmea as a novel and distinct type of modification.

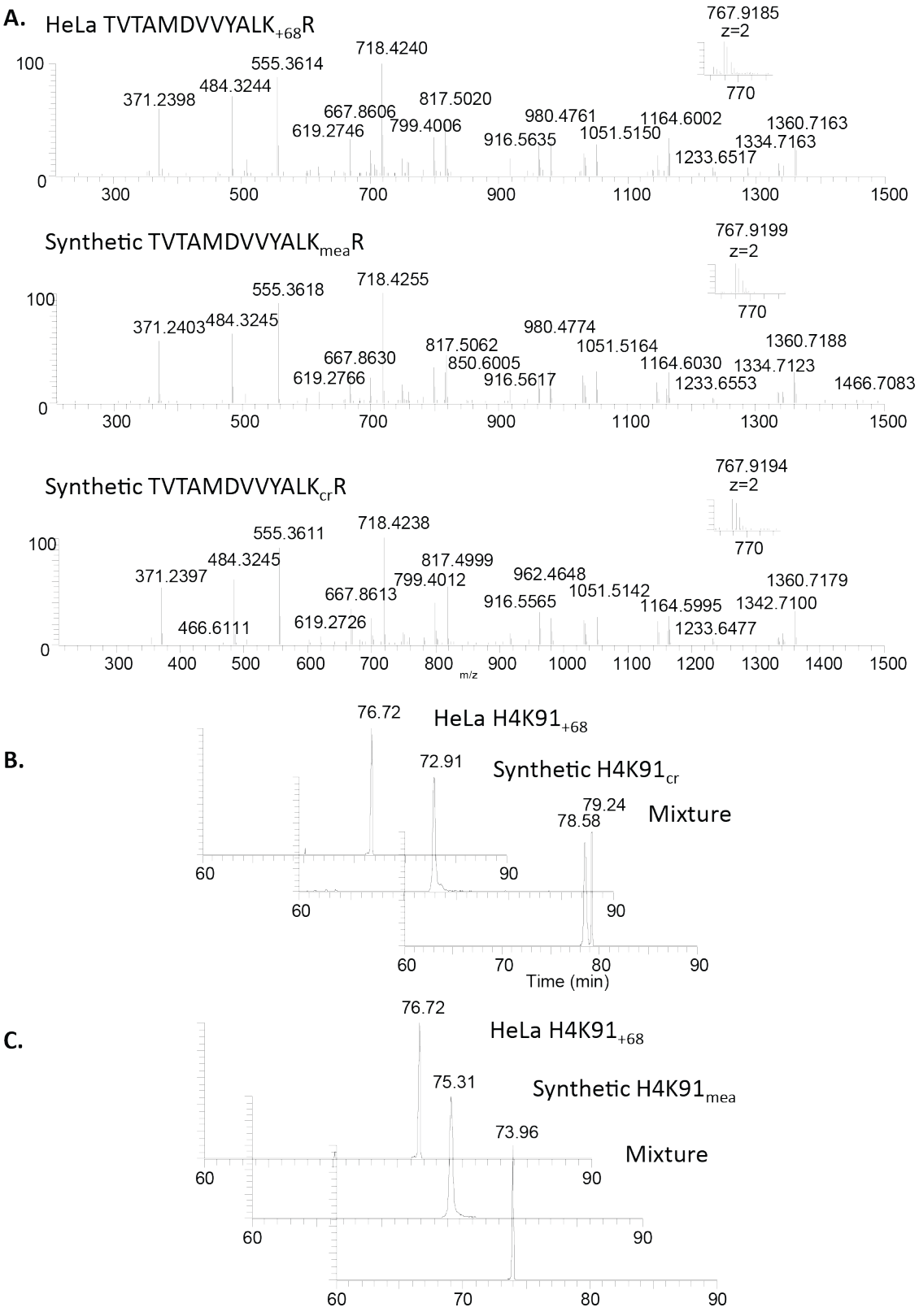

Figure 2. 2 MS/MS fragmentation and validation by co-elution of H4K91mea.

Figure 2.2 (continued) MS/MS fragmentation and validation by co-elution of H4K91mea. (a) MS/MS spectrum of HeLa histone peptide (top), synthetic H4K91ma peptide (middle), and synthetic H4K91cr peptide (bottom). (b) Extraction ion chromatograms of HeLa histone peptide (TVTAMDVVYALK$_{+68}$R) (top), synthetic H4K91cr peptide (middle), and a mixture of both synthetic peptide with *in vivo* sample (bottom). (c) Extraction ion chromatograms of HeLa histone peptide (TVTAMDVVYALK$_{+68}$R) (top), synthetic H4K91mea peptide (middle), and a mixture of both synthetic peptide with *in vivo* sample (bottom).

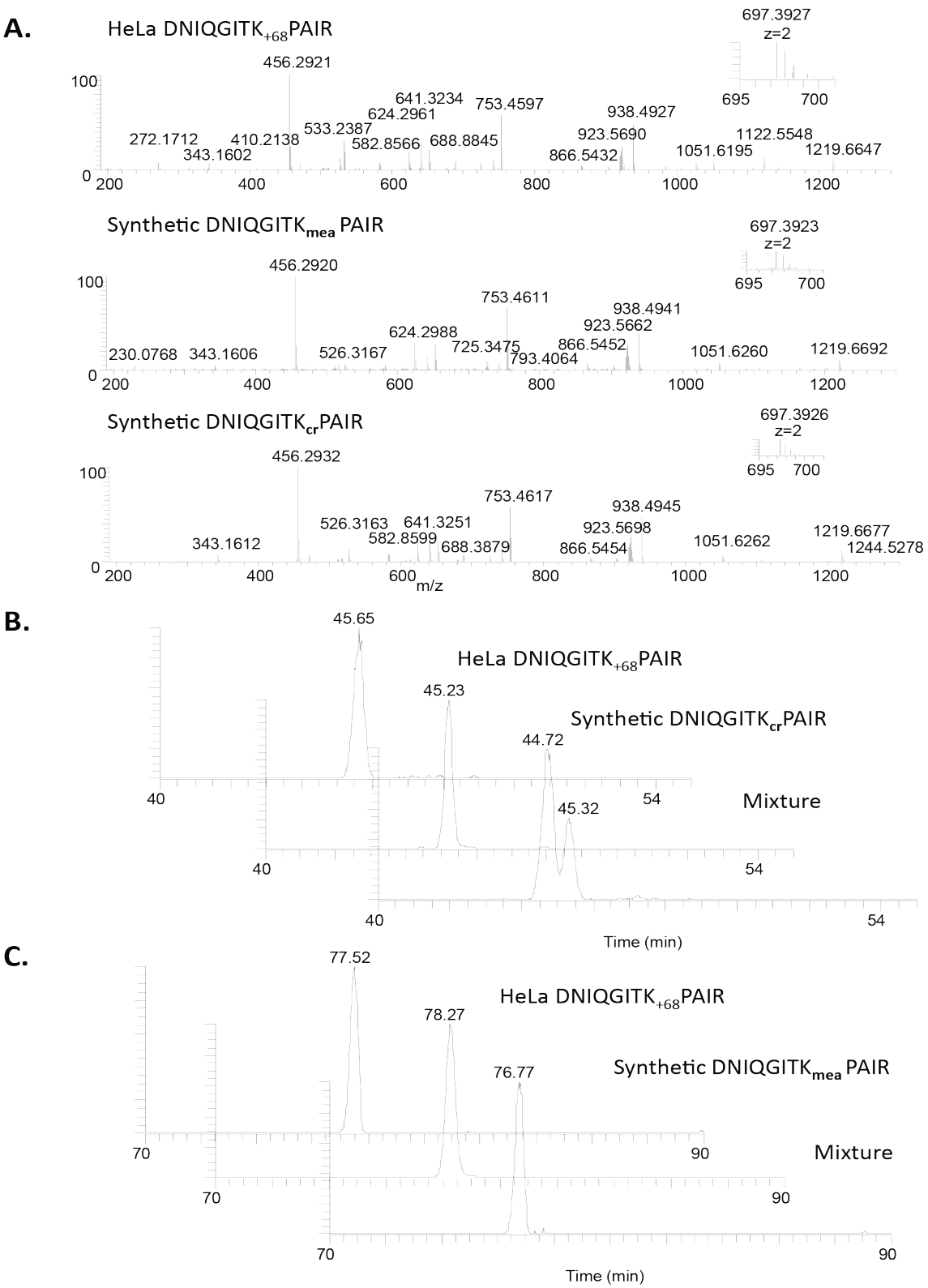

Figure 2. 3 MS/MS fragmentation and validation by co-elution of H4K31mea.

Figure 2.3 (continued) MS/MS fragmentation and validation by co-elution of H4K31mea. (a) MS/MS spectrum of HeLa histone peptide (top), synthetic H4K31ma peptide (middle), and synthetic H4K31cr peptide (bottom). (b) Extraction ion chromatograms of HeLa histone peptide (DNIQGITK$_{+68}$PAIR) (top), synthetic H4K31cr peptide (middle), and a mixture of both synthetic peptide with *in vivo* sample (bottom). (c) Extraction ion chromatograms of HeLa histone peptide (DNIQGITK$_{+68}$PAIR) (top), synthetic H4K31ma peptide (middle), and a mixture of both synthetic peptide with *in vivo* sample (bottom).

In the process of performing co-elution experiments, we encountered two sites, H2AK95 and H4K59, which we were unable to validate on the basis of chromatographic separation alone. To properly identify these sites, we took advantage of the ability of ozonolysis chemistry to differentiate between Kmea and Kcr sites. In an ozonolysis reaction, ozone cleaves molecules at unsaturated bonds. Structural differences between Kmea and Kcr modifications mean that products with different masses will result from the reaction (**Figure 2.4**). We measured the reaction products by LC-MS/MS to validate the identity of the posttranslational modification isolated from cells. Following ozonolysis, the spectra for the HeLa H2AK95+68.023 Da modified peptide matched the same pattern as the synthetic H2AK95mea peptide (**Figure 2.5**). In contrast, fragmentation of H2AK95cr peptide yielded distinct fragmentation patterns with multiple products (**Figure 2.6**). We also validated the identity of H4K59mea by this method (**Figure 2.7**). These experiments further support the existence of the Kmea modification as a naturally occurring PTM.

Chemical oxidation by ozone

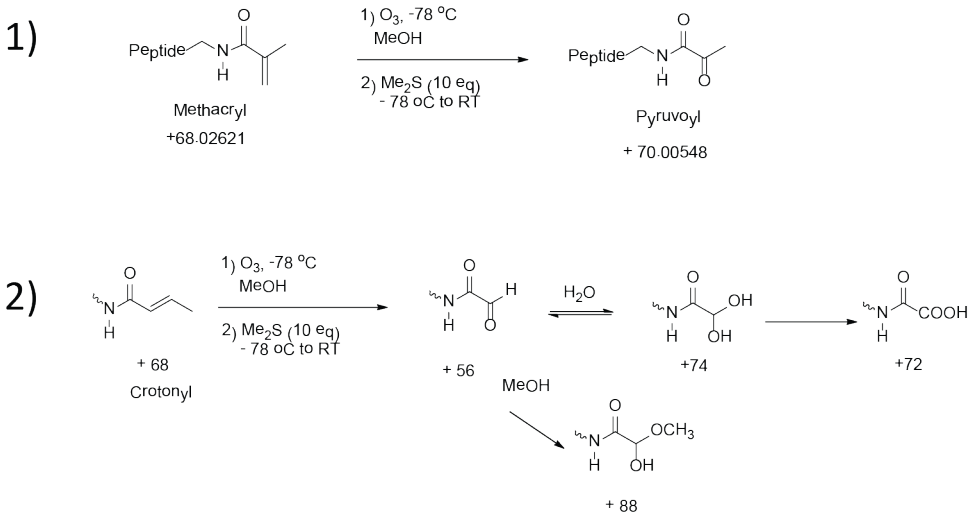

Figure 2. 4 Diagram of ozonolysis reactions.
Chemical reactions for ozonolysis of Kmea (1) and Kcr (2) peptides. The 2 step reaction conditions used for this procedure are indicated. Ozonolysis is predicted to yield an end product lysine modification with +70.00548 Da mass shift for peptides bearing Kmea modification. In contrast, Kcr peptides are expected to yield products with mass shifts of approximately +56, +72, +74, or +88 Da.

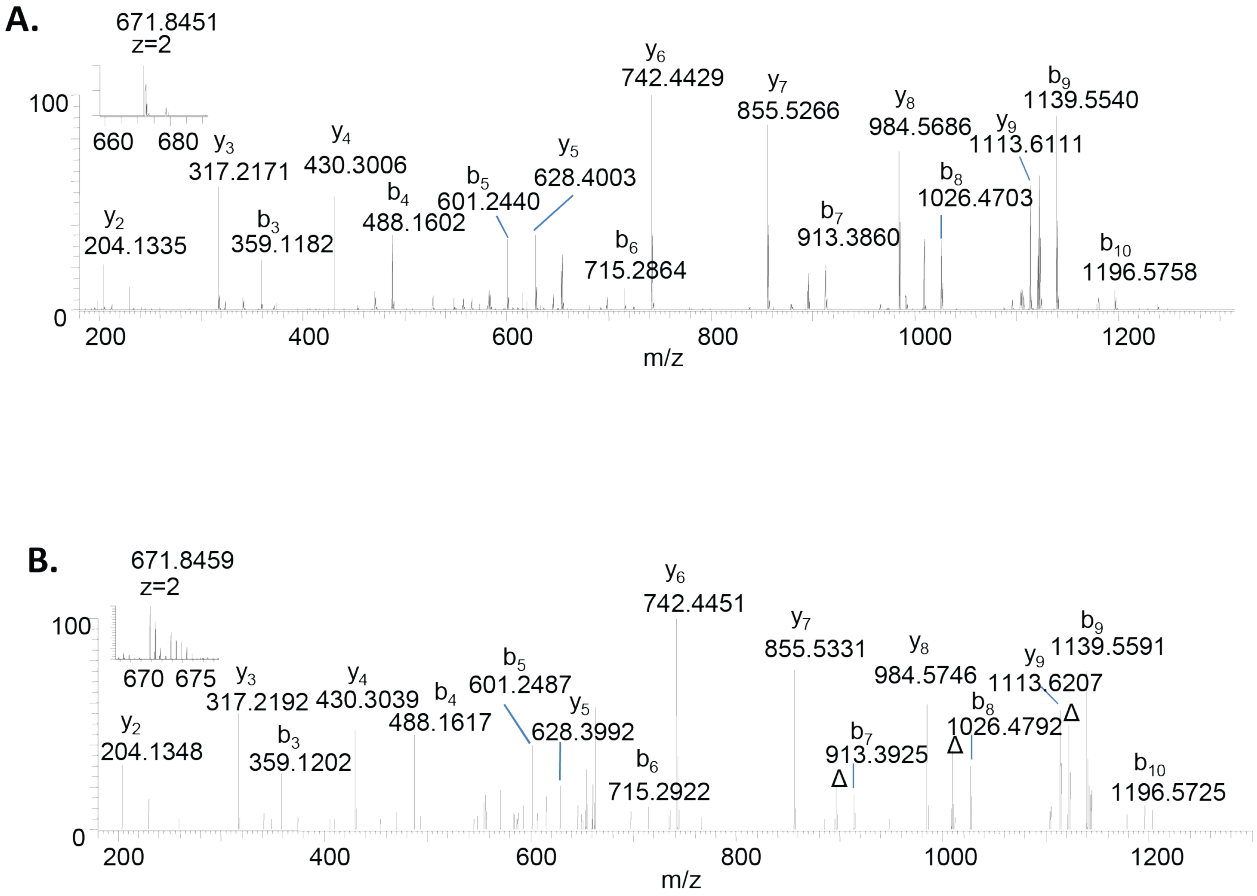

Figure 2. 5 Validation of H2AK95mea peptide by ozonolysis.
(a) MS/MS of synthetic H2AK95mea peptide following ozonolysis reaction. (b) MS/MS of HeLa peptide following ozonolysis reaction. The fragmentation pattern of the peptide from HeLa histones matches that of the synthetic H2AK95mea peptide following ozonolysis.

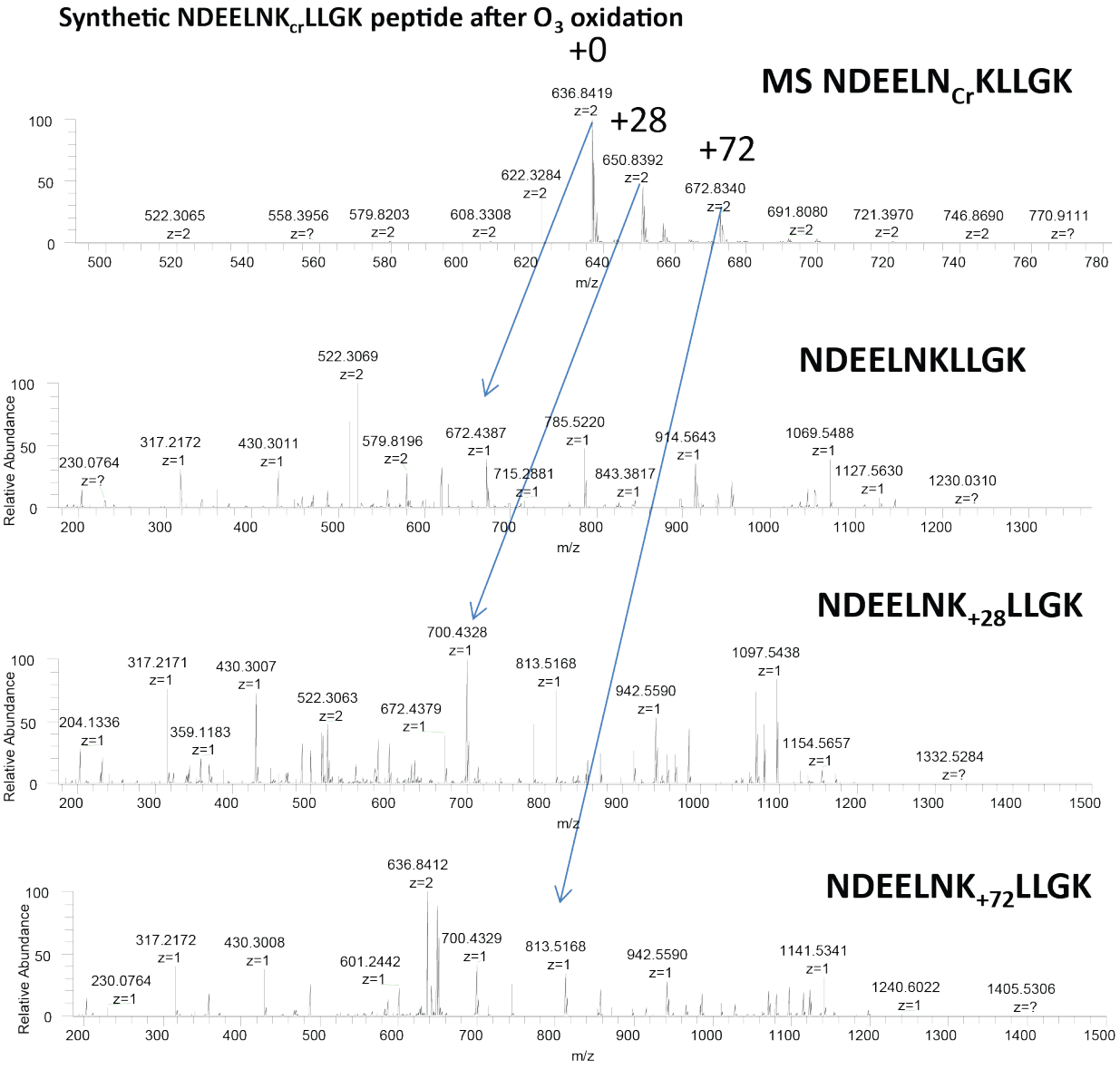

Figure 2. 6 H2AK95cr peptide has distinct fragmentation pattern after ozonolysis. Three peaks were detected by MS1 (top) following ozonolysis of synthetic H2AK95cr peptide. These corresponded to the unmodified, +28 Da, and +72 Da versions of the peptide. The +72 Da peptide is consistent with one of the predicted products listed in Figure 2.4. Importantly, the fragmentation pattern of the H2AK95cr peptide does not match the pattern for the HeLa histone extract peptide shown in Figure 2.5.

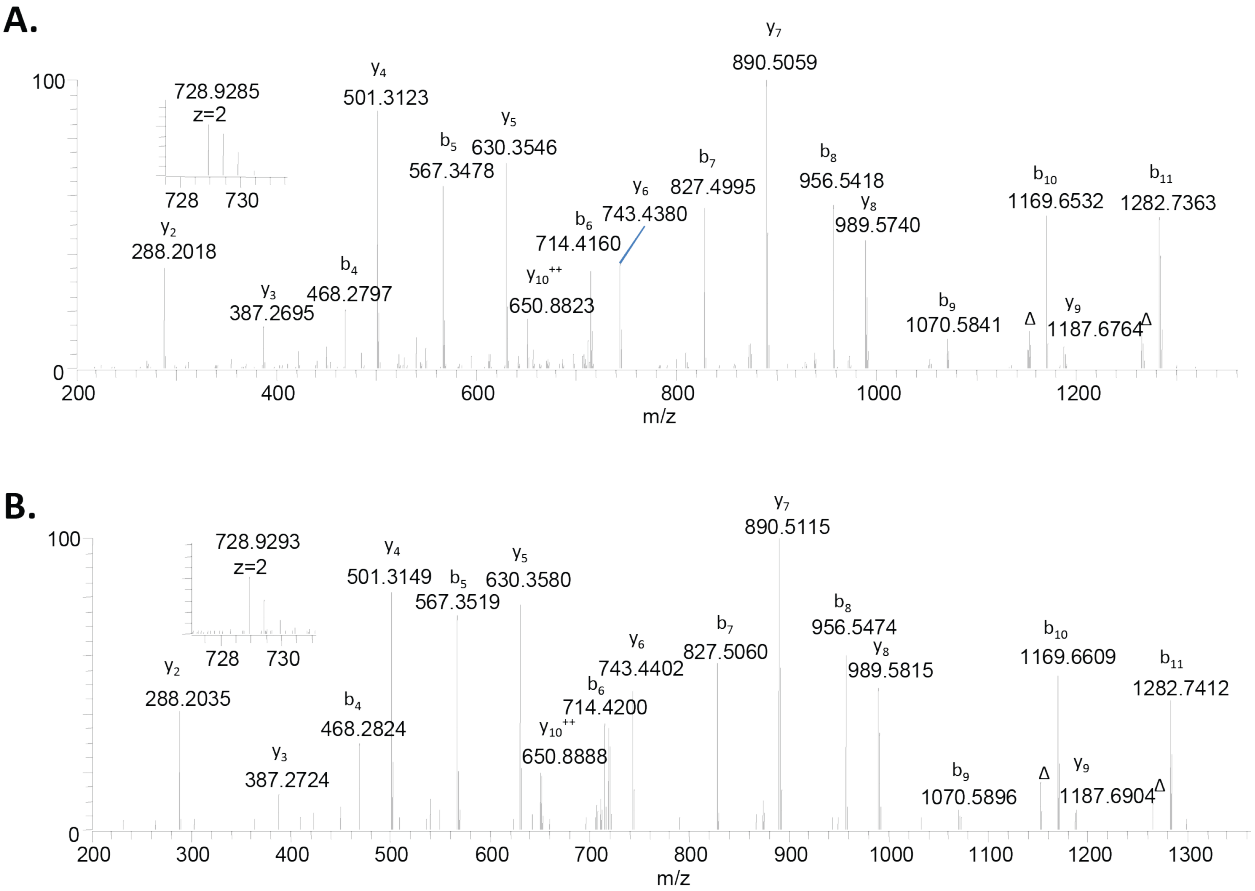

Figure 2. 7 Validation of H4K59mea by ozonolysis.
(a) MS/MS of synthetic H2AK59mea peptide following ozonolysis reaction. (b) MS/MS of HeLa peptide following ozonolysis reaction. The fragmentation pattern of the peptide from HeLa histones matches that of the synthetic H2AK59mea peptide following ozonolysis.

2.2.2 Generation and validation of Kmea antibodies

Antibody based enrichment methods are ideal for detection of low abundance posttranslational modifications. We generated a rabbit polyclonal pan-specific antibody for Kmea. By dot blot analysis, we found that the Kmea antibody was about 20 fold more specific for Kmea peptide library used in its generation than the other acylated peptide libraries we tested (**Figure 2.8A**). The pan Kmea antibody was able to detect a signal when used in immunoblotting with acid extracted histones from HeLa cells (**Figure 2.8B**). We performed a competition assay by incubating the Kmea pan antibody in the presence of various peptide libraries. The immunoblot signal was competed away using synthetic Kmea peptide library to a greater extent than when competition was performed with any other tested synthetic peptide library with unmodified or acylated lysines (**Figure 2.8B**). This confirms that the signal we detected by western blot was due to the presence of antibodies in the polyclonal mixture that are specific for the Kmea peptide library.

2.2.3 Methacrylate is a metabolic precursor for histone Kmea

We hypothesized that methacrylyl-CoA would serve as the precursor for lysine methacrylation. Similar to the effects of acetate and crotonate, we hypothesized that treatment of HeLa cells with sodium methacrylate would provide a substrate for the formation of Kmea. Consistent with our hypothesis, we found that increasing doses of sodium methacrylate coincided with increases in histone Kmea signal (**Figure 2.8C**). Furthermore, the effect of equimolar doses of methacrylate and crotonate had the strongest effects on increasing signal on Kmea and Kcr, respectively (**Figure 2.8C**). This further suggests that Kmea and Kcr antibodies are primarily detecting distinct posttranslational modifications.

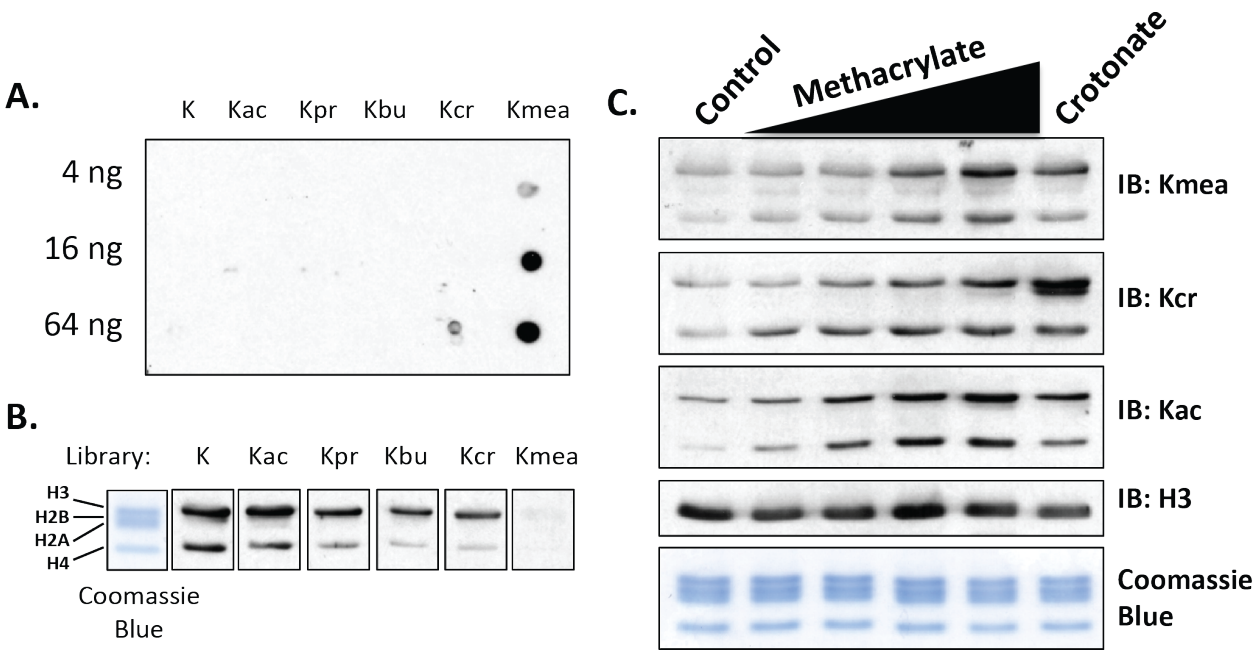

Figure 2. 8 Validation using pan Kmea antibody.
(a) Dot blot for pan anti-Kmea antibody using synthetic peptide libraries spotted onto nitrocellulose membrane. The amount and identity of each peptide library are indicated. (b) Immunoblot results following incubation of the pan anti-Kmea antibody with indicated acylated synthetic peptide libraries. Western blot images are taken from the same film at the same exposure time. Images are cropped for aesthetics. (c) Western blot results for histones extracted from HeLa cells. HeLa cells were treated for 24 hours with 1, 3, 5, or 10 mM sodium methacrylate or 10 mM sodium crotonate.

The previous experiment did not rule out the possibility that the effects that we observed in western blot were not due to factors other than metabolic incorporation. For example, certain short chain fatty acids, most notably butyrate, lead to increases in Kac by acting as histone deacetylase inhibitors.[207] Indeed, crotonate has been reported to also inhibit HDACs *in vitro*.[232] To confirm that methacrylate was capable of serving as a metabolic precursor, we used an isotopic labeling approach. We treated HeLa cells with 20 mM d7-labeled methacrylate for 24 hours before isolating histones through acid extraction. We then tryptically digested the histones and enriched Kmea sites using our newly generated pan Kmea antibody. Through this approach, we detected two sites where the isotopic methacrylate was incorporated into the Kmea modification (**Figures 2.9 and 2.10**). These results clearly demonstrate that methacrylate can serve as a metabolic precursor for histone Kmea. Furthermore, these results further validate the existence of Kmea as a unique modification that is separate from Kcr.

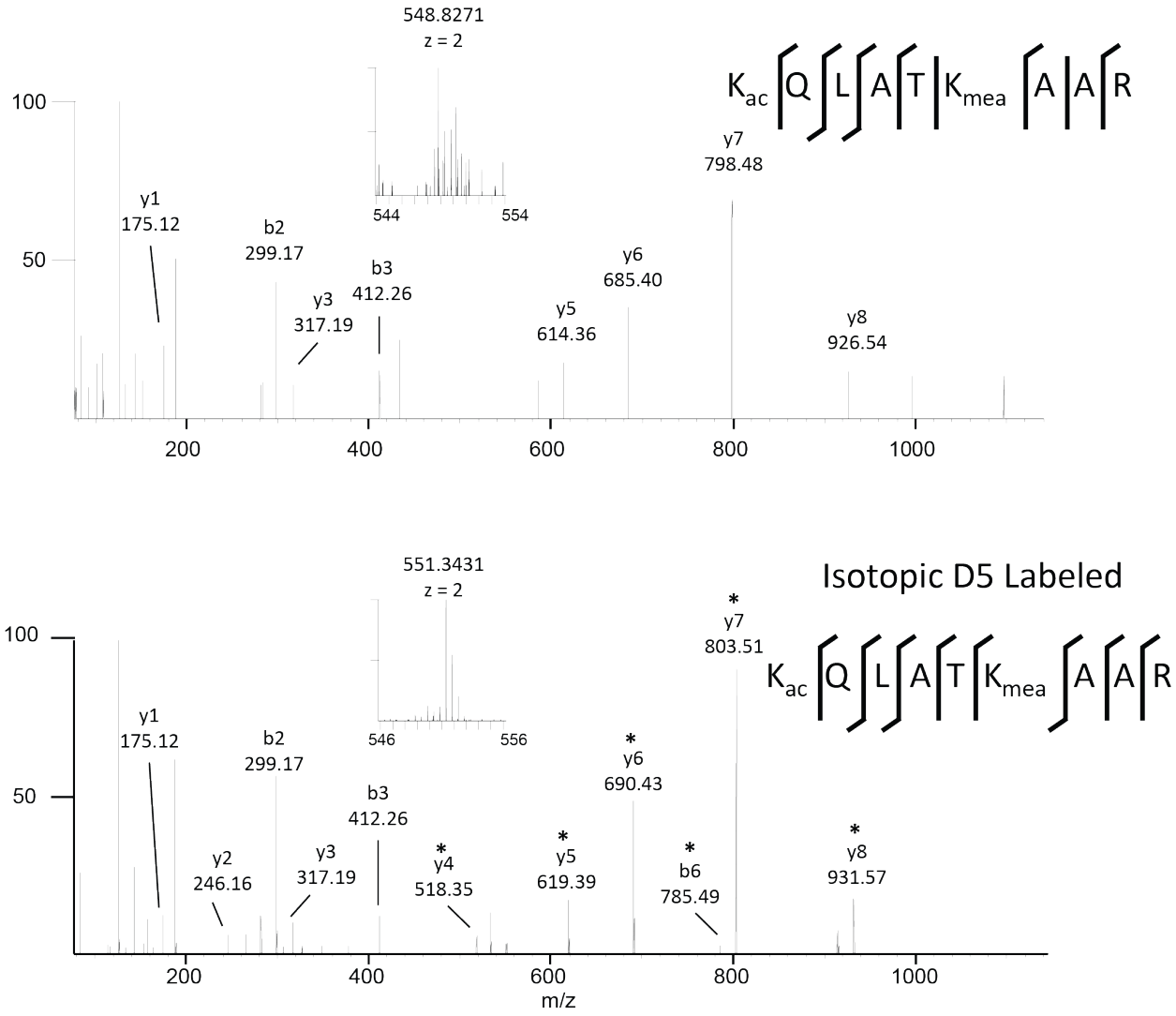

Figure 2. 9 D5 labeled sodium methacrylate is directly incorporated into H3K23mea. MS/MS spectra of H3K23mea isolated from HeLa histones following treatment with 20 mM methacrylate (top). MS/MS spectra of isotopic H3K23mea isolated from HeLa histones following treatment with 20 mM d-7 methacrylate (bottom). (*) indicate b and y ions with 5 Da mass shift consistent with incorporation of the isotopic metabolite.

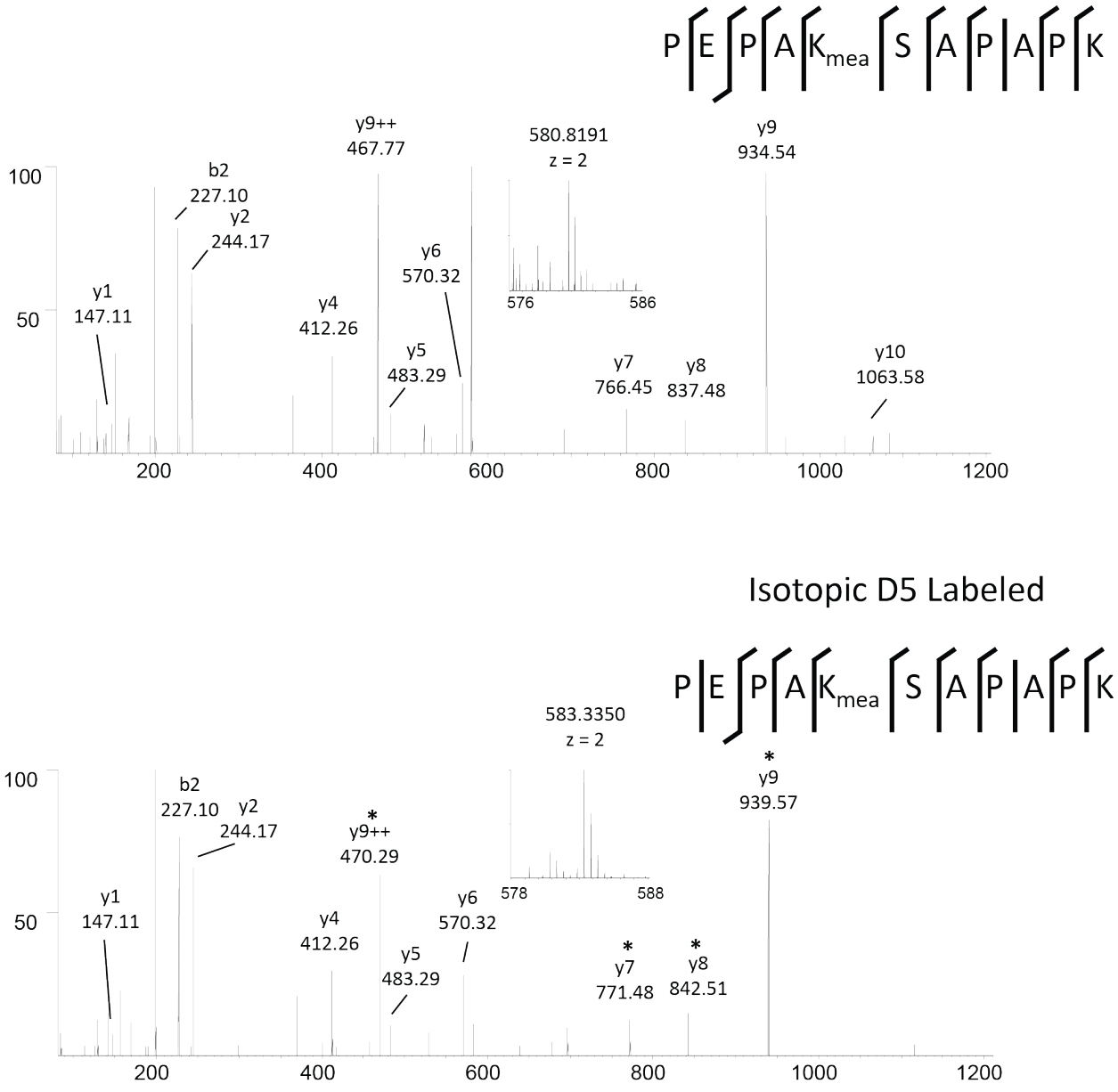

Figure 2. 10 D5 labeled sodium methacrylate is directly incorporated into H2BK5mea. MS/MS spectra of H2BK5mea isolated from HeLa histones following treatment with 20 mM methacrylate (top). MS/MS spectra of isotopic H2BK5mea isolated from HeLa histones following treatment with 20 mM d-7 methacrylate (bottom). (*) indicate b and y ions with 5 Da mass shift consistent with incorporation of the isotopic metabolite.

2.2.4 Mapping histone Kmea sites using IP-MS/MS

An understanding of the potential effects of Kmea will require that we know the modified residues. We treated cells with 20 mM of sodium methacrylate for 24 hours before harvesting cells and performing acid extraction of histones. The histones were tryptically digested and enriched by immunoprecipitation with the pan Kmea antibody. The aforementioned greater specificity of the antibody for Kmea over Kcr is critical as this discrimination is the basis for our referring to sites as Kmea sites when performing MS/MS surveys for Kmea sites. We performed LC-MS/MS on the enriched sample and then analyzed the results using MASCOT to search for lysine residues bearing +68.023 Da additional mass. Spectra with a MASCOT score greater than 20 were further evaluated manually for spectral quality (**Appendix**). From the results of the IP-MS/MS in addition to the sites that we validated by co-elution and ozonolysis, we identified a total 25 sites that represent potential Kmea sites across the core histones (**Figure 2.11**). As indicated in the figure, many of these sites overlapped with previously reported Kac and Kcr sites [92,260,261], This suggests that Kmea is a widespread modification found throughout the core histones similar to Kac and Kcr.

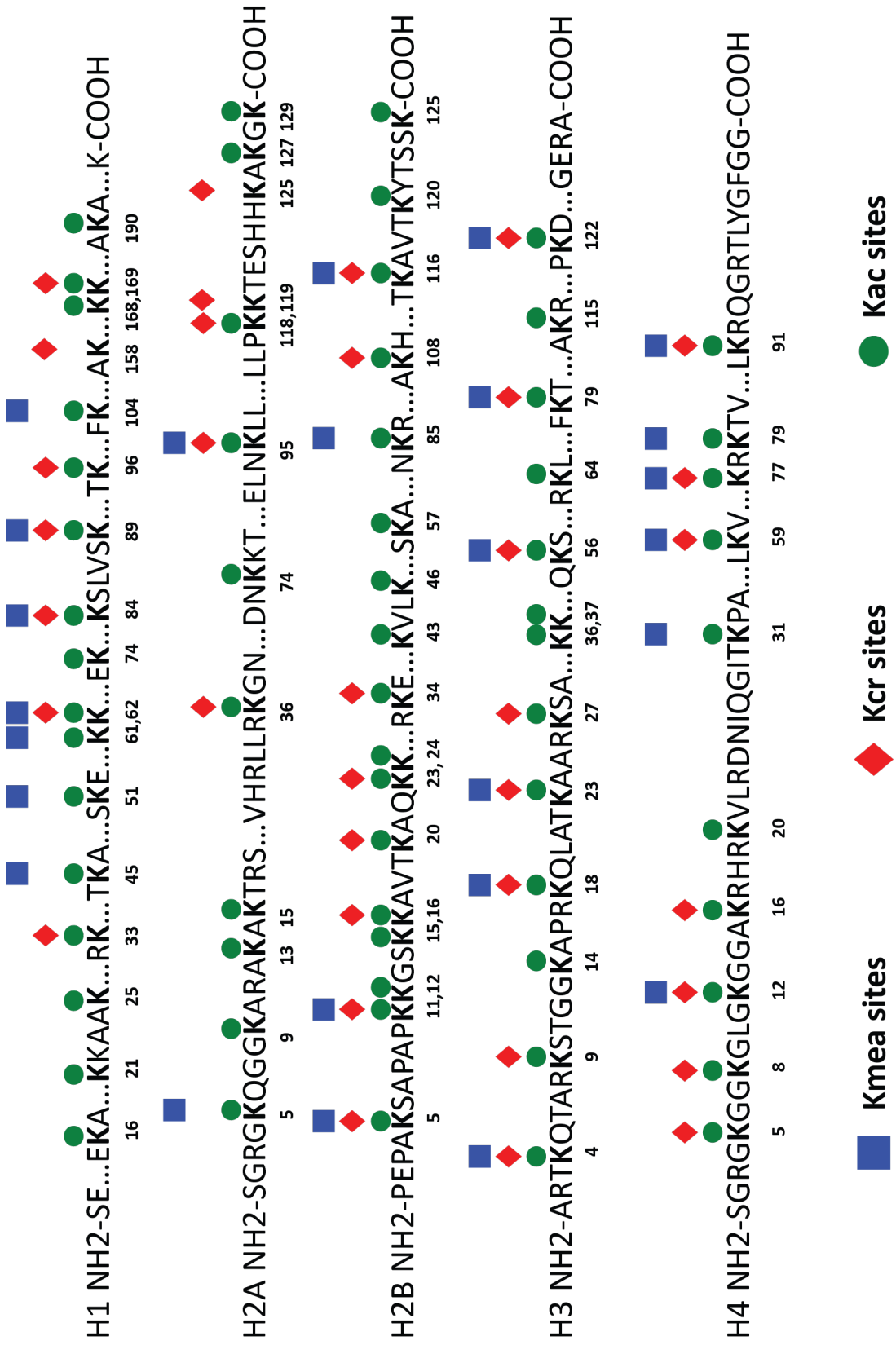

Figure 2. 11 List of all Kmea sites detected in HeLa cells

Figure 2.11 (continued) List of all Kmea sites detected in HeLa cells. Schematic of the sequences of the 5 core histone proteins with sites of Kmea, Kcr, and Kac indicated. The key for the modifications is as follows: Kmea, blue squares; Kcr, orange diamonds; Kac, green circles. Kmea sites include both those detected by IP-MS/MS with pan Kmea antibody as well as sites that were validated by co-elution or ozonolysis.

2.3 Discussion

In summary, these results demonstrate that Kmea is a novel widespread type of histone mark. We comprehensively validated the existence of this modification through MS/MS fragmentation, HPLC co-elution, ozonolysis, isotopic labeling, and antibody validation. This work provides new directions for the study of the effects of methacrylyl-CoA in cell biology. The enzymatic regulation of this new modification is further explored in chapters 3 and 4.

The fact that Kcr and Kmea are structural isomers raises important points regarding the study of each moving forward. It also poses a potential issue for the use of methods that do not distinguish between these two modifications. For example, Bos and Muir proposed that a TCEP conjugated chemical probe can be used in the detection of Kcr due to the presence of an α,β-unsaturated carbonyl.[262] This probe would be likely to cross-react with Kmea as it also contains an α,β-unsaturated carbonyl group. In addition, the recent discovery of tigyllysine presents another case of an α,β-unsaturated carbonyl that would present an off-target substrate.[105] Our work also suggests that careful optimization must be made in separating Kcr and Kmea by HPLC. In our hands, there were sites that we still were unable to confidently separate certain sites based on retention time alone. Certain methods for quantitation of modified peptides or acyl-CoAs rely heavily on retention times for identification.[263,264] Therefore, methods that use such approaches should be validated to demonstrate that they can properly differentiate between methacryl and crotonyl signals.

In this work, we utilized Kmea antibodies for the specific detection of Kmea over Kcr. We limited our analysis to using antibodies that had approximately 20 fold greater specificity for Kmea over other related acyllysine peptides. Nonetheless, the specificity still remains as potential caveat for correct identification. Our laboratory has used the inherent cross-reactivity of

other antibodies to detect new modifications with similar structures.[89] That also applies to the discovery of Kmea as detailed in this work, using pan Kcr antibodies for initial enrichment. While the data overall demonstrates that Kmea is a new and unique modification, there nevertheless remains the possibility that certain signals like those from IP-MS/MS include off-target Kcr detection.

2.4 Methods

Reagents

We developed the pan-Kmea antibody in collaboration with PTM Biolabs (Chicago, IL). We obtained pan Kcr (PTM-501) and pan Kac (PTM-101) antibodies from PTM Biolabs (Chicago, IL). The anti-H3 antibody (ab12079) were obtained from Abcam (Cambridge, MA). Methacrylic acid and crotonic acid were obtained from Sigma-Aldrich (St. Louis, MO). The d7-methacrylic acid was obtained from CDN Isotopes (Pointe-Claire, Quebec, Canada). GL Biochem (Shanghai, China) synthesized the peptide libraries for this work. Sequencing grade modified trypsin was obtained from Promega (Madison, WI). Chemicals used in buffers were obtained from Sigma-Aldrich (St. Louis, MO) unless otherwise noted.

Cell culture

HeLa were obtained from ATCC and not validated further. Cells were grown in high glucose DMEM (Thermo Fisher Scientific, Waltham, MA) with 10% FBS at 37°C in 5% CO_2.

Methacrylate and crotonate treatment

The salt forms of methacrylic acid and crotonic acid were prepared by raising pH to 7.0-7.3 using NaOH. HeLa cells were treated with 0, 1, 3, 5, or 10 mM of methacrylate or 10 mM of crotonate after cells reached approximately 50% confluency. Cells were harvested for histone

extraction at 24 hours post treatment. HeLa cells treated with 20 mM d7-methacrylic acid (CDN Isotopes, Pointe-Claire, Quebec, Canada) were prepared in the same way.

Histone extraction

Acid extraction of histones was performed according to modified version of a published protocol [93]. Briefly, cells were harvested in 10 cm plates after reaching approximately 90% confluency. Cells were washed in phosphate buffered saline (PBS) before detaching from plate by cell scraper. Cells were then washed and pelleted in PBS twice at 1,000 x g for 5 min at 4°C. Cell membranes were lysed in extraction buffer (10 mM HEPES pH 7.0, 10 mM KCl, 1.5 mM MgCl2, 0.34 M sucrose, 0.5% NP-40, 5 mM sodium butyrate, 10 mM nicotinamide) for 10 minutes with gentle agitation at 4°C. Nuclei were then pelleted at 2,000 x g at 4°C for 10 min and supernatant was discarded. Cells were resuspended in extraction buffer without NP-40. Cell nuclei were pelleted at 2,000 x g at 4°C for 5 min. Nuclear pellets were then lysed in a nuclear lysis buffer (3 mM EDTA, 0.2 mM EGTA, 5 mM sodium butyrate, 10 mM nicotinamide) for 30 min with gentle agitation at 4°C. Chromatin was pelleted at 6,500 x g for 5 min at 4°C and then resuspended in 0.4 N H_2SO_4. Chromatin suspension in acid was incubated overnight at 4°C with gentle agitation. After centrifuging at 16,000 x g for 10 min, acid soluble supernatant was collected and used in TCA precipitation. Following TCA precipitation, histones were pelleted and washed three times in acetone. Histones were finally resuspended in deionized H_2O.

Trypsin digestion

Isolated histones were in-solution digested using sequencing grade modified trypsin (Promega) at a ratio of 50:1, respectively. Buffer was adjusted to pH 8 using ammonium bicarbonate. Samples were incubated at 37°C overnight. Following incubation, samples were boiled for 1 minute to inactivate trypsin.

Validation of Methacryllysine Peptides Using HPLC-MS/MS

We injected synthetic methacrylated or crotonylated peptides with or without mixing with tryptically digested histone extract into nano-HPLC system. Peptides were analyzed using LTQ Orbitrap Velos Mass Spectrometer according to the methods in our previous work.[102]

Peptide enrichment by immunoprecipitation and identification by LC-MS/MS

We began by conjugating pan anti-Kmea antibodies to nProtein A Sepharose beads (GE Healthcare Bio-Sciences). The bead conjugated antibodies were then incubated in the presence of tryptically digested peptides overnight at 4°C with gentle agitation. We washed the beads with NETN buffer (50 mM Tris-Cl pH 8.0, 1 mM EDTA, 100 mM NaCl, 0.5% NP-40) three times. This was followed by two washes in ETN buffer which lacked the 0.5% NP-40. This was followed once with deionized water. We then eluted peptides using 0.1% trifluoroacetic acid. The eluted peptides were then dried in a SpeedVac (Thermo Fisher Scientific, Waltham, MA). Dried peptides samples were dissolved in HPLC Buffer A (0.1% formic acid in water, v/v) and loaded into a homemade capillary column (10 cm length x 75 mm ID, 3 μm particle size, Dr. Maisch GmbH) attached to an EASY-nLC 1000 system (Thermo Fisher Scientific, Waltham, MA). We separated and eluted peptides along a gradient of 2% to 90% HPLC Buffer B (0.1% formic acid in acetonitrile, v/v) in HPLC Buffer A at a flow rate of 200 nl min^{-1} over 60 minutes. The peptides were ionized and analyzed using a Q-Exactive mass spectrometer (Thermo Fisher Scientific, Waltham, MA). The MS/MS analysis was performed in accord with our previous publication.[91] RAW files were converted into msm files and then analyzed by MASCOT software. The parameters for the search included the following modifications: Kmea (lysine +68.023 Da), Kac, N-terminal acetylation, K/Rme1, K/Rme2, and Kme3. Histone peptide

matches with Kmea sites were manually verified for correctness for all spectra with MASCOT scores of at least 20.

Dot blot

Synthetic peptides were spotted onto nitrocellulose membrane in the amounts indicated in the figures. Membranes were incubated in blocking buffer (3% bovine serum albumin, 20 mM tris-buffered saline pH 7.6, 0.1% Tween-20) for 1 hour at room temperature with gentle agitation. Membranes were incubated in solution of primary antibody diluted in 1% BSA blocking buffer and incubated for 30 minutes at room temperature with gentle agitation. Blots were washed three times in TBST. Then, membranes were incubated in secondary antibody diluted in 1% BSA in TBST for 30 minutes at room temperature with gentle agitation. Blots were washed three times in TBST and then incubated for 1 minute in enhanced chemiluminescence reagent. Film was exposed in dark room to visualize antibody binding. Film was scanned into digital image and then the entire image contrast adjusted using the autocontrast tool in Photoshop.

Western blot

A total of 4 μg histone extract was loaded per lane in 15% tris-glycine polyacrylamide gel in Mini-Protean electrophoresis system (Bio-Rad, Hercules, CA). SDS-PAGE was performed using running buffer (25 mM tris, 192 mM glycine, 0.1% SDS). Voltage was set to 80V for the first 30 minutes before increasing to 120V until loading dye reached the bottom of the gel. Tank transfer in mini-trans-blot module (Bio-Rad, Hercules, CA) was performed using transfer buffer (25 mM tris, 192 mM glycine, 0.1% SDS) with 20% methanol for 1 hour and 15 minutes at 100 V constant. We transferred proteins to 0.2 μm PVDF membranes. Membranes were incubated in blocking buffer (3% bovine serum albumin, 20 mM tris-buffered saline pH 7.6, 0.1% Tween-20) for 1 hour at room temperature. Membranes were probed with primary antibody in 1% BSA

blocking buffer overnight at 4°C with gentle agitation. Secondary HRP conjugated antibodies were incubated for 1 hour at room temperature. Membranes were washed 3 times for 8 minutes each in TBST (20 mM tris-buffered saline pH 7.6, 0.1% Tween-20) following both primary and secondary antibody incubations. Film was exposed in dark room after incubating for 1 minute in enhanced chemiluminescence reagent with gentle agitation. Film images were scanned into digital files. The entire image contrast for each image was adjusted using the autocontrast tool in Photoshop.

Peptide competition assay

Pan Kmea antibody was incubated in the presence of 500 molar excess of peptide libraries for 4 hours at room temperature with gentle incubation. This solution was used as the primary antibody incubation overnight at 4°C with gentle agitation. All other steps are consistent with the western blot protocol as described.

Coomassie blue stain

SDS-PAGE was performed as described in the western blot protocol. Gel was rinsed briefly in deionized H_2O. Gel was then incubated in Protoblue Safe colloidal coomassie blue G-250 stain (National Diagnostics, Atlanta, Georgia) overnight with gentle agitation according to manufacturer instructions. Gels were then periodically washed in deionized H_2O until bands were clearly visible. Gels were scanned into digital images and contrast adjusted in Photoshop.

CHAPTER 3

HAT1 IS A WRITER FOR KMEA

3.1 Introduction

A central factor that allows for PTMs to be involved in signaling is that they are often reversibly added and removed by enzymes. Enzymes that catalyze the addition of chemical groups to amino acid residues are known as writers. For the new lysine acylations discovered by our lab, the writers identified for lysine acylations thus far consist almost entirely of previously classified lysine acetyltransferases. Carnitine palmitoyltransferase 1A is currently the lone exception as it is a carnitine acyltransferase, but is reported to act as a lysine succinyltransferase.[203] Thus, targeted analysis of previously classified lysine acetyltransferases has been a fruitful avenue for discovering writers for newly identified lysine acylations.

The reasons for the substrate promiscuity of lysine acetyltransferases is perhaps best exemplified by p300, the writer with the most diverse set of substrates identified thus far. With regard to its structure, p300 contains a deep aliphatic pocket in its active site that is capable of accommodating a variety of acyl-CoA substrates.[197] The measured kinetics of p300 activity decrease as a factor of increasing acyl chain length.[55,197] Mutagenesis of a key isoleucine residue in the active site pocket increased or decreased the kinetics for Kcr and Kbu depending on if the substituted residue expanded or occluded the pocket, respectively.[197] Thus, the structure of acetyltransferases can in some cases accommodate alternative substrates to acetyl-CoA.

The activity associated with writers can provide key insight into the potential functional roles of newly identified acylations. For example, p300 was known to be associated with transcriptional activation prior to its identification as an acetyltransferase.[265] Consistent with this previously identified function, p300 can catalyze *in vitro* transcription using Kcr, Kbu, Khib, and

Klac.[91,106,120,128] This does not preclude the possibility that the use of alternative substrates may have distinct functions. We found that p300 regulates glycolysis through Khib of glycolytic enzymes rather than by Kac.[128] This conclusion was reached due to a variety of evidence. There was minimal overlap in proteome wide analysis of p300 associated Khib and Kac sites. Khib sites were uniquely enriched on glycolytic enzymes including enolase 1. We found that enolase 1 activity increases *in vitro* following 2-hydroxyisobutyrylation by p300. Furthermore, enolase 1 had detectable increases in Khib levels following glucose deprivation. Finally, we demonstrated that enolase 1 is modified by Khib at a residue critical for its enzymatic activity. This study demonstrates that identifying additional substrates for KATs can provide key insight into their functions beyond what can be ascribed to Kac alone.

While p300 appears to have tremendous promiscuity in substrate choices, it is unclear to what extent other writers utilize cofactors beyond acetyl-CoA. For example, HAT1 is a KAT with no known cofactors other than acetyl-CoA. Indeed, a recent study measuring competitive binding of other acyl-CoAs for KATs suggested that butyryl-CoA and crotonyl-CoA have low affinity for HAT1.[204] The functional role of HAT1 remains largely unclear despite being the original KAT to be cloned.[134] Given the aforementioned discovery of p300 being able to utilize different acyl-CoAs for different functions, the study of substrates for writers like HAT1 may yield additional clues to their functional activity.

We screened four candidate KATs for the ability to catalyze the addition of Kmea *in vitro*. Of these, HAT1 catalyzed the addition of the Kmea on histone H4 peptide *in vitro*. We generated a H4K5mea specific antibody to test the hypothesis that perturbing HAT1 would affect cellular Kmea. Consistent with this hypothesis, we validated that overexpression, knockdown,

and knockout altered HAT1 in cells altered H4K5mea levels detected by immunoblot. This is the first report of HAT1 using any substrates other acetyl-CoA.

3.2 Results

3.2.1 In vitro acetyltransferase screen and identification of HAT1 as Kmea writer

We hypothesized that previously classified acetyltransferases may be able to catalyze the addition of the methacryl moiety to lysine. We chemically synthesized methacrylyl-CoA. This was then combined with recombinant KAT enzyme and peptide for the *in vitro* assay. The samples was then analyzed by MALDI-TOF MS analysis. We selected four acetyltransferases to identify *in vitro* writers: MOF, GCN5, HAT1, and p300. The synthetic peptide substrate for each experiment corresponded to the first 20 amino acids of either the H3 or H4 peptide.

For the experiments using p300 and GCN5, we used a synthetic peptide substrate that consisted of the first 20 amino acid residues of the H3 histone. As described in the introduction, p300 is a KAT with promiscuous activity for Kpr,[97,196] Kbu,[97,120] Kcr,[106] Khib,[128] Kbhb,[197] and Klac.[91] Surprisingly, p300 did not catalyze the addition of Kmea *in vitro* (**Figure 3.1**). GCN5 (aka. KAT2A) has reported activity for Kpr, Kbu, Ksuc, and Kglu.[118,119,199] However, GCN5 was also unable to catalyze the addition of Kmea *in vitro* (**Figure 3.1**). As expected, both p300 and GCN5 were able to catalyze the addition of Kac to the H3 peptide *in vitro* (**Figure 3.1**). Thus, we conclude that p300 and GCN5 are not writers for Kmea at least under these conditions.

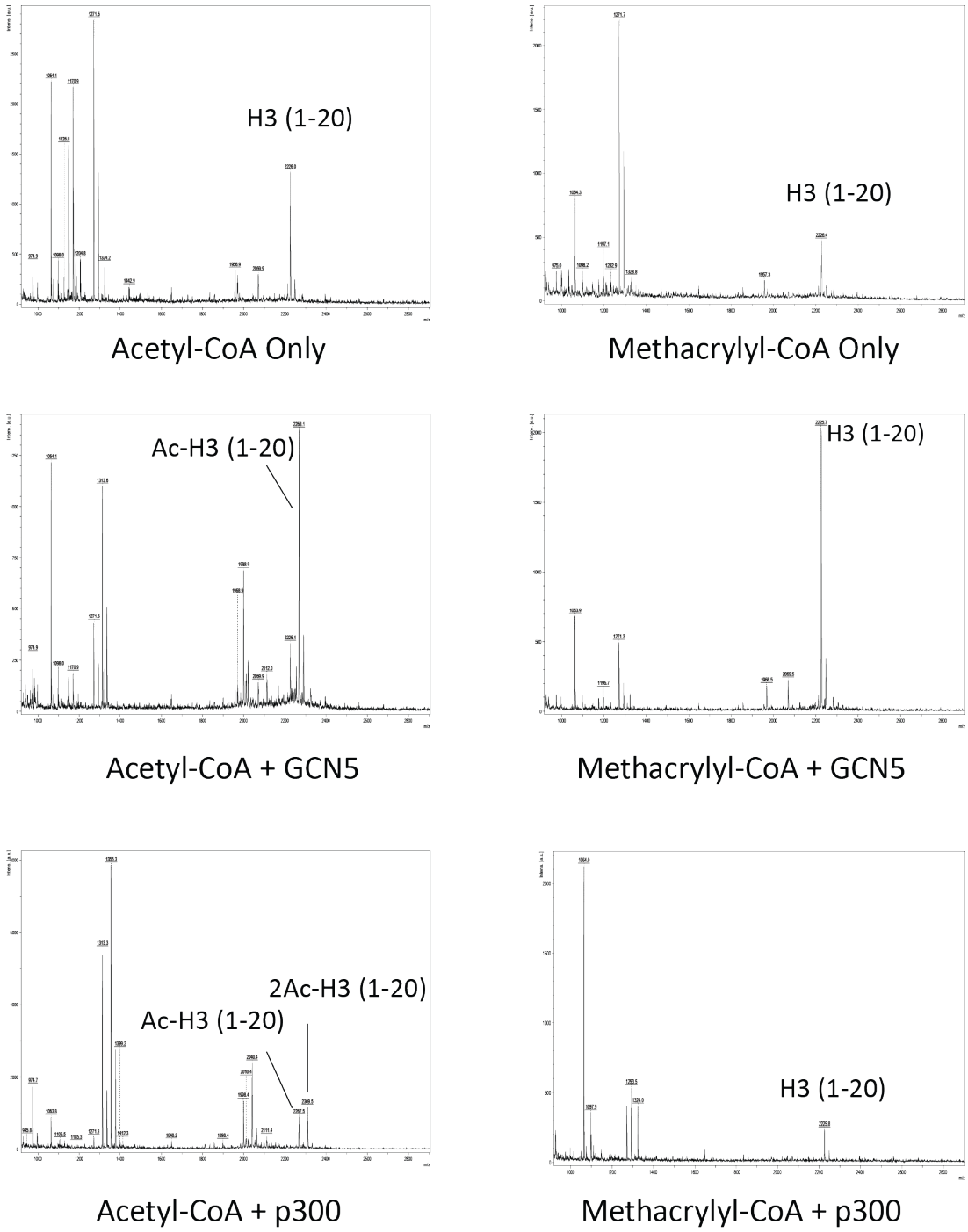

Figure 3. 1 *In vitro* screen of GCN5 and p300 for Kmea writer activity.
Synthetic peptides consisting of the first 20 amino acid residues of the H3 histone were incubated with the indicated acyl-CoA and recombinant enzyme *in vitro*. The samples were subjected to MALDI-TOF analysis to detect modified peptide forms. Experiments using acetyl-CoA were incorporated as positive technical controls. Neither GCN5 nor p300 catalyzed the addition of Kmea in this assay.

For experiments with MOF and HAT1, we used a synthetic peptide substrate consisting of the first 20 amino acids of the H4 histone. MOF (aka KAT8) is a reported writer for Kpr[200] and Kcr.[266] In our assay, MOF had no activity for Kmea even though it successfully catalyzed the addition of Kac (**Figure 3.2**). It should be noted that, while MOF has been ascribed to have crotonyltransferase activity in cells, MOF has not been successfully demonstrated to catalyze Kcr *in vitro*.[106,266] The designation of MOF as a Kcr writer was based upon results using pan and site specific Kcr antibodies for immunofluorescence and immunoblot experiments.[266] The authors speculated that the absence of activity *in vitro* was due the need for protein complex formation for MOF under *in vivo* conditions.[266] As a caveat, other published studies have raised issues for detection of off-targets including Kac for western blots using certain Kcr antibodies.[201,262]. As such, we chose to prioritize enzymes that had *in vitro* enzymatic activity in addition to cellular activity for this study. We did not further pursue MOF activity for Kmea.

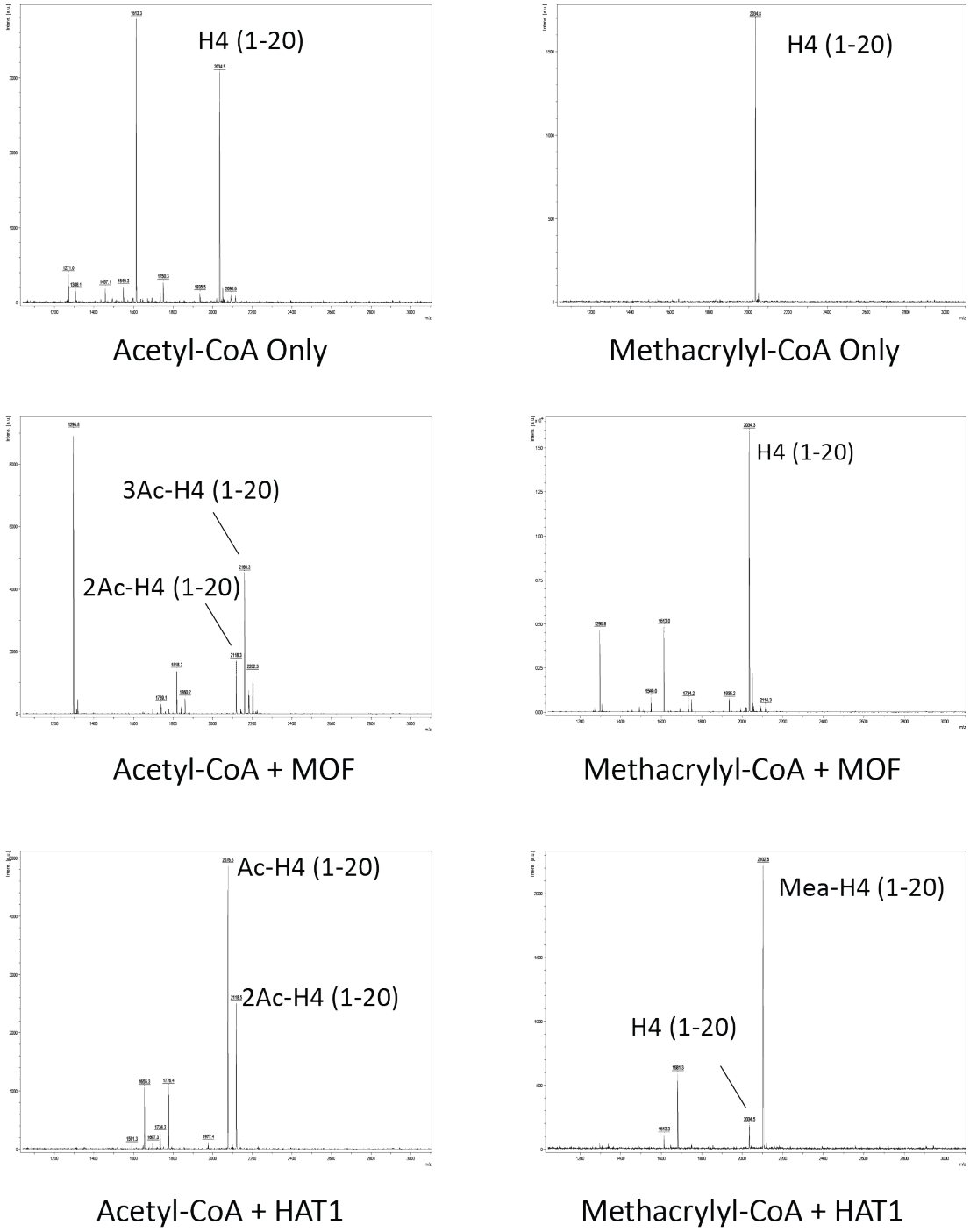

Figure 3. 2 *In vitro* screen of MOF and HAT1 for Kmea writer activity.
Synthetic peptides consisting of the first 20 amino acid residues of the H4 histone were incubated with the indicated acyl-CoA and recombinant enzyme *in vitro*. The samples were subjected to MALDI-TOF analysis to detect modified peptide forms. Experiments using acetyl-CoA were incorporated as positive technical controls. Only HAT1 catalyzed the addition of Kmea to H4 peptides in this assay.

HAT1 is a lysine acetyltransferase with no known cofactors other than acetyl-CoA. Of the tested enzymes, we found that only recombinant HAT1 was able to catalyze the formation of Kmea in the presence of methacrylyl-CoA (**Figure 3.2**). Interestingly, the HAT1 reaction including acetyl-CoA resulted in detection of both mono and diacetylated peptides while reactions with methacrylyl-CoA only yield singly modified peptides (**Figure 3.2**). HAT1 is known to acetylate nascent histones on lysine residues 5 and 12.[150] Thus it is likely that the diacetylated peptides correspond to H4K5K12ac. As we used MALDI-TOF MS to detect peptides, this data does not provide the exact positions modified. For example, the singly modified peaks could be a mixture of singly modified H4K5 and H4K12 peptides. The data does suggest that HAT1 is only capable of modifying a single site with Kmea as opposed to two with Kac. In summary, this *in vitro* data provides the first evidence that the addition of Kmea could be enzymatically catalyzed. It also demonstrates for the first time that HAT1 can use substrates other than acetyl-CoA.

3.2.2 HAT1 is a H4K5mea writer in cells

To test for the effects of HAT1 on Kmea in cells, we developed a site-specific antibody for H4K5mea. This antibody had approximately 20 fold greater specificity for H4K5mea than other acylations tested (**Figure 3.3A**). This assay was performed using synthetic peptides that all contained the same amino acid sequence, but differed with regards to the modification on the center lysine residue. This is important as peptides that differ in sequence composition can yield false negatives for reactivity in this type of assay. To further validate the antibody's ability to detect H4K5mea, we treated HeLa cells for 24 hours with doses of methacrylate or crotonate. We isolated histones through acid extraction and then subjected them to western blot analysis. The H4K5mea antibody responded with increasing signal in a dose dependent fashion to

methacrylate treatment (**Figure 3.3B**). The effect was greatest for the highest methacrylate dosage even when crotonate was used at an equimolar dose. We also observed that H4K5ac increased in a dose dependent manner. This was consistent with the observations for the pan Kac antibody that were detailed in section *2.2.3*. As discussed there, it is entirely possible that some of the observed effects of methacrylate's activity may correspond to its ability to act as an HDAC inhibitor similar to short chain fatty acids like butyrate.

HAT1 exclusively acetylates nascent histone H4 without targeting histones incorporated into chromatin.[150] The HAT1 dependent H4K5ac modifications are rapidly removed following incorporation of nascent histones into chromatin.[169,187] These two factors combined make it imperative to isolate nascent histones when assaying for the effects of HAT1 perturbation. Gruber and colleagues recently published methods for the isolation of nascent and soluble histones using RIPA buffer when studying HAT1.[171] When they used acid extracted histones, they did not detect any effect of HAT1 perturbation on H4K5ac or H4K12ac. Thus, we prepared lysates using RIPA buffer according to their method for all of our experiments involving cellular HAT1 perturbation. We hypothesized that H4K5mea levels on nascent histones would respond to overexpression of HAT1. We transfected HEK 293T for 48 hours with empty vector or flag tagged HAT1 plasmids. Consistent with our hypothesis, both H4K5ac and H4K5mea signals increased following overexpression of HAT1-Flag protein in HEK 293T cells (**Figure 3.3C**).

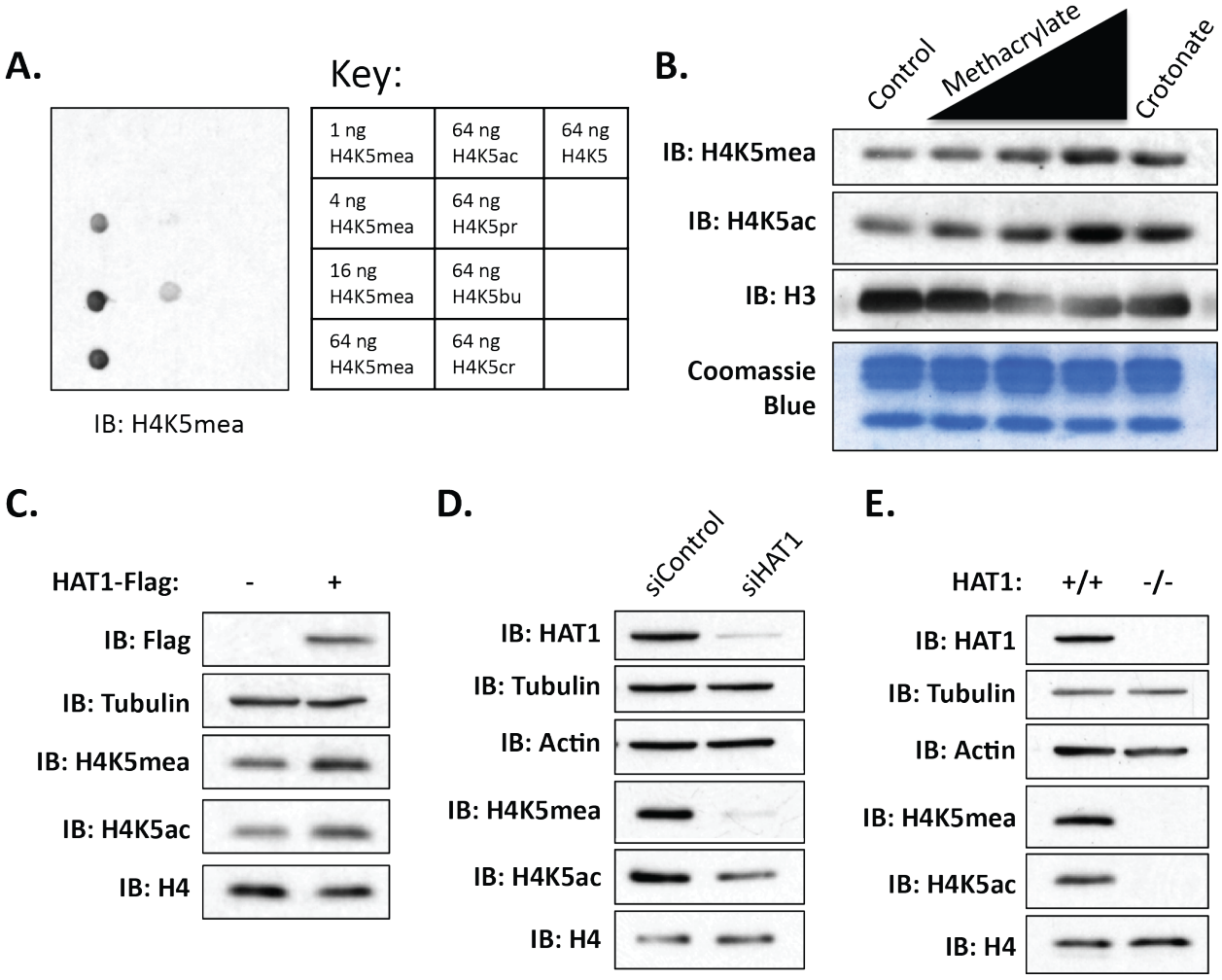

Figure 3. 3 HAT1 regulates H4K5mea in cells.
(a) Dot blot analysis of H4K5mea peptide specificity. Synthetic peptides of the same amino acid sequence that were distinct only by the modification status of the center lysine residue were spotted onto nitrocellulose membrane. The identity and positions of the peptides are indicated in the key. (b) HeLa cells were treated with 0, 1, 3, or 5 mM sodium methacrylate or 5 mM sodium crotonate for 24 hours. Histone were acid extracted and subjected to western blot analysis. (c) HEK 293T were transfected with empty vector or HAT1-Flag plasmid for 48 hours before harvesting. H4K5mea western blot signal increases in HEK 293T cells overexpressing HAT1-Flag relative to empty vector control transfected cells. (d). HEK 293T cells were transfected for 72 hours with 25 nM of control or HAT1 siRNA. H4K5mea signal decreases in HEK 293T cells following knockdown of HAT1 relative to control. (e) H4K5mea signal is lower in MEF HAT1 -/- cells relative to MEF HAT1 +/+ cells.

We treated HEK 293T cells for 72 hours with pooled siRNA that was either specific for HAT1 or non-specific control. Consistent with our hypothesis, knockdown of HAT1 selectively decreased both H4K5ac and H4K5mea signals (**Figure 3.3D**). HAT1 has previously been reported to still maintain near normal levels of H4K12ac following knockdown.[167] In our experiment, we observed dramatic reductions for H4K5ac and H4K5mea. Gruber and colleagues reported that transient knockdown of HAT1 over 72 hours results in decreased H3 and H4 levels in a metabolism dependent manner.[171] We did not observe a decrease in H4 levels. This may be due to the fact that we changed the media every 24 hours post transfection to ensure maintenance of high glucose levels. In any case, the results are consistent with the hypothesis that HAT1 is a writer for H4K5mea in cultured cells.

Mice that are HAT1 knockouts die during late embryogenesis.[169] As such, there are no viable mice lines with whole body HAT1 knockout. However, Parthun and colleagues generated a HAT1 knockout MEF knockout cell line.[169] We hypothesized that H4K5mea levels on nascent and soluble histones would be greatly reduced in HAT1 knockout MEFs relative to controls. Consistent with this hypothesis, both H4K5mea and H4K5ac levels were much lower in MEF HAT1 -/- samples relative to HAT1 +/+ control samples (**Figure 3.3E**). In summary, our results suggest that HAT1 catalyzes the transfer of methacryl moiety to histone H4 *in vitro* and in cultured cells.

3.3 Discussion

In summary, these results demonstrate that HAT1 is a writer for Kmea *in vitro* and in cell culture. Thus, the addition of Kmea can be enzymatically regulated. This is provides an important step for understanding Kmea activity in signaling. For example, our previous work on p300 regulated lysine acylations has found that many of them are correlated with active gene

expression.[91,106,120] The discoveries that these acylations are enzymatically regulated and associated with transcription provides the foundation for their classification as bona fide epigenetic modifications. In contrast, the mechanistic role of Kmea is less clear in part due to the uncertainties surrounding its associated writer, HAT1.

The functional significance of HAT1 has largely remained unclear since its initial discovery. Formerly, the field hypothesized that HAT1 acetylation of histones was critical for H3/H4 import and incorporation into nucleosomes.[164] However, neither histone import nor histone incorporation into replicating chromatin are affected by loss of HAT1 in MEF cells.[169] There is recent evidence that HAT1 regulates cellular metabolism. Mice that are heterozygous for HAT1 expression have defects in their mitochondria and present early aging phenotypes.[163] Another study found that HAT1 phosphorylation by AMPK promoted mitochondrial biogenesis.[162] Indeed, even the HAT1 mediated acetylation of histones has been proposed to act as a nutrient sensor coupling the state of cellular metabolism to signals for cell division.[171] We speculate that HAT1 binding to methacrylyl-CoA may provide additional ways for it to sense and respond to the state of cellular metabolism. Our previous work on p300 suggests that acetyltransferases can use different acyl-CoAs for the regulation of distinct pathways.[128] As such, the discovery of Kmea may provide new insight into deciphering the functions of HAT1.

3.4 Methods

Reagents

We developed the pan-Kmea and H4K5mea antibodies in collaboration with PTM Biolabs (Chicago, IL). We obtained the pan Kac (PTM-101) antibody from PTM Biolabs (Chicago, IL). The anti-Tubulin (ab6160), anti-H4 (ab31830) and anti-H3 antibody (ab12079) were obtained from Abcam (Cambridge, MA). Anti-Flag (F7425) was obtained from Sigma Aldrich (St. Louis,

MO). We obtained anti-H4K5ac antibody (39700) from Active Motif (Carlsbad, CA). The anti-actin antibody (4967S) was from Cell Signaling Technologies (Danvers, MA). Methacrylic acid and crotonic acid were obtained from Sigma-Aldrich (St. Louis, MO). Pooled siRNA for control (D-001810-10-05) and HAT1 (L-011490-00-0005) were obtained from Horizon Discovery (Waterbeach, United Kingdom). GL Biochem (Shanghai, China) synthesized the acylated peptides for this work. Sequencing grade modified trypsin was obtained from Promega (Madison, WI). Chemicals used in buffers were obtained from Sigma-Aldrich (St. Louis, MO) unless otherwise noted.

Cell culture

HeLa and HEK 293T cells were obtained from ATCC and not validated further. MEF HAT1 wild type and knockout cells were a gift from Mark Parthun's lab. Cells were grown in high glucose DMEM (Thermo Fisher Scientific, Waltham, MA) with 10% FBS at 37°C in 5% CO_2.

Methacrylate and crotonate treatment

The salt forms of methacrylic acid and crotonic acid were prepared by raising pH to 7.0-7.3 using NaOH. HeLa cells were treated with 0, 1, 3, or 5 mM of methacrylate or 5 mM of crotonate after cells reached approximately 50% confluency.

Histone extraction

Acid extraction of histones was performed according to modified version of a published protocol [93]. Briefly, cells were harvested in 10 cm plates after reaching approximately 90% confluency. Cells were washed in phosphate buffered saline (PBS) before detaching from plate by cell scraper. Cells were then washed and pelleted in PBS twice at 1,000 x g for 5 min at 4°C. Cell membranes were lysed in extraction buffer (10 mM HEPES pH 7.0, 10 mM KCl, 1.5 mM MgCl2, 0.34 M sucrose, 0.5% NP-40, 5 mM sodium butyrate, 10 mM nicotinamide) for 10

minutes with gentle agitation at 4°C. Nuclei were then pelleted at 2,000 x g at 4°C for 10 min and supernatant was discarded. Cells were resuspended in extraction buffer without NP-40. Cell nuclei were pelleted at 2,000 x g at 4°C for 5 min. Nuclear pellets were then lysed in a nuclear lysis buffer (3 mM EDTA, 0.2 mM EGTA, 5 mM sodium butyrate, 10 mM nicotinamide) for 30 min with gentle agitation at 4°C. Chromatin was pelleted at 6,500 x g for 5 min at 4°C and then resuspended in 0.4 N H_2SO_4. Chromatin suspension in acid was incubated overnight at 4°C with gentle agitation. After centrifuging at 16,000 x g for 10 min, acid soluble supernatant was collected and used in TCA precipitation. Following TCA precipitation, histones were pelleted and washed three times in acetone. Histones were finally resuspended in deionized H_2O.

Plasmid transfection

HEK 293T cells were grown to approximately 80% confluence before transfected 2 μg of plasmid DNA using Lipofectamine 3000 (Thermo Fisher Scientific, Waltham, MA) according to manufacturer instructions. Culture media was replaced with fresh media at 24 hours post-transfection. Cells were harvested by whole cell lysis at 48 hours post-transfection.

RIPA whole cell lysis

For experiments involving HAT1 validation, a lysis approach was used to enrich nascent histones as previously described.[171] Briefly, cells were washed in PBS once before the addition of RIPA buffer (50 mM Tris-HCL, pH 7.4; 150 mM NaCl; 0.1% SDS; 0.5% sodium deoxycholate; 1% Triton X-100) with the additional inhibitors 1 mM PMSF, 10 mM nicotinamide, and 5 mM sodium butyrate. Adherent cells were scraped in lysis buffer using cell scraper. Lysates were briefly vortexed before centrifuging at greater than 16,000 x g for 10 minutes. Supernatants were then transferred to a new tube without disturbing pelleted chromatin. Laemmli buffer was added to samples that were boiled for 5 minutes prior to use in SDS-PAGE.

RNAi transfection

HEK 293T cells were transfected with siRNA using Lipofectamine RNAiMAX (Thermo Fisher Scientific, Waltham, MA) for reverse transfection according to manufacturer instructions. Briefly, we added 62.5 pmol of either siControl (Horizon Discovery, D-001810-10-05) or HAT1 (Horizon Discovery, L-011490-00-0005) to 500 µl Opti-MEM (Thermo Fisher Scientific, Waltham, MA) per well of 6 well plates. Then 10.5 µl of RNAiMAX were added to each well. This mixture was incubated at room temperature for 20 minutes. Then 2 ml of HEK 293T cell suspension in complete media was added to each well. The cells were incubated for 72 hours post-transfection at 37°C in 5% CO_2. We replaced the media at the 24 and 48 hour time points post-transfection with fresh complete media. Cells were then harvested and lysates were prepared using RIPA buffer.

Dot blot

Synthetic peptides were spotted onto nitrocellulose membrane in the amounts indicated in the figures. Membranes were incubated in blocking buffer (3% bovine serum albumin, 20 mM tris-buffered saline pH 7.6, 0.1% Tween-20) for 1 hour at room temperature with gentle agitation. Membranes were incubated in solution of primary antibody diluted in 1% BSA blocking buffer and incubated for 30 minutes at room temperature with gentle agitation. Blots were washed three times in TBST. Then, membranes were incubated in secondary antibody diluted in 1% BSA in TBST for 30 minutes at room temperature with gentle agitation. Blots were washed three times in TBST and then incubated for 1 minute in enhanced chemiluminescence reagent. Film was exposed in dark room to visualize antibody binding.

Western blot

A total of 4 μg histone extract or 20 μg RIPA whole cell lysate was loaded per lane in 15% tris-glycine polyacrylamide gel in Mini-Protean electrophoresis system (Bio-Rad, Hercules, CA). SDS-PAGE was performed using running buffer (25 mM tris, 192 mM glycine, 0.1% SDS). Voltage was set to 80V for the first 30 minutes before increasing to 120V until loading dye reached the bottom of the gel. Tank transfer in mini-trans-blot module (Bio-Rad, Hercules, CA) was performed using transfer buffer (25 mM tris, 192 mM glycine, 0.1% SDS) with 20% methanol for 1 hour and 15 minutes at 100 V constant. We transferred proteins to 0.2 μm PVDF membranes. Membranes were incubated in blocking buffer (3% bovine serum albumin, 20 mM tris-buffered saline pH 7.6, 0.1% Tween-20) for 1 hour at room temperature. Membranes were probed with primary antibody in 1% BSA blocking buffer overnight at 4°C with gentle agitation. Secondary HRP conjugated antibodies were incubated for 1 hour at room temperature. Membranes were washed 3 times for 8 minutes each in TBST (20 mM tris-buffered saline pH 7.6, 0.1% Tween-20) following both primary and secondary antibody incubations. Film was exposed in dark room after incubating for 1 minute in enhanced chemiluminescence reagent with gentle agitation. Film images were scanned into digital files. The entire image contrast for each image was adjusted using the autocontrast tool in Photoshop.

Coomassie blue stain

SDS-PAGE was performed as described in the western blot protocol. Gel was rinsed briefly in deionized H_2O. Gel was then incubated in Protoblue Safe colloidal coomassie blue G-250 stain (National Diagnostics, Atlanta, Georgia) overnight with gentle agitation according to manufacturer instructions. Gels were then periodically washed in deionized H_2O until bands were clearly visible. Gels were scanned into digital images and contrast adjusted in Photoshop.

Synthesis of methacrylyl-CoA

The synthesis of acyl-CoA was performed as previously published.[91] We dissolved methacrylic acid in 5 ml of CH_2Cl_2. Then we added N-hydroxysuccinimide and sonicated the solution until it became clear. Then we added N,N'-dicyclohexylcarboiimide which led to the formation of a white precipitate. The solution was incubated at room temperature overnight with constant stirring. We then evaporated the organic solvent by vacuum to yield crude product methyl-NHS. We dissolved CoA hydrate in 1.5ml of 0.5M $NaHCO_3$ (pH 8.0) and then cooled the solution in an ice bath. Methacryl-NHS in 0.5 ml CH3CN/acetone was then added dropwise to the CoA solution. This solution was then stirred overnight at 4°C which was then quenched by adding 1M HCl to adjust to pH 4.0. We then performed RP-HPLC purification with gradient 5-45% buffer A (0.05% TFA in water) in buffer B (0.05% TFA in acetonitrile) at a flow rate of 5 ml min^{-1} over 30 min. The collected fractions were lyophilized after flash-freeze with liquid nitrogen.

In vitro acetyltransferase assay

In vitro acetyltransferase assays were performed as previously described.[200] We combined 0.5 μM recombinant enzyme, 100 μM acetyl-CoA or methacrylyl-CoA, with 50 μM histone H3 or H4 peptide. Reaction mixtures were incubated at 30°C for 2 hours. Synthetic histone peptides substrates consisted of the first 20 amino acids of the N-terminal tails of histones H3 and H4 with acetylation of the N-terminal peptide amine. The sequences for H3 (1-20) and H4 (1-20) were Ac-ARTKQTARKSTGGKAPRKQL and Ac-SGRGKGGKGLGKGGAKRHRK, respectively. Reactions with GCN5 and p300 as enzymes were paired with synthetic H3 (1-20) peptide as substrate. Similarly, reactions with MOF and HAT1 were paired with synthetic H4 (1-20) as substrate. Samples were analyzed by MALDI-MS to identify if peptide substrates were modified in the reaction.

CHAPTER 4

HDAC3, SIRT1, AND SIRT2 ARE KMEA ERASERS

4.1 Introduction

Enzymes can regulate both the addition and removal of PTMs. The opposing action to the writer discussed in chapter 3 is that of the eraser. While no non-acetyl specific lysine acylation writers have been discovered, there are erasers that are specific for newly discovered acylations. This is the case for SIRT5 that specifically targets negatively charged lysine acylations.[98,99,123] Prior to the discovery of these substrates, it was unclear what the enzymatic function of SIRT5 was. As such, the discovery of new substrates aids in expanding our understanding of the roles of previously classified deacetylases in cellular processes.

Herein we examined the erasers for Kmea. We provide evidence that supports previous literature that HDAC3 is an eraser for Kmea *in vitro.*[110] We also identified for the first time that the class III deacetylases SIRT1 and SIRT2 catalyze the removal of Kmea *in vitro.* Furthermore, overexpression of SIRT2 in cells is associated with decreased H3K18mea signal. Thus, we provide evidence that Kmea is a reversible modification that is regulated through enzymatic removal.

4.2 Results

4.2.1 HDAC3 is an eraser for Kmea in vitro

We and others have shown that many of the previously classified lysine deacetylases are able to enzymatically remove other types of lysine acylations besides lysine acetylation.[267] Crotonyl moieties on lysine residues can be enzymatically removed by HDAC 1-3 and SIRT 1-3.[102,107–109] A recent screen of HDAC 1-11 that included previously discovered and hypothetical lysine acylation substrates revealed that HDAC3 acts an eraser for lysine methacrylation *in*

vitro.[110] Consistent with this report, we observed that *in vitro* incubation of HDAC3 with histone extract reduced the Kmea signal by western blot (**Figure 4.1A**). Similarly, we observed a large increase in Kmea signal in cells treated for 24 hours with the HDAC class I inhibitors butyrate and Trichostatin A (**Figure 4.1B**). Thus, our results are consistent and complimentary to the work published by Moreno-Yruela and colleagues.

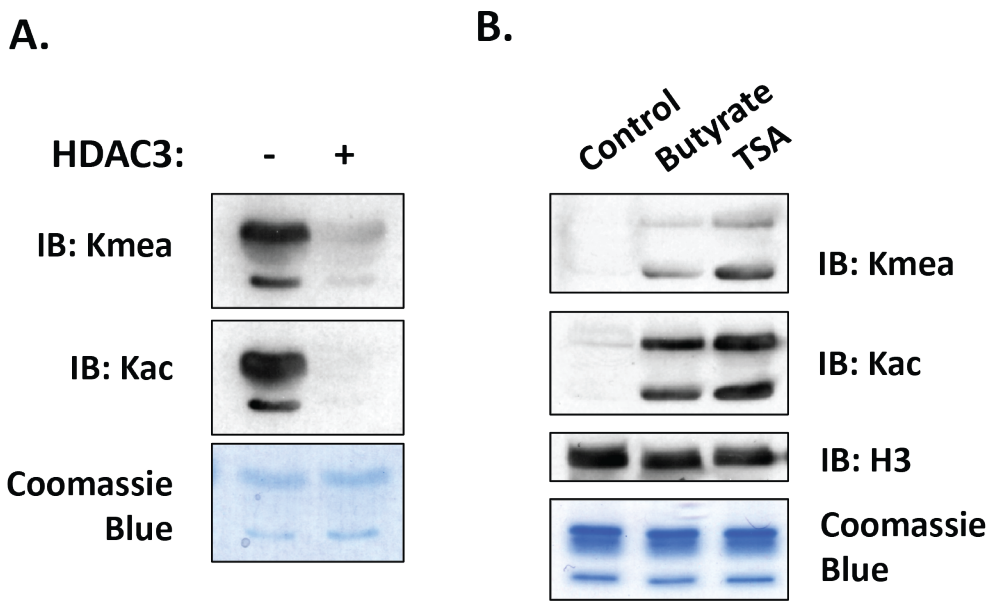

Figure 4. 1 HDAC3 is an eraser for Kmea.
(a) Recombinant HDAC3 was incubated for 12 hours with acid extracted histones. Samples were then analyzed by western blot. (b) HEK 293T cells were treated for 24 hours with 10 mM sodium butyrate or 1 μM TSA. Histones were acid extracted and then subjected to western blot analysis.

4.2.2 In vitro screen reveals SIRT1 and SIRT2 as Kmea erasers

Unlike HDAC 1-11, the sirtuin family of enzymes has not been studied for the removal of methacryllysine. We screened recombinant SIRT 1-7 for the ability to enzymatically remove methacryl moiety from synthetic H3K18mea peptides *in vitro*. We found that SIRT1 and SIRT2 had the strongest methacryllysine eraser activity *in vitro* (**Figure 4.2**). This was in contrast to the H3K18ac control that where removal was efficiently catalyzed by SIRT1-3 (**Figure 4.3**). In general, the deaceylase activity was greater for H3K18ac peptides than H3K18mea peptides. These results suggested that SIRT1 and SIRT2 were the candidate erasers of the sirtuin family.

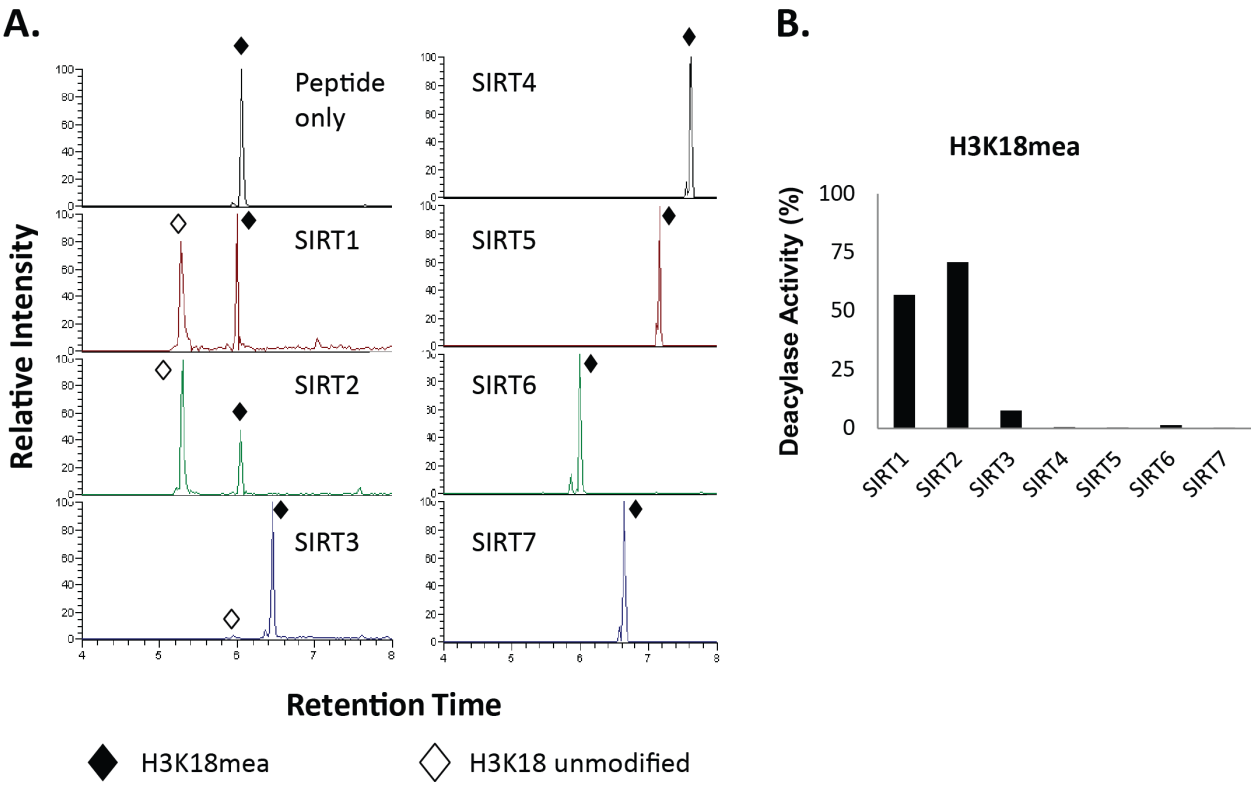

Figure 4. 2 SIRT1 and SIRT2 are Kmea erasers *in vitro*.
(a) Synthetic H3K18mea peptides were incubated with indicated recombinant enzymes and then subjected to LC-MS/MS. Chromatograms of each sample condition is shown. Open diamonds indicate the H3K18 unmodified peptide peaks. Filled diamonds indicate the H3K18mea peptide peaks. (b) Quantitation of *in vitro* screen of SIRT 1-7 against H3K18mea peptide. Deacylase activity percentage is calculated by dividing the area of the H3K18 unmodified chromatogram peak over the sum of the H3K18 unmodified and modified chromatogram peaks.

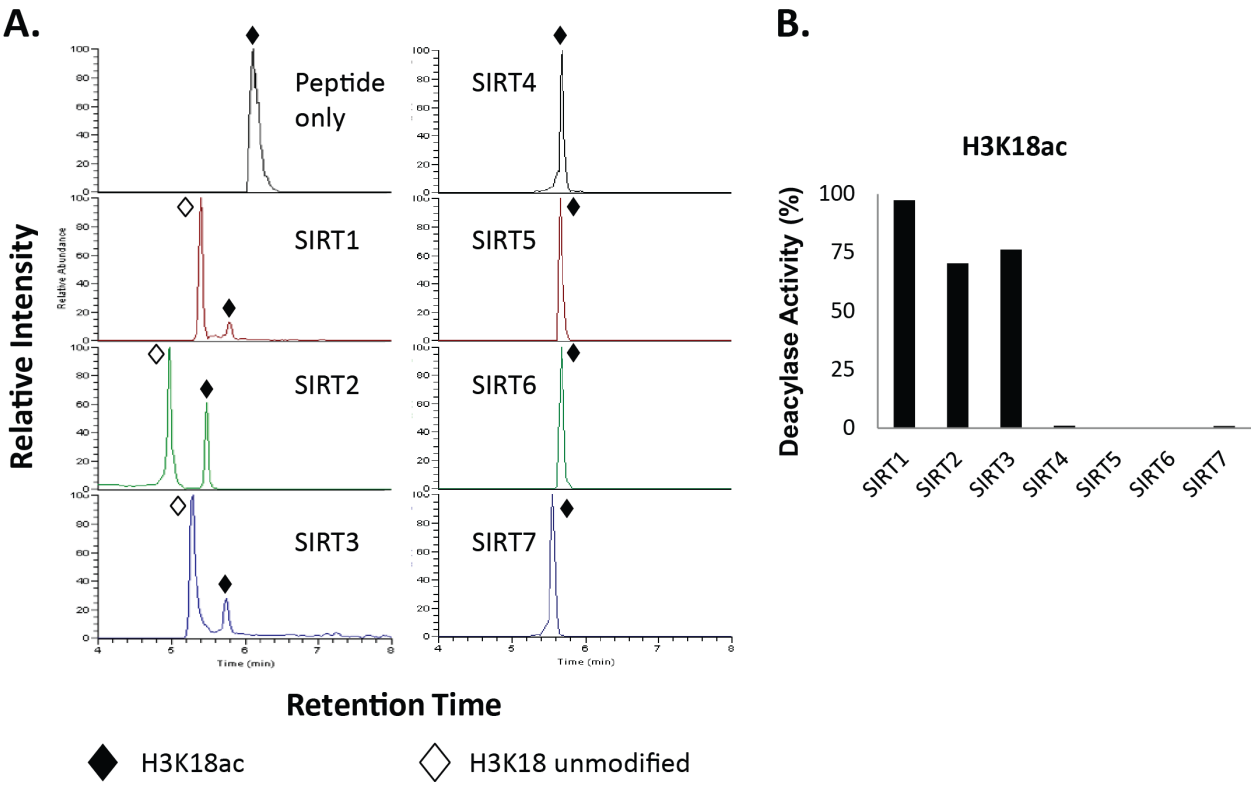

Figure 4. 3 SIRT1-3 catalyze the removal of H3K18ac *in vitro*.
(a) Synthetic H3K18ac peptides were incubated with indicated recombinant enzymes and then subjected to LC-MS/MS. Chromatograms of each sample condition is shown. Open diamonds indicate the H3K18 unmodified peptide peaks. Filled diamonds indicate the H3K18ac peptide peaks. (b) Quantitation of *in vitro* screen of SIRT 1-7 against H3K18ac peptide. Deacylase activity percentage is calculated by dividing the area of the H3K18 unmodified chromatogram peak over the sum of the H3K18 unmodified and modified chromatogram peaks.

We confirmed that the effects of SIRT1 and SIRT2 were due to their enzymatic activity as removal of the essential cofactor NAD+ from the buffer abolished their ability to remove the methacryl moiety from peptide (**Figure 4.4A**). This strongly suggests that SIRT1 and SIRT2 are enzymatically catalyzing the removal of Kmea *in vitro*. As further support for *in vitro* activity, we found that incubation of recombinant SIRT1 and SIRT2 enzymes with histone extract *in vitro* greatly reduced the Kmea western blot signal (**Figure 4.4B**). These experiments confirm that SIRT1 and SIRT2 possess the ability to catalytically remove the methacryl moiety from lysines *in vitro.*

4.2.2 SIRT2 is an eraser for H3K18mea in cells

The sirtuin family of deacylases are reported to work on specific histone marks [205]. One of the SIRT2 substrates is H3K18ac which has been reported to be regulated by the translocation of SIRT2 to the nucleus under certain conditions [268]. We hypothesized that we could simulate these conditions through overexpression of SIRT2-Flag in HEK 293T cells. Consistent with our hypothesis, overexpression of SIRT2-Flag was associated with decreases in the H3K18ac, H3K18cr, and H3K18mea western blot signals relative to the empty vector control (**Figure 4.4C**). In summary, SIRT2 catalyzes the removal of H3K18mea both *in vitro* and in cells.

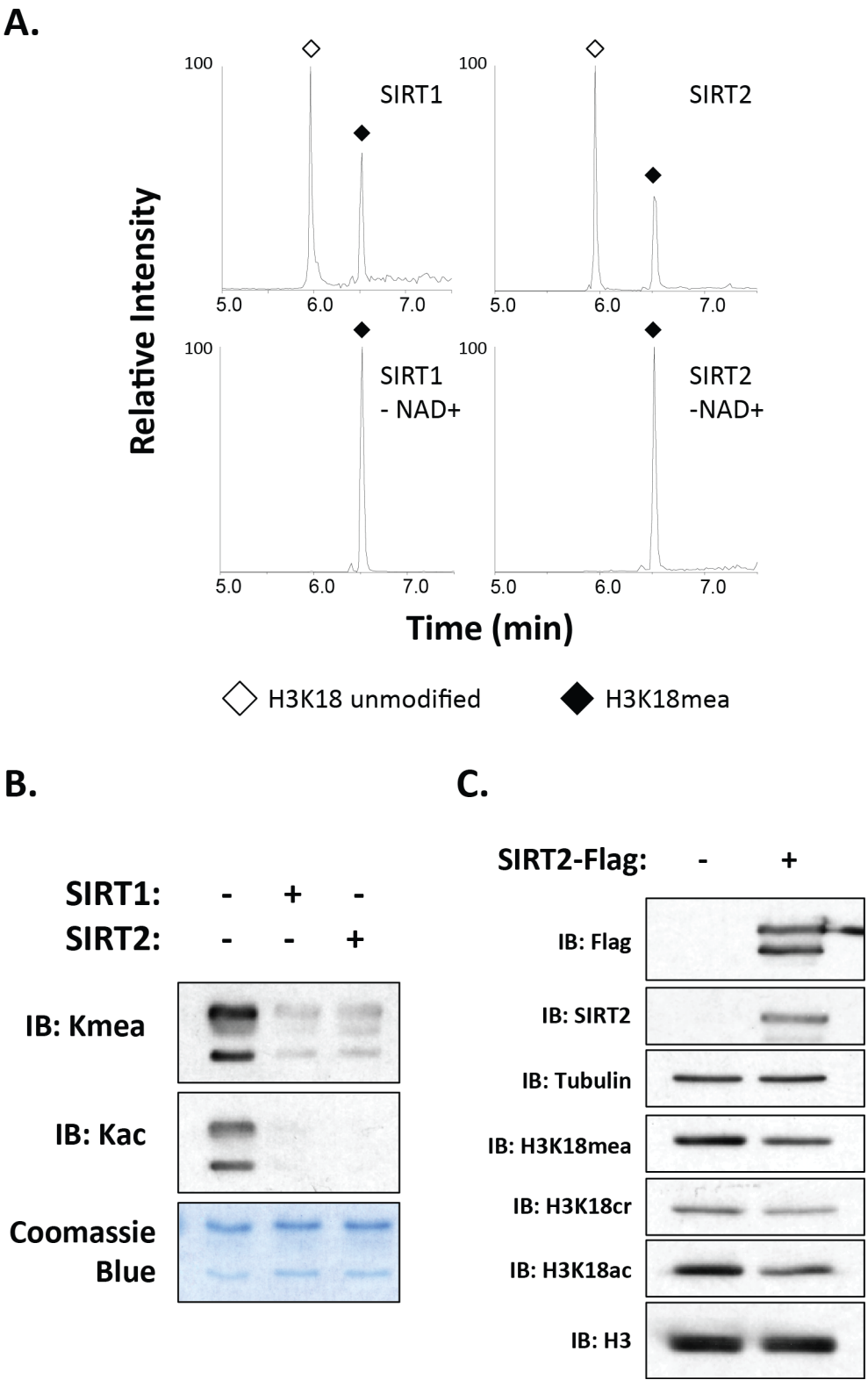

Figure 4. 4 Validation of SIRT1 and SIRT2 as erasers for Kmea.

Figure 4.4 (continued) Validation of SIRT1 and SIRT2 as erasers for Kmea. (a) H3K18mea synthetic peptides were incubated with SIRT1 or SIRT2 in presence of reaction buffer with or without essential cofactor NAD+. Chromatograms of each sample condition are shown. Open diamonds indicate the H3K18 unmodified peptide peaks. Filled diamonds indicate the H3K18mea peptide peaks. (b) Recombinant SIRT1 and SIRT2 were incubated for 12 hours with acid extracted histones. Samples were then analyzed by western blot. (c) HEK 293T cells were transfected with empty vector or SIRT2-Flag plasmids for 48 hours. H3K18mea western blot signal decreased in HEK 293T cells overexpressing SIRT2-Flag relative to empty vector transfected control.

4.3 Discussion

In summary, we have identified that the removal of Kmea is enzymatically regulated and identified erasers that perform this action. This includes the first identification of sirtuins capable of removing Kmea. In addition, our data also supports previous reports that HDAC3 can act as a Kmea eraser *in vitro.*[110] Collectively, these data demonstrate that Kmea is a reversible modification, which provides an important contribution to understanding its potential in cell signaling.

When it comes to histone marks, the sirtuins are reported to regulate specific sites *in vivo*.[267] SIRT1 reportedly targets acetylation on H1K26,[269] H3K9,[269] H3K14,[245] H3K56,[270] and H4K16.[269] Likewise, SIRT2 targets acetylation on H3K18,[268] H3K56,[270] and H4K16.[271] It should be noted that mass spectrometric proteomics analysis by our laboratory and others have found that the major targets for SIRT1 are non-histone proteins.[272,273] Though we have focused on histone substrates in this work, it is possible that SIRT1 and SIRT2 primarily regulate non-histone Kmea substrates. We observed dramatic effects on pan Kmea signal in response to class I HDAC inhibitors (**Figure 4.1B**). Therefore, it is entirely possible that HDAC3 is the predominant eraser for Kmea on histones.

As methacrylyl-CoA is a mitochondrial intermediate in the catabolism of valine, it seems likely that mitochondrial proteins are also modified by Kmea. If so, then it will be of interest to determine which erasers affect mitochondrial substrates of Kmea. Our results suggest that SIRT3, an enzyme predominantly located in mitochondria, has little to no activity for removing Kmea. This is in contrast to the reported activity of SIRT3 for Kcr.[107] Further work is needed to determine the affects of eraser activity on non-histone targets.

4.4 Methods

Reagents

We developed the pan-Kmea and H3K18mea antibodies in collaboration with PTM Biolabs (Chicago, IL). We obtained pan Kac (PTM-101) and H3K18cr (PTM-517) antibodies from PTM Biolabs (Chicago, IL). The H3K18ac (ab1191), anti-Tubulin (ab6160), and anti-H3 antibody (ab12079) were obtained from Abcam (Cambridge, MA). GL Biochem (Shanghai, China) synthesized the H3K18ac and H3K18mea peptides for this work. Chemicals used in buffers were obtained from Sigma-Aldrich (St. Louis, MO) unless otherwise noted.

Cell culture

HEK 293T cells were obtained from ATCC and not validated further. Cells were grown in high glucose DMEM (Thermo Fisher Scientific, Waltham, MA) with 10% FBS at 37°C in 5% CO_2.

Plasmid transfection

HEK 293T cells were grown to approximately 80% confluence before transfected 2 μg of plasmid DNA using Lipofectamine 3000 (Thermo Fisher Scientific, Waltham, MA) according to manufacturer instructions. Culture media was replaced with fresh media at 24 hours post-transfection. Cells were harvested by whole cell lysis at 48 hours post-transfection.

Whole cell lysis

Cells were harvested upon reaching experimental time points and were greater 80% confluent. Cells were washed in PBS once before the addition of lysis buffer (60 mM Tris HCL, pH 6.8; 10% glycerol; 2% SDS; and 5% β-mercaptoethanol) with the additional inhibitors 1 mM PMSF, 10 mM nicotinamide, and 5 mM sodium butyrate. The adherent cell lysate was scraped from dish and transferred to a microcentrifuge tube. The lysate was then briefly vortexed, boiled for 5

minutes, and centrifuged at greater than 16,000 x g for 5 minutes before supernatant was transferred to new tube.

Histone extraction

Acid extraction of histones was performed according to modified version of a published protocol [93]. Briefly, cells were harvested in 10 cm plates after reaching approximately 90% confluency. Cells were washed in phosphate buffered saline (PBS) before detaching from plate by cell scraper. Cells were then washed and pelleted in PBS twice at 1,000 x g for 5 min at 4°C. Cell membranes were lysed in extraction buffer (10 mM HEPES pH 7.0, 10 mM KCl, 1.5 mM MgCl2, 0.34 M sucrose, 0.5% NP-40, 5 mM sodium butyrate, 10 mM nicotinamide) for 10 minutes with gentle agitation at 4°C. Nuclei were then pelleted at 2,000 x g at 4°C for 10 min and supernatant was discarded. Cells were resuspended in extraction buffer without NP-40, cell nuclei were pelleted at 2,000 x g at 4°C for 5 min. Nuclear pellets were then lysed in a nuclear lysis buffer (3 mM EDTA, 0.2 mM EGTA, 5 mM sodium butyrate, 10 mM nicotinamide) for 30 min with gentle agitation at 4°C. Chromatin was pelleted at 6,500 x g for 5 min at 4°C and then resuspended in 0.4 N H_2SO_4. Chromatin suspension in acid was incubated overnight at 4°C with gentle agitation. After centrifuging at 16,000 x g for 10 min, acid soluble supernatant was collected and used in TCA precipitation. Following TCA precipitation, histones were pelleted and washed three times in acetone. Histones were finally resuspended in deionized water.

Western blot

A total of 4 μg histone extract or 20 μg whole cell lysate was loaded per lane in 15% tris-glycine polyacrylamide gel in Mini-Protean electrophoresis system (Bio-Rad, Hercules, CA). SDS-PAGE was performed using running buffer (25 mM tris, 192 mM glycine, 0.1% SDS). Voltage was set to 80V for the first 30 minutes before increasing to 120V until loading dye reached the

bottom of the gel. Tank transfer in mini-trans-blot module (Bio-Rad, Hercules, CA) was performed using transfer buffer (25 mM tris, 192 mM glycine, 0.1% SDS) with 20% methanol for 1 hour and 15 minutes at 100 V constant. We transferred proteins to 0.2 μm PVDF membranes. Membranes were incubated in blocking buffer (3% bovine serum albumin, 20 mM tris-buffered saline pH 7.6, 0.1% Tween-20) for 1 hour at room temperature. Membranes were probed with primary antibody in 1% BSA blocking buffer overnight at 4°C with gentle agitation. Secondary HRP conjugated antibodies were incubated for 1 hour at room temperature. Membranes were washed 3 times for 8 minutes each in TBST (20 mM tris-buffered saline pH 7.6, 0.1% Tween-20) following both primary and secondary antibody incubations. Film was exposed in dark room after incubating for 1 minute in enhanced chemiluminescence reagent with gentle agitation. Film images were scanned into digital files. The entire image contrast for each image was adjusted using the autocontrast tool in Photoshop.

Coomassie blue stain

SDS-PAGE was performed as described in the western blot protocol. Gel was rinsed briefly in deionized H_2O. Gel was then incubated in Protoblue Safe colloidal coomassie blue G-250 stain (National Diagnostics, Atlanta, Georgia) overnight with gentle agitation according to manufacturer instructions. Gels were then periodically washed in deionized H_2O until bands were clearly visible. Gels were scanned into digital images and contrast adjusted in Photoshop.

In vitro recombinant sirtuin screen

Recombinant sirtuin proteins were obtained from BPS Biosciences (San Diego, CA). *In vitro* sirtuin reactions performed by combining 0.5 μM synthetic peptide with 0.25 μM sirtuin in 20 mM Tris-HCL, pH 8 with 1 mM NAD+ and 1 mM DTT in total volume of 50 μl. The peptide sequence for H3K18ac and H3K18mea were GGKAPRK(acetyl)QLATKA and

GGKAPRK(methacryl)QLATKA, respectively. Mixtures incubated at 37°C for 1 hour. Adding 50 µl of 200 mM HCl and 320 mM acetic acid in HPLC grade methanol quenched the reaction. Samples were dried using SpeedVac. Samples were desalted by ZipTip before being subject to LC-MS/MS. Percent deacylase activity was measured by dividing the area of the unmodified peptide chromatographic peak over the sum of the area of the unmodified and modified chromatographic peaks.

In vitro HDAC histone extract assay

Recombinant HDAC3, SIRT1, and SIRT2 were all obtained from BPS Biosciences. The reaction buffer for the sirtuins was 20 mM Tris-HCL, pH 8 with 1 mM NAD+ and 1 mM DTT. HDAC3 reaction buffer consisted of 25 mM Tris pH 8, 130 mM NaCl, 3.0 mM KCl, 1 mM $MgCl_2$, and 0.1% PEG8000, pH 8.0. We treated HeLa cells with 20 mM sodium methacrylate for 24 hours prior to performing histone extraction. Recombinant enzyme was mixed with histone extract at a ratio of 0.2 µg enzyme per 2 µg of histone extract in the appropriate buffer. Mixtures incubated at 37°C for 12 hours. Adding laemmli buffer followed by boiling of samples ended the reaction. The samples were then analyzed by western blotting.

CHAPTER 5

DISCUSSION AND FUTURE DIRECTIONS

In summary, we have discovered the new modification Kmea as wells as enzymes capable of regulating it. We validated the existence of the modification by multiple complimentary methods including MS/MS fragmentation, HPLC co-elution, ozonolysis, isotopic labeling, and antibody-based detection. We demonstrated that methacrylate increases Kmea signals by western blot and demonstrated its direct incorporation in the modification by isotopic labeling. We found a total of 25 Kmea sites across the core histone proteins in HeLa cells through a combination of IP-MS/MS and synthetic peptide validation approaches. We identified HAT1 as a writer for Kmea through a combination of *in vitro* and cell based experiments. This is particularly notable as methacrylyl-CoA is the first known metabolic cofactor for HAT1 outside of acetyl-CoA. In addition, we identified erasers for Kmea that include HDAC3, SIRT1, and SIRT2. Taken all together, this work lays the foundation Kmea as a new type of reversible histone mark. This work also raises a number of questions for future analysis.

The functional significance of Kmea in physiological processes will be an area for future study. For other lysine acylations that our laboratory has discovered, enzymatic writers can provide clues for functional relevance. For example, p300 is a known transcriptional activator and the newly discovered lysine acylations that it utilizes can also activate transcription *in vitro*.[91,106,120,128] In this work, we discovered that HAT1 is a writer for Kmea. Due to the enigmatic nature of HAT1's activity, the function of HAT1 catalyzed Kmea is not immediately clear. Given that methacrylyl-CoA and acetyl-CoA are distinct metabolites, we speculate that the utilization of these substrates by HAT1 could provide a mechanism for sensing and responding to changes in metabolism. There are a number of recent publications that support the notion that

HAT1 serves as a metabolic sensor. AMPK phosphorylates HAT1 to promote mitochondrial biogenesis.[162] Mice that are heterozygous for HAT1 have defects in mitochondria and exhibit early aging phenotypes.[163] HAT1 acetylation of nascent histone H4 has been proposed to serve as a mechanism sense cytoplasmic acetyl-CoA and shuttle acetate into the nucleus to support cell division.[171] Therefore, we speculate that HAT1 may similarly be able to respond to levels of methacrylyl-CoA in ways that affect metabolism. Our previous work suggests that p300 uses different acyl-CoAs to regulate distinct pathways.[128] Future experiments are needed to determine if HAT1 regulates different pathways through Kmea and Kac as well.

Kcr has become established in the literature as a bona fide epigenetic histone mark. This is in part due to the identification of Kcr writers, erasers, and readers.[89] Furthermore, Kcr is associated with transcriptional activation.[102,106] Given the significance of Kcr, it will be important for the field to properly parse the roles of Kcr and Kmea. Our experiments highlight some of the potential technical caveats for previously relied upon methods. For example, the existence of Kmea creates issues for the validity of chemical probes that were proposed to uniquely react with Kcr.[262] Similarly, mass spectrometric methods that rely on a combination of retention time and MS/MS to detect Kcr may require further optimization to demonstrate that the detected signals do not include co-eluting Kmea peptides. In this work, we have attempted to circumvent these pitfalls primarily through the use of antibodies with greater than 20 fold specificity to separately detect Kcr and Kmea signals. It is imperative that the field considers the technical issues associated with separating Kcr and Kmea signals for research moving forward.

Crotonyl-CoA and methacrylyl-CoA are the products of distinct metabolic pathways in mitochondria (**Figure 5.1**). As such there is reason to think that their roles in cellular biology may be differentially regulated. How methacrylyl-CoA accumulates in the nucleus is another

subject that requires further study. The evidence from other acylations suggests that the acyl-CoA species used for histone modifications are produced within the nucleus. The major source of acetyl-CoA for histones is derived from the metabolism of citrate by nuclear ACLY.[43] Similarly, nuclear α-KGDH complexes provide succinyl-CoA for histone lysine succinylation.[118] We previously reported that ACSS2 was able to produce nuclear crotonyl-CoA for histone crotonylation.[106] In addition, the nuclear pools of crotonyl-CoA can be further metabolized into β-hydroxybutyryl-CoA by CDYL.[274] Whether similar enzymes regulate nuclear methacrylyl-CoA pools is still to be determined (**Figure 5.1**).

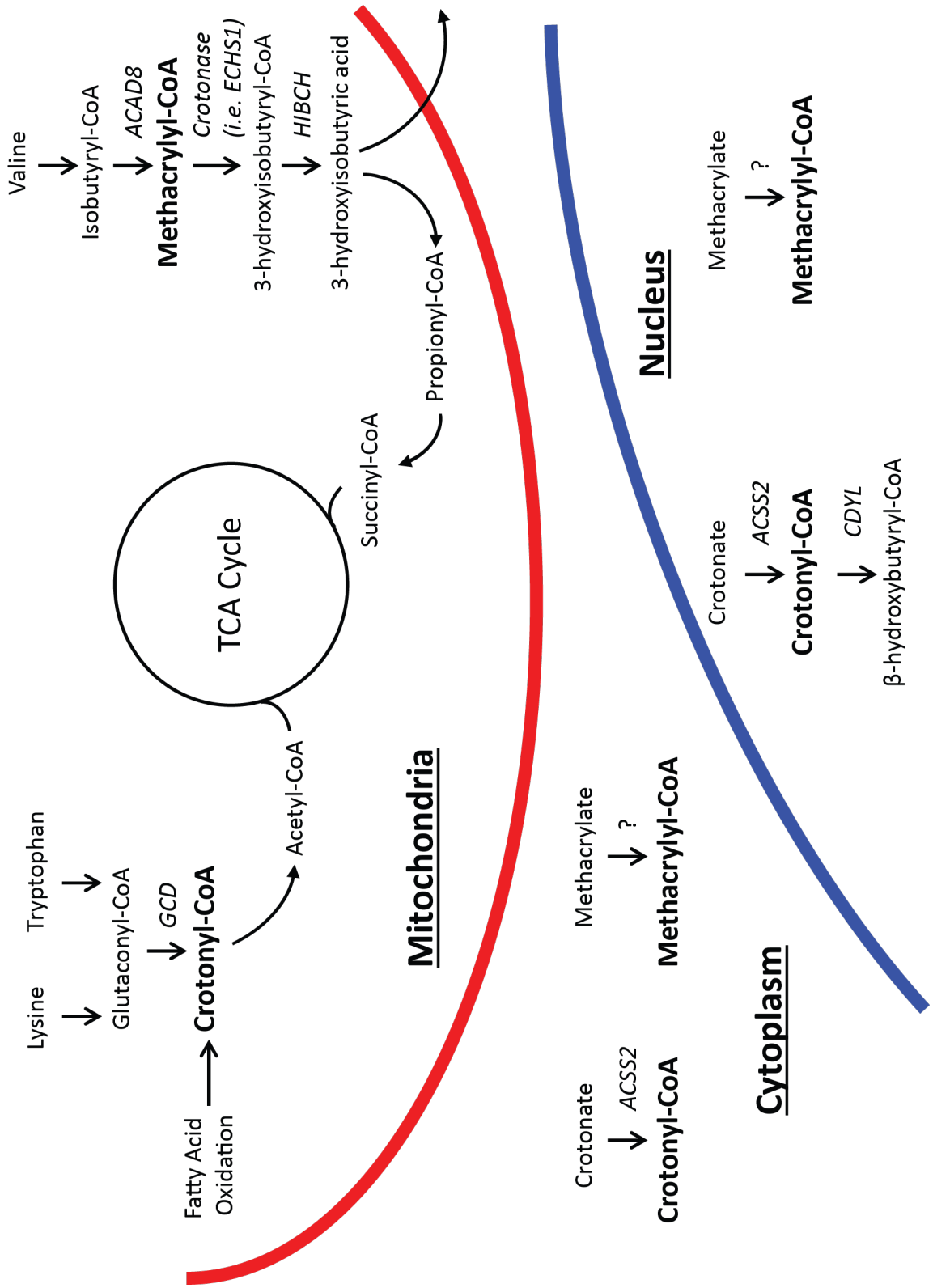

Figure 5. 1 Metabolic pathways for methacrylyl-CoA and crotonyl-CoA.

Figure 5.1 (continued) Metabolic pathways for methacrylyl-CoA and crotonyl-CoA. Diagram of known and speculative pathways for the metabolism of methacrylyl-CoA and crotonyl-CoA separated by compartment. For simplicity, portions of the pathways are condensed that involve multiple steps. Reaction arrows that indicate multiple steps are unaccompanied by enzyme name. The relevant enzyme or enzyme complex are abbreviated next to the reaction arrow for single step portions of the pathway. The abbreviations represent the following enzymes or enzyme complexes: *ACAD8*, acyl-CoA dehydrogenase family member 8 (aka isobutyryl-CoA dehydrogenase); *ACSS2,* acyl-CoA sythetase short-chain family member 2; *CDYL,* chromodomain Y like; *crotonase* (aka enoyl-CoA hydratase), multiple members of the crotonase family have been implicated in this interaction including ECHS1; *ECHS1*, enoyl-CoA hydratase short chain 1; *GCD,* glutaconyl-CoA decarboxylase complex; *HIBCH*, 3-hydroxyisobutyryl-CoA hydrolase. Question marks denote speculative single step reactions where the enzyme is unidentified. The mitochondrial export of 3-hydroxyisobutyric acid is indicated by a single arrow in the figure.

Another consideration for determining functional relevance is whether the abundance of a given modification exceeds a level to impose a physiological function. There is currently limited data available on the abundances of newly discovered lysine acylations. We did not measure Kmea abundance in this work. Given the aforementioned technical caveats for separating Kcr and Kmea, it is possible that some of the measured Kcr abundances include measurements of Kmea levels. With regards to Kcr, certain sites like H3K9cr, H3K122cr, H4K59cr, and H4K91cr have been reported within one log of Kac levels at those sites for certain models.[55,275] Other sites like H3K18cr and H4K5cr have either been unreported or below the limit of quantitation despite measurements being available for Kac at the same positions.[55,275] Current technology for quantitation of abundance at specific sites has the technical caveat that it is a measure of relative rather than absolute abundance. Baldensperger and colleagues recently reported quantitative measurements of acyllysine amino acids following extensive proteolytic digestion of proteins extracted from different mouse tissues.[105] Their measurements suggest that Kcr levels are approximately 3 logs below that of Kac in mouse liver, kidney, heart, and brain.[105] Crotonyl-CoA levels have been measured to be approximately 2 to 3 logs below acetyl-CoA levels in different samples.[55] Further work is needed to determine how Kmea and methacrylyl-CoA levels compare to these measurements.

Many of the newly discovered lysine acylations have been found to be associated with active gene transcription through ChIP-Seq analysis.[91,102,103,106,117–119] It is possible that Kmea serves a similar function in transcription and should be the subject of further study. ChIP-Seq is highly dependent upon the use of specific antibodies in order to obtain biologically meaningful results. Previous surveys of commercially available ChIP-grade antibodies have found widespread issues with specificity.[276–282] Antibodies against lysine acylations have also been

reported to detect off target modifications in immunoblot and western assays.[55,201,262,283] While synthetic peptides arrays have been the gold standard for determining specificity, a recent publication by Alex Ruthenburg and colleagues suggests that peptide array results only weakly correlate with specificity in ChIP assays.[281] The authors went on to demonstrate that ChIP-Seq data from previous publications using insufficiently specific H3K4me3 antibodies was confounded by off target detection of H3Kme2 modification.[281] H3Kme2 is approximately 1 log more abundant than the structurally similar H3Kme3.[284] It is unclear to what extent off target Kac binding may affect ChIP-Seq results for structurally similar lysine acylations that are 2 to 3 logs lower in abundance. Interestingly, Bos and Muir reported that covalent binding of TCEP to Kcr can selectively block antibody binding.[262] They proposed that this could provide a method to test for off target detection of Kcr antibody signals. As both Kcr and Kmea have reactive α,β-unsaturated carbonyl groups, antibodies against these modifications may be uniquely positioned to interrogate issues regarding specificity in biological samples with varying PTM abundances.

While our work was focused on histones, the existence of methacrylyl-CoA in the mitochondria suggest that there are likely to be mitochondrial Kmea substrates. The pH of the inner mitochondrial matrix is particularly suitable for non-enzymatic reaction of acyl-CoAs with lysines.[39] Hirschey and colleagues hypothesize that the accumulation of lysine acylations creates a form of carbon stress that interferes with biological processes.[285,286] In support of this hypothesis, proximal cysteine and lysine pairs are less conserved in species with longer lifespans suggesting evolutionary selection to prevent detrimental acylations.[287] The concept of reactive acyllysine accumulation has been tested in multiple models with varying results. Acyl modifications have been discovered on lysines critical for enzymatic function.[54,99,116,128] This has been confirmed through point mutations of the acylated lysine residues. A potential caveat to this

is that the point mutants mimic effects of a fully modified state in cases where the levels of the modification are unknown. The effects in certain models have been less pronounced or situational. Fisher-Wellman and colleagues measured the effects of deletion of malonyl decarboxylase, SIRT5, or SIRT3 on a variety of metabolic phenotypes.[288] They found that the only consistent effect was a marginal reduction in ATP synthetase activity across the tested conditions. Despite causing major changes in the acetylproteome, the effects of SIRT3 knockout in mice were limited to a modest decrease in insulin secretion and only for mice fed high-sucrose and high-fat diets.[289] The localization and effects of Kmea mitochondrial substrates will be a subject of future study.

The potential for Kmea to modify mitochondrial proteins may be especially relevant for leigh syndrome, a neurological disorder characterized by mitochondrial defects.[59] Inherited mutations in the ECHS1 and HIBCH enzymes of the valine catabolic pathway lead to the development of Leigh syndrome.[60,61,63] Methacrylyl-CoA accumulates in patients with these mutations and has been hypothesized to act as a causal factor in the disease through its electrophilic capacity to alkylate cysteines.[60] The discovery of Kmea raises a potential alternative mechanism for pathological effects of methacrylyl-CoA accumulation. In other in-born-errors of metabolism, elevated levels of acyl-CoAs correlate with higher levels of lysine acylations.[290] An overabundance of certain lysine acylations is reported to have negative effects on ATP synthase activity, albeit to a relatively small amount.[288] We speculate that Kmea accumulation on mitochondrial proteins could be associated with impaired mitochondrial function. However, it may be informative that isobutyryl-CoA accumulation resulting from ACAD8 mutation leads to a different metabolic disorder, namely isobutyryl-CoA dehydrogenase deficiency.[291] Assuming that isobutyryl-CoA would also be capable of forming non-enzymatic lysine acylations, the

pathological significance may be more complicated than simply accumulation of lysine acylations in the presence of incomplete valine metabolism. Future work should examine the modifications incurred through methacrylyl-CoA both at lysine and cysteine residues with regards to leigh syndrome.

While they are often useful, cell culture models have caveats for the study of BCAA catabolism. Cell culture media was not designed to be representative of physiological conditions and its composition can lead to metabolic phenomena in culture that are unrepresentative to *in vivo* conditions.[292] Culturing cardiomyocytes in the high glucose conditions commonly found in cell culture suppresses BCAA catabolism.[293] Furthermore, downregulation of BCAA catabolic enzymes promotes proliferation of culture cell lines in part through activation of mTORC1.[78] A similar mechanism of mTOR activation through degradation of ECHS1 has also been reported.[294] Better culture models may therefore be reliant on post mitotic differentiation systems. Preadipocyte NIH 3T3-L1 cells significantly upregulate BCAA catabolism following differentiation into adipocytes.[295] Similarly, C2C12 cells that have been differentiated to myotubes and overexpress PGC-1α secrete notable amounts of 3-hydroxyisobutyrate consistent with upregulated valine catabolism.[88] Thus careful selection of culture models are necessary for the study of BCAA catabolic conditions that will be informative of *in vivo* conditions. As such, the study of Kmea associated with BCAA perturbation will require careful selection and optimization cell culture systems.

There are currently no genetic mouse model knockouts for either HIBCH or ECHS1. The effects of deletion of these enzymes have been studied in other model organisms, albeit without yielding phenotypes that resemble leigh syndrome in humans. In drosophila melanogaster, deletion of HIBCH was associated with delayed degeneration of axons and synapses following

injury.[296] Knockdown of a crotonase (HADHA) and HIBCH also exacerbated the degenerative phenotype observed in CLN mutant expressing drosophila.[297] In caenorhabditis elegans, the accumulation of acrylyl-CoA through deletion of ech-6 (enoyl-CoA hydratase) and hach-1 (3-hydroxyisobutyryl-CoA hydrolase) reduced growth and viability relative to wild type controls.[298] Thus while none of these models are representative of leigh syndrome, they do provide *in vivo* evidence that the accumulation of acryl-CoA compounds can have neurodegenerative and lethal effects depending on the organism. These models may be informative for understanding the effects of Kmea and should be considered for future work.

The discovery of Kmea provides further evidence that a multitude of reactive metabolites are capable of serving as sources for histone PTMs. The work described herein has the potential to broaden our understanding of the mechanisms at play in the regulation of cellular processes. In order for the field to understand the effects of PTMs on pathophysiological processes, it is necessary to identify all of the relevant PTMs. This author hopes that the discovery of Kmea will prove to be useful in decoding such processes in future work.

REFERENCES:

1. Piovesan A, Antonaros F, Vitale L, Strippoli P, Pelleri MC, Caracausi M. Human protein-coding genes and gene feature statistics in 2019. *BMC Res Notes*. 2019. doi:10.1186/s13104-019-4343-8

2. Walsh CT, Garneau-Tsodikova S, Gatto GJ. Protein posttranslational modifications: The chemistry of proteome diversifications. *Angew Chemie - Int Ed*. 2005. doi:10.1002/anie.200501023

3. Bateman A, Martin MJ, O'Donovan C, et al. UniProt: The universal protein knowledgebase. *Nucleic Acids Res*. 2017. doi:10.1093/nar/gkw1099

4. Aebersold R, Agar JN, Amster IJ, et al. How many human proteoforms are there? *Nat Chem Biol*. 2018. doi:10.1038/nchembio.2576

5. Hanahan D, Weinberg RA. Hallmarks of cancer: the next generation. *Cell*. 2011;144(5):646-674. doi:10.1016/j.cell.2011.02.013

6. Garraway LA, Lander ES. Lessons from the cancer genome. *Cell*. 2013. doi:10.1016/j.cell.2013.03.002

7. Jones PA, Issa JPJ, Baylin S. Targeting the cancer epigenome for therapy. *Nat Rev Genet*. 2016. doi:10.1038/nrg.2016.93

8. Dawson MA, Kouzarides T. Cancer epigenetics: from mechanism to therapy. *Cell*. 2012;150(1):12-27. doi:10.1016/j.cell.2012.06.013

9. Mullard A. FDA approves an inhibitor of a novel "epigenetic writer." *Nat Rev Drug Discov*. 2020. doi:10.1038/d41573-020-00024-0

10. Nacev BA, Feng L, Bagert JD, et al. The expanding landscape of 'oncohistone' mutations in human cancers. *Nature*. 2019. doi:10.1038/s41586-019-1038-1

11. Bloch K, Borek E. Biological acetylation of natural amino acids. *J Biol Chem*. 1946.

12. Phillips DMP. The presence of acetyl groups in histones. *Biochem J*. 1963;87(2):258-263. doi:10.1042/bj0870258

13. Allfrey VG, Faulkner R, Mirsky AE. Acetylation and methylation of histones and their possible role in the regulation of RNA synthesis. *Proc Natl Acad Sci*. 1964;51(5):786-794. doi:10.1073/pnas.51.5.786

14. Hebbes TR, Thorne AW, Crane-Robinson C. A direct link between core histone acetylation and transcriptionally active chromatin. *EMBO J*. 1988. doi:10.1002/j.1460-2075.1988.tb02956.x

15. Johnson LM, Kayne PS, Kahn ES, Grunstein M. Genetic evidence for an interaction

between SIR3 and histone H4 in the repression of the silent mating loci in Saccharomyces cerevisiae. *Proc Natl Acad Sci U S A*. 1990. doi:10.1073/pnas.87.16.6286

16. Megee PC, Morgan BA, Mittman BA, Smith MM. Genetic analysis of histone H4: Essential role of lysines subject to reversible acetylation. *Science (80-)*. 1990. doi:10.1126/science.2106160

17. Park EC, Szostak JW. Point mutations in the yeast histone H4 gene prevent silencing of the silent mating type locus HML. *Mol Cell Biol*. 1990. doi:10.1128/mcb.10.9.4932

18. Aparicio OM, Billington BL, Gottschling DE. Modifiers of position effect are shared between telomeric and silent mating-type loci in S. cerevisiae. *Cell*. 1991. doi:10.1016/0092-8674(91)90049-5

19. Brownell JE, Zhou J, Ranalli T, et al. Tetrahymena histone acetyltransferase A: A homolog to yeast Gcn5p linking histone acetylation to gene activation. *Cell*. 1996;84:843-851. doi:10.1016/S0092-8674(00)81063-6

20. Taunton J, Hassig CA, Schreiber SL. A mammalian histone deacetylase related to the yeast transcriptional regulator Rpd3p. *Science (80-)*. 1996. doi:10.1126/science.272.5260.408

21. Verdin E, Ott M. 50 years of protein acetylation: from gene regulation to epigenetics, metabolism and beyond. *Nat Rev Mol Cell Biol*. 2014;16(4):258-264. doi:10.1038/nrm3931

22. Jenuwein T, Allis CD. Translating the histone code. *Science*. 2001;293(5532):1074-1080. doi:10.1126/science.1063127

23. Dhalluin C, Carlson JE, Zeng L, He C, Aggarwal AK, Zhou MM. Structure and ligand of a histone acetyltransferase bromodomain. *Nature*. 1999. doi:10.1038/20974

24. Barski A, Cuddapah S, Cui K, et al. High-Resolution Profiling of Histone Methylations in the Human Genome. *Cell*. 2007;129(4):823-837. doi:10.1016/j.cell.2007.05.009

25. Robertson G, Hirst M, Bainbridge M, et al. Genome-wide profiles of STAT1 DNA association using chromatin immunoprecipitation and massively parallel sequencing. *Nat Methods*. 2007. doi:10.1038/nmeth1068

26. Mikkelsen TS, Ku M, Jaffe DB, et al. Genome-wide maps of chromatin state in pluripotent and lineage-committed cells. *Nature*. 2007. doi:10.1038/nature06008

27. Johnson DS, Mortazavi A, Myers RM, Wold B. Genome-wide mapping of in vivo protein-DNA interactions. *Science (80-)*. 2007. doi:10.1126/science.1141319

28. L'Hernault SW, Rosenbaum JL. Chlamydomonas α-tubulin is posttranslationally modified in the flagella during flagellar assembly. *J Cell Biol*. 1983. doi:10.1083/jcb.97.1.258

29. Tang Y, Zhao W, Chen Y, Zhao Y, Gu W. Acetylation Is Indispensable for p53 Activation. *Cell*. 2008. doi:10.1016/j.cell.2008.03.025

30. Gu W, Roeder RG. Activation of p53 sequence-specific DNA binding by acetylation of the p53 C-terminal domain. *Cell*. 1997. doi:10.1016/S0092-8674(00)80521-8

31. Kim SC, Sprung R, Chen Y, et al. Substrate and Functional Diversity of Lysine Acetylation Revealed by a Proteomics Survey. *Mol Cell*. 2006;23(4):607-618. doi:10.1016/j.molcel.2006.06.026

32. Choudhary C, Kumar C, Gnad F, et al. Lysine acetylation targets protein complexes and co-regulates major cellular functions. *Science (80-)*. 2009. doi:10.1126/science.1175371

33. Zhao S, Xu W, Jiang W, et al. Regulation of cellular metabolism by protein lysine acetylation. *Science (80-)*. 2010. doi:10.1126/science.1179689

34. Krebs EG, Beavo JA. Phosphorylation-Dephosphorylation of Enzymes. *Annu Rev Biochem*. 1979. doi:10.1146/annurev.bi.48.070179.004423

35. Clarke S. Protein methylation. *Curr Opin Cell Biol*. 1993. doi:10.1016/0955-0674(93)90080-A

36. Schieber M, Chandel NS. ROS function in redox signaling and oxidative stress. *Curr Biol*. 2014. doi:10.1016/j.cub.2014.03.034

37. Esterbauer H, Schaur RJ, Zollner H. Chemistry and biochemistry of 4-hydroxynonenal, malonaldehyde and related aldehydes. *Free Radic Biol Med*. 1991. doi:10.1016/0891-5849(91)90192-6

38. Allaman I, Bélanger M, Magistretti PJ. Methylglyoxal, the dark side of glycolysis. *Front Neurosci*. 2015. doi:10.3389/fnins.2015.00023

39. Wagner GR, Payne RM. Widespread and enzyme-independent Nε-acetylation and Nε-succinylation of proteins in the chemical conditions of the mitochondrial matrix. *J Biol Chem*. 2013. doi:10.1074/jbc.M113.486753

40. Lipmann F, Kaplan NO. Coenzyme for acetylation, a pantothenic acid derivative. *J Biol Chem*. 1947.

41. Lipmann F. Development of the acetylation problem, a personal account. *Science (80-)*. 1954. doi:10.1126/science.120.3126.855

42. Su X, Wellen KE, Rabinowitz JD. Metabolic control of methylation and acetylation. *Curr Opin Chem Biol*. 2016. doi:10.1016/j.cbpa.2015.10.030

43. Wellen KE, Hatzivassiliou G, Sachdeva UM, Bui T V, Cross JR, Thompson CB. ATP-citrate lyase links cellular metabolism to histone acetylation. *Science*. 2009;324(5930):1076-1080. doi:10.1126/science.1164097

44. Houten SM, Wanders RJA. A general introduction to the biochemistry of mitochondrial fatty acid β-oxidation. *J Inherit Metab Dis*. 2010. doi:10.1007/s10545-010-9061-2

45. Madiraju P, Pande S V., Prentki M, Madiraju SRM. Mitochondrial acetylcarnitine provides acetyl groups for nuclear histone acetylation. *Epigenetics*. 2009. doi:10.4161/epi.4.6.9767

46. Watkins PA, Maiguel D, Jia Z, Pevsner J. Evidence for 26 distinct acyl-coenzyme A synthetase genes in the human genome. *J Lipid Res*. 2007. doi:10.1194/jlr.M700378-JLR200

47. Kamphorst JJ, Chung MK, Fan J, Rabinowitz JD. Quantitative analysis of acetyl-CoA production in hypoxic cancer cells reveals substantial contribution from acetate. *Cancer Metab*. 2014. doi:10.1186/2049-3002-2-23

48. Mashimo T, Pichumani K, Vemireddy V, et al. Acetate Is a Bioenergetic Substrate for Human Glioblastoma and Brain Metastases. *Cell*. 2014;159(7):1603-1614. doi:10.1016/j.cell.2014.11.025

49. Sutendra G, Kinnaird A, Dromparis P, et al. A nuclear pyruvate dehydrogenase complex is important for the generation of acetyl-CoA and histone acetylation. *Cell*. 2014;158(1):84-97. doi:10.1016/j.cell.2014.04.046

50. Lee J V., Carrer A, Shah S, et al. Akt-dependent metabolic reprogramming regulates tumor cell Histone acetylation. *Cell Metab*. 2014. doi:10.1016/j.cmet.2014.06.004

51. Mews P, Donahue G, Drake AM, Luczak V, Abel T, Berger SL. Acetyl-CoA synthetase regulates histone acetylation and hippocampal memory. *Nature*. 2017;546(7658):381-386. doi:10.1038/nature22405

52. Li X, Yu W, Qian X, et al. Nucleus-Translocated ACSS2 Promotes Gene Transcription for Lysosomal Biogenesis and Autophagy. *Mol Cell*. 2017;66(5):684-697.e9. doi:10.1016/j.molcel.2017.04.026

53. Matsuda S, Adachi J, Ihara M, et al. Nuclear pyruvate kinase M2 complex serves as a transcriptional coactivator of arylhydrocarbon receptor. *Nucleic Acids Res*. 2016;44(2):636-647. doi:10.1093/nar/gkv967

54. Wagner GR, Bhatt DP, O'Connell TM, et al. A Class of Reactive Acyl-CoA Species Reveals the Non-enzymatic Origins of Protein Acylation. *Cell Metab*. 2017. doi:10.1016/j.cmet.2017.03.006

55. Simithy J, Sidoli S, Yuan Z-F, et al. Characterization of histone acylations links chromatin modifications with metabolism. *Nat Commun*. 2017;8(1):1141. doi:10.1038/s41467-017-01384-9

56. Bachhawat BK, Coon MJ, Kupiecki FP, Nagle R, Robinson WG. Coenzyme A thiol esters of isobutyric, methacrylic, and beta-hydroxyisobutyric acids as intermediates in the

enzymatic degradation of valine. *J Biol Chem*. 1957.

57. Brosnan JT, Brosnan ME. Branched-chain amino acids: enzyme and substrate regulation. *J Nutr*. 2006;136(1 Suppl):207S-11S. http://www.ncbi.nlm.nih.gov/pubmed/16365084. Accessed October 5, 2017.

58. Neinast MD, Jang C, Hui S, et al. Quantitative Analysis of the Whole-Body Metabolic Fate of Branched-Chain Amino Acids. *Cell Metab*. 2019;29(2):417-429.e4. doi:10.1016/j.cmet.2018.10.013

59. Lake NJ, Compton AG, Rahman S, Thorburn DR. Leigh syndrome: One disorder, more than 75 monogenic causes. *Ann Neurol*. 2016;79(2):190-203. doi:10.1002/ana.24551

60. Brown GK, Hunt SM, Scholem R, et al. beta-hydroxyisobutyryl coenzyme A deacylase deficiency: a defect in valine metabolism associated with physical malformations. *Pediatrics*. 1982;70(4):532-538. http://www.ncbi.nlm.nih.gov/pubmed/7122152. Accessed September 25, 2017.

61. Peters H, Buck N, Wanders R, et al. ECHS1 mutations in Leigh disease: a new inborn error of metabolism affecting valine metabolism. *Brain*. 2014;137(Pt 11):2903-2908. doi:10.1093/brain/awu216

62. Shayota BJ, Soler-Alfonso C, Bekheirnia MR, et al. Case report and novel treatment of an autosomal recessive Leigh syndrome caused by short-chain enoyl-CoA hydratase deficiency. *Am J Med Genet Part A*. 2019. doi:10.1002/ajmg.a.61074

63. Loupatty FJ, Clayton PT, Ruiter JPN, et al. Mutations in the Gene Encoding 3-Hydroxyisobutyryl-CoA Hydrolase Results in Progressive Infantile Neurodegeneration. *Am J Hum Genet*. 2007;80(1):195-199. doi:10.1086/510725

64. Haack TB, Jackson CB, Murayama K, et al. Deficiency of ECHS1 causes mitochondrial encephalopathy with cardiac involvement. *Ann Clin Transl Neurol*. 2015;2(5):492-509. doi:10.1002/acn3.189

65. Ferdinandusse S, Waterham HR, Heales SJR, et al. HIBCH mutations can cause Leigh-like disease with combined deficiency of multiple mitochondrial respiratory chain enzymes and pyruvate dehydrogenase. *Orphanet J Rare Dis*. 2013;8(1):188. doi:10.1186/1750-1172-8-188

66. Sakai C, Yamaguchi S, Sasaki M, Miyamoto Y, Matsushima Y, Goto Y. ECHS1 mutations cause combined respiratory chain deficiency resulting in Leigh syndrome. *Hum Mutat*. 2015;36(2):232-239. doi:10.1002/humu.22730

67. Yamada K, Naiki M, Hoshino S, et al. Clinical and biochemical characterization of 3-hydroxyisobutyryl-CoA hydrolase (HIBCH) deficiency that causes Leigh-like disease and ketoacidosis. *Mol Genet Metab Reports*. 2014;1:455-460. doi:10.1016/j.ymgmr.2014.10.003

68. Soler-Alfonso C, Enns GM, Koenig MK, Saavedra H, Bonfante-Mejia E, Northrup H. Identification of HIBCH Gene Mutations Causing Autosomal Recessive Leigh Syndrome: A Gene Involved in Valine Metabolism. *Pediatr Neurol*. 2015;52(3):361-365. doi:10.1016/j.pediatrneurol.2014.10.023

69. Reuter MS, Sass JO, Leis T, et al. HIBCH deficiency in a patient with phenotypic characteristics of mitochondrial disorders. *Am J Med Genet Part A*. 2014;164(12):3162-3169. doi:10.1002/ajmg.a.36766

70. Fitzsimons PE, Alston CL, Bonnen PE, et al. Clinical, biochemical, and genetic features of four patients with short-chain enoyl-CoA hydratase (ECHS1) deficiency. *Am J Med Genet Part A*. 2018. doi:10.1002/ajmg.a.38658

71. Yamada K, Aiba K, Kitaura Y, et al. Clinical, biochemical and metabolic characterisation of a mild form of human short-chain enoyl-CoA hydratase deficiency: significance of increased N-acetyl-S-(2-carboxypropyl)cysteine excretion. *J Med Genet*. 2015;52(10):691-698. doi:10.1136/jmedgenet-2015-103231

72. Shimomura Y, Murakami T, Fujitsuka N, et al. Purification and partial characterization of 3-hydroxyisobutyryl-coenzyme A hydrolase of rat liver. *J Biol Chem*. 1994;269(19):14248-14253. http://www.ncbi.nlm.nih.gov/pubmed/8188708. Accessed September 25, 2017.

73. Taniguchi K, Nonami T, Nakao A, et al. The valine catabolic pathway in human liver: Effect of cirrhosis on enzyme activities. *Hepatology*. 1996;24(6):1395-1398. doi:10.1002/hep.510240614

74. Ooiwa T, Goto H, Tsukamoto Y, et al. Regulation of valine catabolism in canine tissues: tissue distributions of branched-chain aminotransferase and 2-oxo acid dehydrogenase complex, methacrylyl-CoA hydratase and 3-hydroxyisobutyryl-CoA hydrolase. *Biochim Biophys Acta*. 1995;1243(2):216-220. http://www.ncbi.nlm.nih.gov/pubmed/7873565. Accessed October 5, 2017.

75. Ishigure K, Shimomura Y, Murakami T, et al. Human liver disease decreases methacrylyl-CoA hydratase and beta-hydroxyisobutyryl-CoA hydrolase activities in valine catabolism. *Clin Chim Acta*. 2001;312(1-2):115-121. http://www.ncbi.nlm.nih.gov/pubmed/11580916. Accessed October 6, 2017.

76. Mayers JR, Wu C, Clish CB, et al. Elevation of circulating branched-chain amino acids is an early event in human pancreatic adenocarcinoma development. *Nat Med*. 2014. doi:10.1038/nm.3686

77. Mayers JR, Torrence ME, Danai L V., et al. Tissue of origin dictates branched-chain amino acid metabolism in mutant Kras-driven cancers. *Science (80-)*. 2016. doi:10.1126/science.aaf5171

78. Ericksen RE, Lim SL, McDonnell E, et al. Loss of BCAA Catabolism during Carcinogenesis Enhances mTORC1 Activity and Promotes Tumor Development and

Progression. *Cell Metab*. January 2019. doi:10.1016/j.cmet.2018.12.020

79. Tönjes M, Barbus S, Park YJ, et al. BCAT1 promotes cell proliferation through amino acid catabolism in gliomas carrying wild-type IDH1. *Nat Med*. 2013. doi:10.1038/nm.3217

80. Felig P, Marliss E, Cahill GF. Plasma amino acid levels and insulin secretion in obesity. *N Engl J Med*. 1969. doi:10.1056/NEJM196910092811503

81. Felig P, Wahren J, Hendler R, Brundin T. Splanchnic glucose and amino acid metabolism in obesity. *J Clin Invest*. 1974. doi:10.1172/JCI107593

82. Newgard CB, An J, Bain JR, et al. A Branched-Chain Amino Acid-Related Metabolic Signature that Differentiates Obese and Lean Humans and Contributes to Insulin Resistance. *Cell Metab*. 2009. doi:10.1016/j.cmet.2009.02.002

83. White PJ, Lapworth AL, An J, et al. Branched-chain amino acid restriction in Zucker-fatty rats improves muscle insulin sensitivity by enhancing efficiency of fatty acid oxidation and acyl-glycine export. *Mol Metab*. 2016. doi:10.1016/j.molmet.2016.04.006

84. Fontana L, Cummings NE, Arriola Apelo SI, et al. Decreased Consumption of Branched-Chain Amino Acids Improves Metabolic Health. *Cell Rep*. 2016. doi:10.1016/j.celrep.2016.05.092

85. Newgard CB. Interplay between lipids and branched-chain amino acids in development of insulin resistance. *Cell Metab*. 2012. doi:10.1016/j.cmet.2012.01.024

86. She P, Van Horn C, Reid T, Hutson SM, Cooney RN, Lynch CJ. Obesity-related elevations in plasma leucine are associated with alterations in enzymes involved in branched-chain amino acid metabolism. *Am J Physiol - Endocrinol Metab*. 2007. doi:10.1152/ajpendo.00134.2007

87. Lackey DE, Lynch CJ, Olson KC, et al. Regulation of adipose branched-chain amino acid catabolism enzyme expression and cross-adipose amino acid flux in human obesity. *Am J Physiol - Endocrinol Metab*. 2013. doi:10.1152/ajpendo.00630.2012

88. Jang C, Oh SF, Wada S, et al. A branched-chain amino acid metabolite drives vascular fatty acid transport and causes insulin resistance. *Nat Med*. 2016;22(4):421-426. doi:10.1038/nm.4057

89. Sabari BR, Zhang D, Allis CD, Zhao Y. Metabolic regulation of gene expression through histone acylations. *Nat Rev Mol Cell Biol*. 2017;18(2):90-101. doi:10.1038/nrm.2016.140

90. Huang H, Zhang D, Wang Y, et al. Lysine benzoylation is a histone mark regulated by SIRT2. *Nat Commun*. 2018;9(1):3374. doi:10.1038/s41467-018-05567-w

91. Zhang D, Tang Z, Huang H, et al. Metabolic regulation of gene expression by histone lactylation. *Nature*. 2019;574(7779):575-580. doi:10.1038/s41586-019-1678-1

92. Huang H, Sabari BR, Garcia BA, et al. SnapShot: Histone modifications. *Cell*. 2014;159(2):458-458.e1. doi:10.1016/j.cell.2014.09.037

93. Shechter D, Dormann HL, Allis CD, Hake SB. Extraction, purification and analysis of histones. *Nat Protoc*. 2007. doi:10.1038/nprot.2007.202

94. Müller MM, Muir TW. Histones: At the crossroads of peptide and protein chemistry. *Chem Rev*. 2015. doi:10.1021/cr5003529

95. James AM, Hoogewijs K, Logan A, et al. Non-enzymatic N-acetylation of Lysine Residues by AcetylCoA Often Occurs via a Proximal S-acetylated Thiol Intermediate Sensitive to Glyoxalase II. *Cell Rep*. 2017. doi:10.1016/j.celrep.2017.02.018

96. Merkley ED, Metz TO, Smith RD, Baynes JW, Frizzell N. The succinated proteome. *Mass Spectrom Rev*. 2014;33(2):98-109. doi:10.1002/mas.21382

97. Chen Y, Sprung R, Tang Y, et al. Lysine propionylation and butyrylation are novel post-translational modifications in histones. *Mol Cell Proteomics*. 2007;6:812-819. doi:10.1074/mcp.M700021-MCP200

98. Peng C, Lu Z, Xie Z, et al. The First Identification of Lysine Malonylation Substrates and Its Regulatory Enzyme. *Mol Cell Proteomics*. 2011;10(12):M111.012658-M111.012658. doi:10.1074/mcp.M111.012658

99. Tan M, Peng C, Anderson K a., et al. Lysine glutarylation is a protein posttranslational modification regulated by SIRT5. *Cell Metab*. 2014;19(4):605-617. doi:10.1016/j.cmet.2014.03.014

100. Chen Y, Chen W, Cobb MH, Zhao Y. PTMap - A sequence alignment software for unrestricted, accurate, and full-spectrum identification of post-translational modification sites. *Proc Natl Acad Sci U S A*. 2009. doi:10.1073/pnas.0811739106

101. Kong AT, Leprevost F V., Avtonomov DM, Mellacheruvu D, Nesvizhskii AI. MSFragger: Ultrafast and comprehensive peptide identification in mass spectrometry-based proteomics. *Nat Methods*. 2017. doi:10.1038/nmeth.4256

102. Tan M, Luo H, Lee S, et al. Identification of 67 histone marks and histone lysine crotonylation as a new type of histone modification. *Cell*. 2011;146:1016-1028. doi:10.1016/j.cell.2011.08.008

103. Dai L, Peng C, Montellier E, et al. Lysine 2-hydroxyisobutyrylation is a widely distributed active histone mark. *Nat Chem Biol*. 2014;10(5):365-370. doi:10.1038/nchembio.1497

104. Anderson KA, Huynh FK, Fisher-Wellman K, et al. SIRT4 Is a Lysine Deacylase that Controls Leucine Metabolism and Insulin Secretion. *Cell Metab*. 2017;25(4):838-855.e15. doi:10.1016/j.cmet.2017.03.003

105. Baldensperger T, Sanzo S Di, Ori A, Glomb MA. Quantitation of Reactive Acyl-CoA

Species Mediated Protein Acylation by HPLC-MS/MS. *Anal Chem*. 2019. doi:10.1021/acs.analchem.9b02656

106. Sabari BR, Tang Z, Huang H, et al. Intracellular Crotonyl-CoA Stimulates Transcription through p300-Catalyzed Histone Crotonylation. *Mol Cell*. 2015;58(2):203-215. doi:10.1016/j.molcel.2015.02.029

107. Bao X, Wang Y, Li X, et al. Identification of 'erasers' for lysine crotonylated histone marks using a chemical proteomics approach. *Elife*. 2014;3. doi:10.7554/eLife.02999

108. Wei W, Liu X, Chen J, et al. Class I histone deacetylases are major histone decrotonylases: evidence for critical and broad function of histone crotonylation in transcription. *Cell Res*. 2017;27(7):898-915. doi:10.1038/cr.2017.68

109. Feldman JL, Baeza J, Denu JM. Activation of the Protein Deacetylase SIRT6 by Long-chain Fatty Acids and Widespread Deacylation by Mammalian Sirtuins. *J Biol Chem*. 2013;288(43):31350-31356. doi:10.1074/jbc.C113.511261

110. Moreno-Yruela C, Galleano I, Madsen AS, Correspondence CAO, Olsen CA. Histone Deacetylase 11 Is an ε-N-Myristoyllysine Hydrolase Article Histone Deacetylase 11 Is an ε-N-Myristoyllysine Hydrolase. *Cell Chem Biol*. 2018;25:849-856. doi:10.1016/j.chembiol.2018.04.007

111. Kelly RDW, Chandru A, Watson PJ, et al. Histone deacetylase (HDAC) 1 and 2 complexes regulate both histone acetylation and crotonylation in vivo. *Sci Rep*. 2018. doi:10.1038/s41598-018-32927-9

112. Li Y, Sabari BRR, Panchenko T, et al. Molecular Coupling of Histone Crotonylation and Active Transcription by AF9 YEATS Domain. *Mol Cell*. 2016;62(2):181-193. doi:10.1016/j.molcel.2016.03.028

113. Andrews FH, Shinsky SA, Shanle EK, et al. The Taf14 YEATS domain is a reader of histone crotonylation. *Nat Chem Biol*. 2016;12(6):396-398. doi:10.1038/nchembio.2065

114. Zhao D, Guan H, Zhao S, et al. YEATS2 is a selective histone crotonylation reader. *Cell Res*. 2016;26(5):629-632. doi:10.1038/cr.2016.49

115. Xiong X, Panchenko T, Yang S, et al. Selective recognition of histone crotonylation by double PHD fingers of MOZ and DPF2. *Nat Chem Biol*. 2016;12(12):1111-1118. doi:10.1038/nchembio.2218

116. Zhang Z, Tan M, Xie Z, Dai L, Chen Y, Zhao Y. Identification of lysine succinylation as a new post-translational modification. *Nat Chem Biol*. 2011;7(1):58-63. doi:10.1038/nchembio.495

117. Xie Z, Zhang D, Chung D, et al. Metabolic Regulation of Gene Expression by Histone Lysine β-Hydroxybutyrylation. *Mol Cell*. 2016;62(2):194-206. doi:10.1016/j.molcel.2016.03.036

118. Wang Y, Guo YR, Liu K, et al. KAT2A coupled with the α-KGDH complex acts as a histone H3 succinyltransferase. *Nature*. 2017;552(7684):273-277. doi:10.1038/nature25003

119. Bao X, Liu Z, Zhang W, et al. Glutarylation of Histone H4 Lysine 91 Regulates Chromatin Dynamics. *Mol Cell*. 2019. doi:10.1016/j.molcel.2019.08.018

120. Goudarzi A, Zhang D, Huang H, et al. Dynamic Competing Histone H4 K5K8 Acetylation and Butyrylation Are Hallmarks of Highly Active Gene Promoters. *Mol Cell*. 2016;62(2):169-180. doi:10.1016/j.molcel.2016.03.014

121. Reed LJ. Multienzyme Complexes. *Acc Chem Res*. 1974. doi:10.1021/ar50074a002

122. Knowles JR. The Mechanism of Biotin-Dependent Enzymes. *Annu Rev Biochem*. 1989. doi:10.1146/annurev.bi.58.070189.001211

123. Du J, Zhou Y, Su X, et al. Sirt5 Is a NAD-Dependent Protein Lysine Demalonylase and Desuccinylase. *Science (80-)*. 2011;334(November):806-809. doi:10.1126/science.1207861

124. Park J, Chen Y, Tishkoff DX, et al. SIRT5-Mediated Lysine Desuccinylation Impacts Diverse Metabolic Pathways. *Mol Cell*. 2013;50(6):919-930. doi:10.1016/j.molcel.2013.06.001

125. Rardin MJ, He W, Nishida Y, et al. SIRT5 Regulates the Mitochondrial Lysine Succinylome and Metabolic Networks. *Cell Metab*. 2013;18(6):920-933. doi:10.1016/j.cmet.2013.11.013

126. Nishida Y, Rardin MJ, Carrico C, et al. SIRT5 Regulates both Cytosolic and Mitochondrial Protein Malonylation with Glycolysis as a Major Target. *Mol Cell*. 2015;59(2):321-332. doi:10.1016/j.molcel.2015.05.022

127. Galván-Peña S, Carroll RG, Newman C, et al. Malonylation of GAPDH is an inflammatory signal in macrophages. *Nat Commun*. 2019. doi:10.1038/s41467-018-08187-6

128. Huang H, Tang S, Ji M, et al. EP300-Mediated Lysine 2-Hydroxyisobutyrylation Regulates Glycolysis. *Mol Cell*. 2018. doi:10.1016/j.molcel.2018.04.011

129. Stevenson FT, Bursten SL, Locksley RM, Lovett DH. Myristyl acylation of the tumor necrosis factor α precursor on specific lysine residues. *J Exp Med*. 1992. doi:10.1084/jem.176.4.1053

130. Jing H, Zhang X, Wisner SA, et al. SIRT2 and lysine fatty acylation regulate the transforming activity of K-Ras4a. *Elife*. 2017. doi:10.7554/eLife.32436

131. Lanyon-Hogg T, Faronato M, Serwa RA, Tate EW. Dynamic Protein Acylation: New Substrates, Mechanisms, and Drug Targets. *Trends Biochem Sci*. 2017.

doi:10.1016/j.tibs.2017.04.004

132. Smuda M, Voigt M, Glomb MA. Degradation of 1-deoxy-d-erythro-hexo-2,3-diulose in the presence of lysine leads to formation of carboxylic acid amides. *J Agric Food Chem*. 2010. doi:10.1021/jf100334r

133. Baldensperger T, Jost T, Zipprich A, Glomb MA. Novel α-Oxoamide Advanced-Glycation Endproducts within the N6-Carboxymethyl Lysine and N6-Carboxyethyl Lysine Reaction Cascades. *J Agric Food Chem*. 2018. doi:10.1021/acs.jafc.7b05813

134. Kleff S, Andrulis ED, Anderson CW, Sternglanz R. Identification of a gene encoding a yeast histone H4 acetyltransferase. *J Biol Chem*. 1995. doi:10.1074/jbc.270.42.24674

135. Marmorstein R, Zhou M-M. Writers and readers of histone acetylation: structure, mechanism, and inhibition. *Cold Spring Harb Perspect Biol*. 2014;6(7):a018762. doi:10.1101/cshperspect.a018762

136. Spencer TE, Jenster G, Burcin MM, et al. Steroid receptor coactivator-1 is a histone acetyltransferase. *Nature*. 1997. doi:10.1038/38304

137. Mizzen CA, Yang XJ, Kokubo T, et al. The TAF(II)250 subunit of TFIID has histone acetyltransferase activity. *Cell*. 1996. doi:10.1016/S0092-8674(00)81821-8

138. Kawasaki H, Schiltz L, Chiu R, et al. ATF-2 has intrinsic histone acetyltransferase activity which is modulated by phosphorylation. *Nature*. 2000. doi:10.1038/35012097

139. Doi M, Hirayama J, Sassone-Corsi P. Circadian Regulator CLOCK Is a Histone Acetyltransferase. *Cell*. 2006. doi:10.1016/j.cell.2006.03.033

140. Allis CD, Berger SL, Cote J, et al. New Nomenclature for Chromatin-Modifying Enzymes. *Cell*. 2007. doi:10.1016/j.cell.2007.10.039

141. Chicoine LG, Schulman IG, Richman R, Cook RG, Allis CD. Nonrandom utilization of acetylation sites in histones isolated from Tetrahymena. Evidence for functionally distinct H4 acetylation sites. *J Biol Chem*. 1986.

142. Sobel RE, Cook RG, Perry CA, Annunziato AT, Allis CD. Conservation of deposition-related acetylation sites in newly synthesized histones H3 and H4. *Proc Natl Acad Sci U S A*. 1995;92(4):1237-1241. doi:10.1073/pnas.92.4.1237

143. Wiegand RC, Brutlag DL. Histone acetylase from Drosophila melanogaster specific for H4. *J Biol Chem*. 1981.

144. López-Rodas G, Tordera V, del Pino MSM, Franco L. Subcellular Localization and Nucleosome Specificity of Yeast Histone Acetyltransferases. *Biochemistry*. 1991. doi:10.1021/bi00229a020

145. Lopez-Rodas G, Tordera V, Sanchez del Pino MM, Franco L. Yeast contains multiple

forms of histone acetyltransferase. *J Biol Chem*. 1989.

146. Lopez-Rodas G, Perez-Ortin JE, Tordera V, Salvador ML, Franco L. Partial purification and properties of two histone acetyltransferases from the yeast, Saccharomyces cerevisiae. *Arch Biochem Biophys*. 1985. doi:10.1016/0003-9861(85)90825-2

147. Sobel RE, Cook RG, Allis CD. Non-random acetylation of histone H4 by a cytoplasmic histone acetyltransferase as determined by novel methodology. *J Biol Chem*. 1994.

148. Richman R, Chicoine LG, Collini MP, Cook RG, Allis CD. Micronuclei and the cytoplasm of growing Tetrahymena contain a histone acetylase activity which is highly specific for free histone H4. *J Cell Biol*. 1988. doi:10.1083/jcb.106.4.1017

149. Mingarro I, Sendra R, Salvador ML, Franco L. Site specificity of pea histone acetyltransferase B in vitro. *J Biol Chem*. 1993.

150. Parthun MR, Widom J, Gottschling DE. The major cytoplasmic histone acetyltransferase in yeast: Links to chromatin replication and histone metabolism. *Cell*. 1996. doi:10.1016/S0092-8674(00)81325-2

151. Chang L, Loranger SS, Mizzen C, Ernst SG, Allis CD, Annunziato AT. Histones in transit: Cytosolic histone complexes and diacetylation of H4 during nucleosome assembly in human cells. *Biochemistry*. 1997. doi:10.1021/bi962069i

152. Kölle D, Sarg B, Lindner H, Loidl P. Substrate and sequential site specificity of cytoplasmic histone acetyltransferases of maize and rat liver. *FEBS Lett*. 1998. doi:10.1016/S0014-5793(97)01544-5

153. Garcea RL, Alberts BM. Comparative studies of histone acetylation in nucleosomes, nuclei, and intact cells. Evidence for special factors which modify acetylase action. *J Biol Chem*. 1980.

154. Sures I, Gallwitz D. Histone-Specific Acetyltransferases from Calf Thymus. Isolation, Properties, and Substrate Specificity of Three Different Enzymes. *Biochemistry*. 1980. doi:10.1021/bi00546a019

155. Verreault A, Kaufman PD, Kobayashi R, Stillman B. Nucleosomal DNA regulates the core-histone-binding subunit of the human Hat1 acetyltransferase. *Curr Biol*. 1998. doi:10.1016/S0960-9822(98)70040-5

156. Ai X, Parthun MR. The nuclear Hat1p/Hat2p complex: A molecular link between type B histone acetyltransferases and chromatin assembly. *Mol Cell*. 2004. doi:10.1016/S1097-2765(04)00184-4

157. Ruiz-García AB, Sendra R, Galiana M, Pamblanco M, Pérez-Ortín JE, Tordera V. Hat1 and Hat2 proteins are components of a yeast nuclear histone acetyltransferase enzyme specific for free histone H4. *J Biol Chem*. 1998. doi:10.1074/jbc.273.20.12599

158. Poveda A, Pamblanco M, Tafrov S, Tordera V, Sternglanz R, Sendra R. Hif1 Is a Component of Yeast Histone Acetyltransferase B, a Complex Mainly Localized in the Nucleus. *J Biol Chem*. 2004. doi:10.1074/jbc.M314228200

159. Kelly TJ, Qin S, Gottschling DE, Parthun MR. Type B Histone Acetyltransferase Hat1p Participates in Telomeric Silencing. *Mol Cell Biol*. 2000. doi:10.1128/mcb.20.19.7051-7058.2000

160. Mersfelder EL, Parthun MR. Involvement of Hat1p (Kat1p) catalytic activity and subcellular localization in telomeric silencing. *J Biol Chem*. 2008. doi:10.1074/jbc.M802564200

161. Tong K, Keller T, Hoffman CS, Annunziato AT. Schizosaccharomyces pombe Hat1 (Kat1) is associated with Mis16 and is required for telomeric silencing. *Eukaryot Cell*. 2012. doi:10.1128/EC.00123-12

162. Marin TL, Gongol B, Zhang F, et al. AMPK promotes mitochondrial biogenesis and function by phosphorylating the epigenetic factors DNMT1, RBBP7, and HAT1. *Sci Signal*. 2017. doi:10.1126/scisignal.aaf7478

163. Nagarajan P, Agudelo Garcia PA, Iyer CC, Popova L V., Arnold WD, Parthun MR. Early-onset aging and mitochondrial defects associated with loss of histone acetyltransferase 1 (Hat1). *Aging Cell*. 2019. doi:10.1111/acel.12992

164. Parthun MR. Histone acetyltransferase 1: More than just an enzyme? *Biochim Biophys Acta - Gene Regul Mech*. 2012. doi:10.1016/j.bbagrm.2011.07.006

165. Ejlassi-Lassallette A, Mocquard E, Arnaud MC, Thiriet C. H4 replication-dependent diacetylation and Hat1 promote s-phase chromatin assembly in vivo. *Mol Biol Cell*. 2011. doi:10.1091/mbc.E10-07-0633

166. Alvarez F, Muñoz F, Schilcher P, Imhof A, Almouzni G, Loyola A. Sequential establishment of marks on soluble histones H3 and H4. *J Biol Chem*. 2011. doi:10.1074/jbc.M111.223453

167. Campos EI, Fillingham J, Li G, et al. The program for processing newly synthesized histones H3.1 and H4. *Nat Struct Mol Biol*. 2010. doi:10.1038/nsmb.1911

168. Jasencakova Z, Scharf AND, Ask K, et al. Replication Stress Interferes with Histone Recycling and Predeposition Marking of New Histones. *Mol Cell*. 2010. doi:10.1016/j.molcel.2010.01.033

169. Nagarajan P, Ge Z, Sirbu B, et al. Histone Acetyl Transferase 1 Is Essential for Mammalian Development, Genome Stability, and the Processing of Newly Synthesized Histones H3 and H4. *PLoS Genet*. 2013. doi:10.1371/journal.pgen.1003518

170. Garcia PAA, Hoover ME, Zhang P, Nagarajan P, Freitas MA, Parthun MR. Identification of multiple roles for histone acetyltransferase 1 in replication-coupled chromatin

assembly. *Nucleic Acids Res*. 2017. doi:10.1093/nar/gkx545

171. Gruber JJ, Geller B, Lipchik AM, et al. HAT1 Coordinates Histone Production and Acetylation via H4 Promoter Binding. *Mol Cell*. 2019;75(4):711-724.e5. doi:10.1016/j.molcel.2019.05.034

172. Varga J, Korbai S, Neller A, Zsindely N, Bodai L. Hat1 acetylates histone H4 and modulates the transcriptional program in Drosophila embryogenesis. *Sci Rep*. 2019. doi:10.1038/s41598-019-54497-0

173. Tagami H, Ray-Gallet D, Almouzni G, Nakatani Y. Histone H3.1 and H3.3 Complexes Mediate Nucleosome Assembly Pathways Dependent or Independent of DNA Synthesis. *Cell*. 2004. doi:10.1016/S0092-8674(03)01064-X

174. Ma XJ, Wu J, Altheim BA, Schultz MC, Grunstein M. Deposition-related sites K5/K12 in histone H4 are not required for nucleosome deposition in yeast. *Proc Natl Acad Sci U S A*. 1998. doi:10.1073/pnas.95.12.6693

175. Shibahara KI, Verreault A, Stillman B. The N-terminal domains of histories H3 and H4 are not necessary for chromatin assembly factor-1-mediated nucleosome assembly onto replicated DNA in vitro. *Proc Natl Acad Sci U S A*. 2000.

176. Kim HS, Mukhopadhyay R, Rothbart SB, et al. Identification of a BET family bromodomain/casein kinase II/TAF-containing complex as a regulator of mitotic condensin function. *Cell Rep*. 2014. doi:10.1016/j.celrep.2014.01.029

177. Boltengagen M, Huang A, Boltengagen A, et al. A novel role for the histone acetyltransferase Hat1 in the CENP-A/CID assembly pathway in Drosophila melanogaster. *Nucleic Acids Res*. 2015. doi:10.1093/nar/gkv1235

178. Shang WH, Hori T, Westhorpe FG, et al. Acetylation of histone H4 lysine 5 and 12 is required for CENP-A deposition into centromeres. *Nat Commun*. 2016. doi:10.1038/ncomms13465

179. Hoffmann G, Samel-Pommerencke A, Weber J, Cuomo A, Bonaldi T, Ehrenhofer-Murray AE. A role for CENP-A/Cse4 phosphorylation on serine 33 in deposition at the centromere. *FEMS Yeast Res*. 2018. doi:10.1093/femsyr/fox094

180. Ge Z, Wang H, Parthun MR. Nuclear Hat1p complex (NuB4) components participate in DNA repair-linked chromatin reassembly. *J Biol Chem*. 2011. doi:10.1074/jbc.M110.216846

181. Verzijlbergen KF, van Welsem T, Sie D, et al. A barcode screen for epigenetic regulators reveals a role for the NuB4/HAT-B histone acetyltransferase complex in histone turnover. *PLoS Genet*. 2011. doi:10.1371/journal.pgen.1002284

182. Yang X, Li L, Liang J, et al. Histone acetyltransferase 1 promotes homologous recombination in DNA repair by facilitating histone turnover. *J Biol Chem*. 2013.

doi:10.1074/jbc.M113.473199

183. Qin S, Parthun MR. Histone H3 and the Histone Acetyltransferase Hat1p Contribute to DNA Double-Strand Break Repair. *Mol Cell Biol*. 2002. doi:10.1128/mcb.22.23.8353-8365.2002

184. Barman HK, Takami Y, Ono T, et al. Histone acetyltransferase 1 is dispensable for replication-coupled chromatin assembly but contributes to recover DNA damages created following replication blockage in vertebrate cells. *Biochem Biophys Res Commun*. 2006. doi:10.1016/j.bbrc.2006.05.079

185. Benson LJ, Phillips JA, Gu Y, Parthun MR, Hoffman CS, Annunziato AT. Properties of the type B histone acetyltransferase Hat1: H4 tail interaction, site preference, and involvement in DNA repair. *J Biol Chem*. 2007. doi:10.1074/jbc.M607464200

186. Qin S, Parthun MR. Recruitment of the Type B Histone Acetyltransferase Hat1p to Chromatin Is Linked to DNA Double-Strand Breaks. *Mol Cell Biol*. 2006. doi:10.1128/mcb.26.9.3649-3658.2006

187. Sirbu BM, Couch FB, Feigerle JT, Bhaskara S, Hiebert SW, Cortez D. Analysis of protein dynamics at active, stalled, and collapsed replication forks. *Genes Dev*. 2011. doi:10.1101/gad.2053211

188. Xia P, Gu R, Zhang W, et al. MicroRNA-377 exerts a potent suppressive role in osteosarcoma through the involvement of the histone acetyltransferase 1-mediated Wnt axis. *J Cell Physiol*. 2019. doi:10.1002/jcp.28843

189. Zhang J, Liu M, Liu W, Wang W. Ras-ERK1/2 signalling promotes the development of osteosarcoma through regulation of H4K12ac through HAT1. *Artif Cells, Nanomedicine Biotechnol*. 2019. doi:10.1080/21691401.2019.1593857

190. Fan P, Zhao J, Meng Z, et al. Overexpressed histone acetyltransferase 1 regulates cancer immunity by increasing programmed death-ligand 1 expression in pancreatic cancer. *J Exp Clin Cancer Res*. 2019;38(1). doi:10.1186/s13046-019-1044-z

191. Miao BP, Zhang RS, Yang G, et al. Histone acetyltransferase 1 up regulates Bcl2L12 expression in nasopharyngeal cancer cells. *Arch Biochem Biophys*. 2018. doi:10.1016/j.abb.2018.03.040

192. Han N, Shi L, Guo Q, et al. HAT1 induces lung cancer cell apoptosis via up regulating Fas. *Oncotarget*. 2017. doi:10.18632/oncotarget.21205

193. Jin X, Tian S, Li P. Histone acetyltransferase 1 promotes cell proliferation and induces cisplatin resistance in hepatocellular carcinoma. *Oncol Res*. 2017. doi:10.3727/096504016X14809827856524

194. Pogribny IP, Tryndyak VP, Muskhelishvili L, Rusyn I, Ross SA. Methyl Deficiency, Alterations in Global Histone Modifications, and Carcinogenesis. *J Nutr*. 2007.

doi:10.1093/jn/137.1.216s

195. Seiden-Long IM, Brown KR, Shih W, et al. Transcriptional targets of hepatocyte growth factor signaling and Ki-ras oncogene activation in colorectal cancer. *Oncogene*. 2006. doi:10.1038/sj.onc.1209005

196. Cheng Z, Tang Y, Chen Y, et al. Molecular characterization of propionyllysines in non-histone proteins. *Mol Cell Proteomics*. 2009;8(1):45-52. doi:10.1074/mcp.M800224-MCP200

197. Kaczmarska Z, Ortega E, Goudarzi A, et al. Structure of p300 in complex with acyl-CoA variants. *Nat Chem Biol*. 2016;13(1):21-29. doi:10.1038/nchembio.2217

198. Leemhuis H, Packman LC, Nightingale KP, Hollfelder F. The Human Histone Acetyltransferase P/CAF is a Promiscuous Histone Propionyltransferase. *ChemBioChem*. 2008;9(4):499-503. doi:10.1002/cbic.200700556

199. Ringel AE, Wolberger C. Structural basis for acyl-group discrimination by human Gcn5L2. *Acta Crystallogr Sect D Struct Biol*. 2016;72(7):841-848. doi:10.1107/S2059798316007907

200. Han Z, Wu H, Kim S, et al. Revealing the protein propionylation activity of the histone acetyltransferase MOF (males absent on the first). *J Biol Chem*. 2018. doi:10.1074/jbc.RA117.000529

201. Yan K, Rousseau J, Machol K, et al. Deficient histone H3 propionylation by BRPF1-KAT6 complexes in neurodevelopmental disorders and cancer. *Sci Adv*. 2020. doi:10.1126/sciadv.aax0021

202. Huang H, Luo Z, Qi S, et al. Landscape of the regulatory elements for lysine 2-hydroxyisobutyrylation pathway. *Cell Res*. 2018;28(1):111-125. doi:10.1038/cr.2017.149

203. Kurmi K, Hitosugi S, Wiese EK, et al. Carnitine Palmitoyltransferase 1A Has a Lysine Succinyltransferase Activity. *Cell Rep*. 2018. doi:10.1016/j.celrep.2018.01.030

204. Levy M, Montgomery D, Sardiu M, et al. A systems chemoproteomic analysis of acyl-CoA/protein interaction networks. *Cell Chem Biol*. 2019. doi:10.1101/665281

205. Seto E, Yoshida M. Erasers of histone acetylation: the histone deacetylase enzymes. *Cold Spring Harb Perspect Biol*. 2014;6(4):a018713. doi:10.1101/cshperspect.a018713

206. Riggs MG, Whittaker RG, Neumann JR, Ingram VM. n-Butyrate causes histone modification in HeLa and Friend erythroleukaemia cells. *Nature*. 1977. doi:10.1038/268462a0

207. Candido EPM, Reeves R, Davie JR. Sodium butyrate inhibits histone deacetylation in cultured cells. *Cell*. 1978. doi:10.1016/0092-8674(78)90305-7

208. Vidali G, Boffa LC, Bradbury EM, Allfrey VG. Butyrate suppression of histone deacetylation leads to accumulation of multiacetylated forms of histones H3 and H4 and increased DNase I sensitivity of the associated DNA sequence. *Proc Natl Acad Sci U S A*. 1978. doi:10.1073/pnas.75.5.2239

209. Yoshida M, Horinouchi S, Beppu T. Trichostatin A and trapoxin: Novel chemical probes for the role of histone acetylation in chromatin structure and function. *BioEssays*. 1995. doi:10.1002/bies.950170510

210. Kijima M, Yoshida M, Sugita K, Horinouchi S, Beppu T. Trapoxin, an antitumor cyclic tetrapeptide, is an irreversible inhibitor of mammalian histone deacetylase. *J Biol Chem*. 1993.

211. Vidal M, Gaber RF. RPD3 encodes a second factor required to achieve maximum positive and negative transcriptional states in Saccharomyces cerevisiae. *Mol Cell Biol*. 1991. doi:10.1128/mcb.11.12.6317

212. Yang WM, Inouye C, Zeng Y, Bearss D, Seto E. Transcriptional repression by YY1 is mediated by interaction with a mammalian homolog of the yeast global regulator RPD3. *Proc Natl Acad Sci U S A*. 1996. doi:10.1073/pnas.93.23.12845

213. Laherty CD, Yang WM, Jian-Min S, Davie JR, Seto E, Eisenman RN. Histone deacetylases associated with the mSin3 corepressor mediate Mad transcriptional repression. *Cell*. 1997. doi:10.1016/S0092-8674(00)80215-9

214. Yang WM, Yao YL, Sun JM, Davie JR, Seto E. Isolation and characterization of cDNAs corresponding to an additional member of the human histone deacetylase gene family. *J Biol Chem*. 1997. doi:10.1074/jbc.272.44.28001

215. Zeng Y, Tang CM, Yao YL, Yang WM, Seto E. Cloning and characterization of the mouse histone deacetylase-2 gene. *J Biol Chem*. 1998. doi:10.1074/jbc.273.44.28921

216. Dangond F, Hafler DA, Tong JK, et al. Differential display cloning of a novel human histone deacetylase (HDAC3) cDNA from PHA-activated immune cells. *Biochem Biophys Res Commun*. 1998. doi:10.1006/bbrc.1997.8033

217. Emiliani S, Fischle W, Van Lint C, Al-Abed Y, Verdin E. Characterization of a human RPD3 ortholog, HDAC3. *Proc Natl Acad Sci U S A*. 1998. doi:10.1073/pnas.95.6.2795

218. Grozinger CM, Hassig CA, Schreiber SL. Three proteins define a class of human histone deacetylases related to yeast Hda1p. *Proc Natl Acad Sci U S A*. 1999. doi:10.1073/pnas.96.9.4868

219. Kao HY, Downes M, Ordentlich P, Evans RM. Isolation of a novel histone deacetylase reveals that class I and class II deacetylases promote SMRT-mediated repression. *Genes Dev*. 2000. doi:10.1101/gad.14.1.55

220. Hu E, Chen Z, Fredrickson T, et al. Cloning and characterization of a novel human class I

histone deacetylase that functions as a transcription repressor. *J Biol Chem*. 2000. doi:10.1074/jbc.M908988199

221. Zhou X, Marks PA, Rifkind RA, Richon VM. Cloning and characterization of a histone deacetylase, HDAC9. *Proc Natl Acad Sci U S A*. 2001. doi:10.1073/pnas.191375098

222. Sparrow DB, Miska EA, Langley E, et al. MEF-2 function is modified by a novel co-repressor, MITR. *EMBO J*. 1999. doi:10.1093/emboj/18.18.5085

223. Zhang CL, McKinsey TA, Lu JR, Olson EN. Association of COOH-terminal-binding protein (CtBP) and MEF2-interacting transcription repressor (MITR) contributes to transcriptional repression of the MEF2 transcription factor. *J Biol Chem*. 2001. doi:10.1074/jbc.M007364200

224. Li Zhang C, McKinsey TA, Olson EN. The transcriptional corepressor MITR is a signal-responsive inhibitor of myogenesis. *Proc Natl Acad Sci U S A*. 2001. doi:10.1073/pnas.131198498

225. Zhou X, Richon VM, Rifkind RA, Marks PA. Identification of a transcriptional repressor related to the noncatalytic domain of histone deacetylases 4 and 5. *Proc Natl Acad Sci U S A*. 2000. doi:10.1073/pnas.97.3.1056

226. Tong JJ, Liu J, Bertos NR, Yang XJ. Identification of HDAC10, a novel class II human histone deacetylase containing a leucine-rich domain. *Nucleic Acids Res*. 2002. doi:10.1093/nar/30.5.1114

227. Fischer DD, Cai R, Bhatia U, et al. Isolation and characterization of a novel class II histone deacetylase, HDAC10. *J Biol Chem*. 2002. doi:10.1074/jbc.M108055200

228. Kao HY, Lee CH, Komarov A, Han CC, Evans RM. Isolation and characterization of mammalian HDAC10, a novel histone deacetylase. *J Biol Chem*. 2002. doi:10.1074/jbc.M108931200

229. Guardiola AR, Yao TP. Molecular cloning and characterization of a novel histone deacetylase HDAC10. *J Biol Chem*. 2002. doi:10.1074/jbc.M109861200

230. Gao L, Cueto MA, Asselbergs F, Atadja P. Cloning and functional characterization of HDAC11, a novel member of the human histone deacetylase family. *J Biol Chem*. 2002. doi:10.1074/jbc.M111871200

231. Madsen AS, Olsen CA. Profiling of substrates for zinc-dependent lysine deacylase enzymes: HDAC3 exhibits decrotonylase activity in vitro. *Angew Chemie - Int Ed*. 2012. doi:10.1002/anie.201203754

232. Fellows R, Denizot J, Stellato C, et al. Microbiota derived short chain fatty acids promote histone crotonylation in the colon through histone deacetylases. *Nat Commun*. 2018;9(1):105. doi:10.1038/s41467-017-02651-5

233. Zhang X, Cao R, Niu J, et al. Molecular basis for hierarchical histone de-β-hydroxybutyrylation by SIRT3. *Cell Discov*. 2019. doi:10.1038/s41421-019-0103-0

234. Lahm A, Paolini C, Pallaoro M, et al. Unraveling the hidden catalytic activity of vertebrate class IIa histone deacetylases. *Proc Natl Acad Sci U S A*. 2007. doi:10.1073/pnas.0706487104

235. Aramsangtienchai P, Spiegelman NA, He B, et al. HDAC8 Catalyzes the Hydrolysis of Long Chain Fatty Acyl Lysine. *ACS Chem Biol*. 2016. doi:10.1021/acschembio.6b00396

236. Kutil Z, Novakova Z, Meleshin M, Mikesova J, Schutkowski M, Barinka C. Histone Deacetylase 11 Is a Fatty-Acid Deacylase. *ACS Chem Biol*. 2018. doi:10.1021/acschembio.7b00942

237. Radhakrishnan R, Li Y, Xiang S, et al. Histone deacetylase 10 regulates DNA mismatch repair and may involve the deacetylation of MutS homolog 2. *J Biol Chem*. 2015. doi:10.1074/jbc.M114.612945

238. Oehme I, Linke JP, Böck BC, et al. Histone deacetylase 10 promotes autophagy-mediated cell survival. *Proc Natl Acad Sci U S A*. 2013. doi:10.1073/pnas.1300113110

239. Hai Y, Shinsky SA, Porter NJ, Christianson DW. Histone deacetylase 10 structure and molecular function as a polyamine deacetylase. *Nat Commun*. 2017. doi:10.1038/ncomms15368

240. Rine J, Strathern JN, Hicks JB, Herskowitz I. A suppressor of mating-type locus mutations in Saccharomyces cerevisiae: Evidence for and identification of cryptic mating-type loci. *Genetics*. 1979.

241. Schnell R, Rine J. A position effect on the expression of a tRNA gene mediated by the SIR genes in Saccharomyces cerevisiae. *Mol Cell Biol*. 1986. doi:10.1128/mcb.6.2.494

242. Tanny JC, Dowd GJ, Huang J, Hilz H, Moazed D. An enzymatic activity in the yeast Sir2 protein that is essential for gene silencing. *Cell*. 1999. doi:10.1016/S0092-8674(00)81671-2

243. Frye RA. Characterization of five human cDNAs with homology to the yeast SIR2 gene: Sir2-like proteins (Sirtuins) metabolize NAD and may have protein ADP-ribosyltransferase activity. *Biochem Biophys Res Commun*. 1999. doi:10.1006/bbrc.1999.0897

244. Tanner KG, Landry J, Sternglanz R, Denu JM. Silent information regulator 2 family of NAD-dependent histone/protein deacetylases generates a unique product, 1-O-acetyl-ADP-ribose. *Proc Natl Acad Sci U S A*. 2000. doi:10.1073/pnas.250422697

245. Imai SI, Armstrong CM, Kaeberlein M, Guarente L. Transcriptional silencing and longevity protein Sir2 is an NAD-dependent histone deacetylase. *Nature*. 2000. doi:10.1038/35001622

246. Smith JS, Brachmann CB, Celic I, et al. A phylogenetically conserved NAD+-dependent protein deacetylase activity in the Sir2 protein family. *Proc Natl Acad Sci U S A*. 2000. doi:10.1073/pnas.97.12.6658

247. Landry J, Sutton A, Tafrov ST, et al. The silencing protein SIR2 and its homologs are NAD-dependent protein deacetylases. *Proc Natl Acad Sci U S A*. 2000. doi:10.1073/pnas.110148297

248. Frye RA. Phylogenetic classification of prokaryotic and eukaryotic Sir2-like proteins. *Biochem Biophys Res Commun*. 2000. doi:10.1006/bbrc.2000.3000

249. Jackson MD, Denu JM. Structural identification of 2′- and 3′-O-acetyl-ADP-ribose as novel metabolites derived from the Sir2 family β-NAD+ -dependent histone/protein deacetylases. *J Biol Chem*. 2002. doi:10.1074/jbc.M200671200

250. Haigis MC, Sinclair DA. Mammalian Sirtuins: Biological Insights and Disease Relevance. *Annu Rev Pathol Mech Dis*. 2010. doi:10.1146/annurev.pathol.4.110807.092250

251. Houtkooper RH, Pirinen E, Auwerx J. Sirtuins as regulators of metabolism and healthspan. *Nat Rev Mol Cell Biol*. 2012. doi:10.1038/nrm3293

252. Bosch-Presegué L, Vaquero A. Sirtuin-dependent epigenetic regulation in the maintenance of genome integrity. *FEBS J*. 2015. doi:10.1111/febs.13053

253. Sadhukhan S, Liu X, Ryu D, et al. Metabolomics-assisted proteomics identifies succinylation and SIRT5 as important regulators of cardiac function. *Proc Natl Acad Sci U S A*. 2016. doi:10.1073/pnas.1519858113

254. Colak G, Pougovkina O, Dai L, et al. Proteomic and Biochemical Studies of Lysine Malonylation Suggest Its Malonic Aciduria-associated Regulatory Role in Mitochondrial Function and Fatty Acid Oxidation. *Mol Cell Proteomics*. 2015;14(11):3056-3071. doi:10.1074/mcp.M115.048850

255. Li L, Shi L, Yang S, et al. SIRT7 is a histone desuccinylase that functionally links to chromatin compaction and genome stability. *Nat Commun*. 2016;7:12235. doi:10.1038/ncomms12235

256. Mathias RA, Greco TM, Oberstein A, et al. Sirtuin 4 Is a Lipoamidase Regulating Pyruvate Dehydrogenase Complex Activity. *Cell*. 2014;159(7):1615-1625. doi:10.1016/j.cell.2014.11.046

257. Jiang H, Khan S, Wang Y, et al. SIRT6 regulates TNF-α secretion through hydrolysis of long-chain fatty acyl lysine. *Nature*. 2013;496(7443):110-113. doi:10.1038/nature12038

258. Gil R, Barth S, Kanfi Y, Cohen HY. SIRT6 exhibits nucleosome-dependent deacetylase activity. *Nucleic Acids Res*. 2013. doi:10.1093/nar/gkt642

259. Lee S, Tan M, Dai L, et al. MS/MS of synthetic peptide is not sufficient to confirm new

types of protein modifications. *J Proteome Res*. 2013. doi:10.1021/pr300667e

260. Zhao Y, Garcia BA. Comprehensive catalog of currently documented histone modifications. *Cold Spring Harb Perspect Biol*. 2015. doi:10.1101/cshperspect.a025064

261. Nie L, Shuai L, Zhu M, et al. The landscape of histone modifications in a high-fat diet-induced obese (DIO) mouse model. *Mol Cell Proteomics*. 2017. doi:10.1074/mcp.M117.067553

262. Bos J, Muir TW. A Chemical Probe for Protein Crotonylation. *J Am Chem Soc*. 2018. doi:10.1021/jacs.7b13141

263. Yuan ZF, Sidoli S, Marchione DM, et al. EpiProfile 2.0: A Computational Platform for Processing Epi-Proteomics Mass Spectrometry Data. *J Proteome Res*. 2018. doi:10.1021/acs.jproteome.8b00133

264. Liu X, Sadhukhan S, Sun S, et al. High-Resolution Metabolomics with Acyl-CoA Profiling Reveals Widespread Remodeling in Response to Diet. *Mol Cell Proteomics*. 2015;14(6):1489-1500. doi:10.1074/mcp.M114.044859

265. Ogryzko V V., Schiltz RL, Russanova V, Howard BH, Nakatani Y. The transcriptional coactivators p300 and CBP are histone acetyltransferases. *Cell*. 1996;87:953-959. doi:10.1016/S0092-8674(00)82001-2

266. Liu X, Wei W, Liu Y, et al. MOF as an evolutionarily conserved histone crotonyltransferase and transcriptional activation by histone acetyltransferase-deficient and crotonyltransferase-competent CBP/p300. *Cell Discov*. 2017. doi:10.1038/celldisc.2017.16

267. Bheda P, Jing H, Wolberger C, Lin H. The Substrate Specificity of Sirtuins. *Annu Rev Biochem*. 2016. doi:10.1146/annurev-biochem-060815-014537

268. Eskandarian HA, Impens F, Nahori M-A, et al. A Role for SIRT2-Dependent Histone H3K18 Deacetylation in Bacterial Infection. *Science (80-)*. 2013;341(6145):1238858-1238858. doi:10.1126/science.1238858

269. Vaquero A, Scher M, Lee D, Erdjument-Bromage H, Tempst P, Reinberg D. Human SirT1 interacts with histone H1 and promotes formation of facultative heterochromatin. *Mol Cell*. 2004. doi:10.1016/j.molcel.2004.08.031

270. Das C, Lucia MS, Hansen KC, Tyler JK. CBP/p300-mediated acetylation of histone H3 on lysine 56. *Nature*. 2009. doi:10.1038/nature07861

271. Vaquero A, Scher MB, Dong HL, et al. SirT2 is a histone deacetylase with preference for histone H4 Lys 16 during mitosis. *Genes Dev*. 2006. doi:10.1101/gad.1412706

272. Schölz C, Weinert BT, Wagner SA, et al. Acetylation site specificities of lysine deacetylase inhibitors in human cells. *Nat Biotechnol*. 2015. doi:10.1038/nbt.3130

273. Chen Y, Zhao W, Yang JS, et al. Quantitative acetylome analysis reveals the roles of SIRT1 in regulating diverse substrates and cellular pathways. *Mol Cell Proteomics*. 2012. doi:10.1074/mcp.M112.019547

274. Liu S, Yu H, Liu Y, et al. Chromodomain Protein CDYL Acts as a Crotonyl-CoA Hydratase to Regulate Histone Crotonylation and Spermatogenesis. *Mol Cell*. 2017;67(5):853-866.e5. doi:10.1016/j.molcel.2017.07.011

275. Tweedie-Cullen RY, Brunner AM, Grossmann J, et al. Identification of combinatorial patterns of post-translational modifications on individual histones in the mouse brain. *PLoS One*. 2012. doi:10.1371/journal.pone.0036980

276. Bock I, Dhayalan A, Kudithipudi S, Brandt O, Rathert P, Jeltsch A. Detailed specificity analysis of antibodies binding to modified histone tails with peptide arrays. *Epigenetics*. 2011. doi:10.4161/epi.6.2.13837

277. Egelhofer TA, Minoda A, Klugman S, et al. An assessment of histone-modification antibody quality. *Nat Struct Mol Biol*. 2011. doi:10.1038/nsmb.1972

278. Rothbart SB, Dickson BM, Raab JR, et al. An Interactive Database for the Assessment of Histone Antibody Specificity. *Mol Cell*. 2015. doi:10.1016/j.molcel.2015.06.022

279. Nishikori S, Hattori T, Fuchs SM, et al. Broad ranges of affinity and specificity of anti-histone antibodies revealed by a quantitative peptide immunoprecipitation assay. *J Mol Biol*. 2012. doi:10.1016/j.jmb.2012.09.022

280. Fuchs SM, Krajewski K, Baker RW, Miller VL, Strahl BD. Influence of combinatorial histone modifications on antibody and effector protein recognition. *Curr Biol*. 2011. doi:10.1016/j.cub.2010.11.058

281. Shah RN, Grzybowski AT, Cornett EM, et al. Examining the Roles of H3K4 Methylation States with Systematically Characterized Antibodies. *Mol Cell*. 2018. doi:10.1016/j.molcel.2018.08.015

282. Grzybowski AT, Chen Z, Ruthenburg AJ. Calibrating ChIP-Seq with Nucleosomal Internal Standards to Measure Histone Modification Density Genome Wide. *Mol Cell*. 2015. doi:10.1016/j.molcel.2015.04.022

283. Gattner MJ, Vrabel M, Carell T. Synthesis of ε-N-propionyl-, ε-N-butyryl-, and ε-N-crotonyl-lysine containing histone H3 using the pyrrolysine system. *Chem Commun*. 2013. doi:10.1039/c2cc37836a

284. Leroy G, Dimaggio PA, Chan EY, et al. A quantitative atlas of histone modification signatures from human cancer cells. *Epigenetics Chromatin*. 2013;6(1):20. doi:10.1186/1756-8935-6-20

285. Wagner GR, Hirschey MD. Nonenzymatic protein acylation as a carbon stress regulated by sirtuin deacylases. *Mol Cell*. 2014;54(1):5-16. doi:10.1016/j.molcel.2014.03.027

286. Trub AG, Hirschey MD. Reactive Acyl-CoA Species Modify Proteins and Induce Carbon Stress. *Trends Biochem Sci*. 2018. doi:10.1016/j.tibs.2018.02.002

287. James AM, Smith AC, Smith CL, Robinson AJ, Murphy MP. Proximal Cysteines that Enhance Lysine N-Acetylation of Cytosolic Proteins in Mice Are Less Conserved in Longer-Living Species. *Cell Rep*. 2018. doi:10.1016/j.celrep.2018.07.007

288. Fisher-Wellman KH, Draper JA, Davidson MT, et al. Respiratory Phenomics across Multiple Models of Protein Hyperacylation in Cardiac Mitochondria Reveals a Marginal Impact on Bioenergetics. *Cell Rep*. 2019;26(6):1557-1572.e8. doi:10.1016/j.celrep.2019.01.057

289. Peterson BS, Campbell JE, Ilkayeva O, Grimsrud PA, Hirschey MD, Newgard CB. Remodeling of the Acetylproteome by SIRT3 Manipulation Fails to Affect Insulin Secretion or β Cell Metabolism in the Absence of Overnutrition. *Cell Rep*. 2018. doi:10.1016/j.celrep.2018.05.088

290. Pougovkina O, Te Brinke H, Wanders RJA, Houten SM, de Boer VCJ. Aberrant protein acylation is a common observation in inborn errors of acyl-CoA metabolism. *J Inherit Metab Dis*. 2014;37(5):709-714. doi:10.1007/s10545-014-9684-9

291. Yun JW, Jo KI, Woo HI, et al. A novel ACAD8 mutation in asymptomatic patients with isobutyryl-CoA dehydrogenase deficiency and a review of the ACAD8 mutation spectrum. *Clin Genet*. 2015. doi:10.1111/cge.12350

292. Muir A, Danai L V., Gui DY, Waingarten CY, Lewis CA, Vander Heiden MG. Environmental cystine drives glutamine anaplerosis and sensitizes cancer cells to glutaminase inhibition. *Elife*. 2017. doi:10.7554/eLife.27713

293. Shao D, Villet O, Zhang Z, et al. Glucose promotes cell growth by suppressing branched-chain amino acid degradation. *Nat Commun*. 2018. doi:10.1038/s41467-018-05362-7

294. Zhang Y-K, Qu Y-Y, Lin Y, et al. Enoyl-CoA hydratase-1 regulates mTOR signaling and apoptosis by sensing nutrients. *Nat Commun*. 2017;8(1):464. doi:10.1038/s41467-017-00489-5

295. Green CR, Wallace M, Divakaruni AS, et al. Branched-chain amino acid catabolism fuels adipocyte differentiation and lipogenesis. *Nat Chem Biol*. 2016;12(1):15-21. doi:10.1038/nchembio.1961

296. Wishart TM, Rooney TM, Lamont DJ, et al. Combining Comparative Proteomics and Molecular Genetics Uncovers Regulators of Synaptic and Axonal Stability and Degeneration In Vivo. *PLoS Genet*. 2012. doi:10.1371/journal.pgen.1002936

297. Llavero Hurtado M, Fuller HR, Wong AMS, et al. Proteomic mapping of differentially vulnerable pre-synaptic populations identifies regulators of neuronal stability in vivo. *Sci Rep*. 2017;7(1):12412. doi:10.1038/s41598-017-12603-0

298. Watson E, Olin-Sandoval V, Hoy MJ, et al. Metabolic network rewiring of propionate flux compensates vitamin B12 deficiency in C. elegans. *Elife*. 2016. doi:10.7554/eLife.17670

APPENDIX

Appendix Figure 1 Spectra for Kmea sites identified by IP-MS/MS.
Annotated MASCOT images for the 22 histone Kmea sites identified by IP-MS/MS using pan Kmea antibody. The parameters for the search included the following modifications: Kmea (lysine +68.023 Da), Kac, N-terminal acetylation, K/Rme1, K/Rme2, and Kme3. Histone peptide matches with Kmea sites were manually verified for correctness for all spectra with MASCOT scores of at least 20. All spectra were manually verified for quality.

H1K45ma

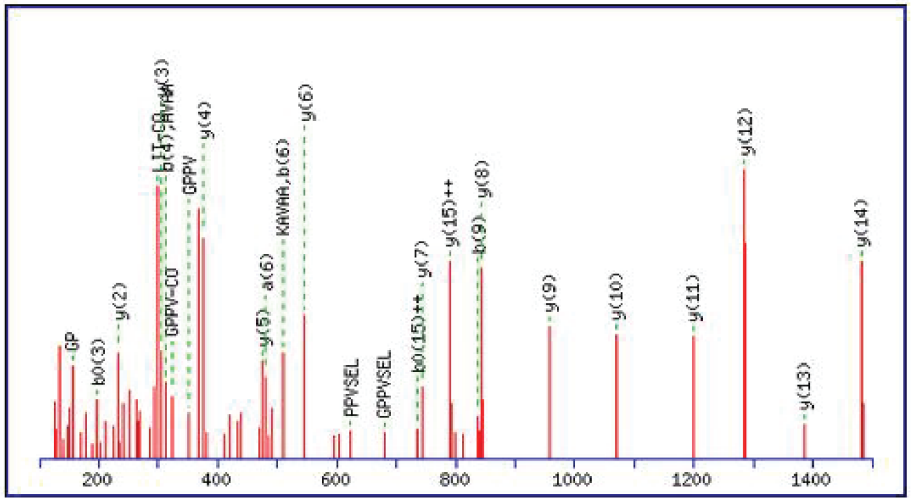

MS/MS Fragmentation of **ASGPPVSELITKAVAASK**
Found in **P16402**, Histone H1.3

Match to Query 2445: 1792.987550 from(897.501051,2+)

Monoisotopic mass of neutral peptide Mr(calc): 1792.99
Variable modifications:
K12 : Methacryl (K)
Ions Score: 90 **Expect:** 1.1e-006
Matches (Bold Red): 28/408 fragment ions using 40 most intense peaks

#	Immon.	a	a^{++}	a^{*}	a^{*++}	a^{0}	a^{0++}	b	b^{++}	b^{*}	b^{*++}	b^{0}	b^{0++}	Seq.	y	y^{++}	y^{*}	y^{*++}	y^{0}	y^{0++}	#
1	44.05	44.05	22.53					72.04	36.53					A							18
2	60.04	131.08	66.04			113.07	57.04	159.08	80.04			141.07	71.04	S	1722.96	861.99	1705.94	853.47	1704.95	852.98	17
3	30.03	188.10	94.56			170.09	85.55	216.10	108.55			**198.09**	99.55	G	1635.93	818.47	1618.90	809.96	1617.92	809.46	16
4	70.07	285.16	143.08			267.15	134.08	**313.15**	157.08			295.14	148.07	P	1578.91	**789.96**	1561.88	781.45	1560.90	780.95	15
5	70.07	382.21	191.61			364.20	182.60	410.20	205.61			392.19	196.60	P	**1481.86**	741.43	1464.83	732.92	1463.85	732.43	14
6	72.08	**481.28**	241.14			463.27	232.14	**509.27**	255.14			491.26	246.13	V	**1384.80**	692.91	1367.78	684.39	1366.79	683.90	13
7	60.04	568.31	284.66			550.30	275.65	596.30	298.66			578.29	289.65	S	**1285.74**	643.37	1268.71	634.86	1267.73	634.37	12
8	102.05	697.35	349.18			679.34	340.17	725.35	363.18			707.34	354.17	E	**1198.70**	599.86	1181.68	591.34	1180.69	590.85	11
9	86.10	810.44	405.72			792.43	396.72	**838.43**	419.72			820.42	410.71	L	**1069.66**	535.33	1052.63	526.82	1051.65	526.33	10
10	86.10	923.52	462.26			905.51	453.26	951.51	476.26			933.50	467.26	I	**956.58**	478.79	939.55	470.28	938.57	469.79	9
11	74.06	1024.57	512.79			1006.56	503.78	1052.56	526.78			1034.55	517.78	T	**843.49**	422.25	826.47	413.74	825.48	413.25	8
12	169.13	1220.69	610.85	1203.66	602.33	1202.68	601.84	1248.68	624.85	1231.66	616.33	1230.67	615.84	K	**742.45**	371.73	725.42	363.21	724.44	362.72	7
13	44.05	1291.73	646.37	1274.70	637.85	1273.71	637.36	1319.72	660.36	1302.69	651.85	1301.71	651.36	A	**546.32**	273.67	529.30	265.15	528.31	264.66	6
14	72.08	1390.79	695.90	1373.77	687.39	1372.78	686.90	1418.79	709.90	1401.76	701.38	1400.78	700.89	V	**475.29**	238.15	458.26	229.63	457.28	229.14	5
15	44.05	1461.83	731.42	1444.80	722.91	1443.82	722.41	1489.83	745.42	1472.80	736.90	1471.82	**736.41**	A	**376.22**	188.61	359.19	180.10	358.21	179.61	4
16	44.05	1532.87	766.94	1515.84	758.42	1514.86	757.93	1560.86	780.94	1543.84	772.42	1542.85	771.93	A	**305.18**	153.09	288.16	144.58	287.17	144.09	3
17	60.04	1619.90	810.45	1602.87	801.94	1601.89	801.45	1647.90	824.45	1630.87	815.94	1629.88	815.45	S	**234.14**	117.58	217.12	109.06	216.13	108.57	2
18	101.11													K	147.11	74.06	130.09	65.55			1

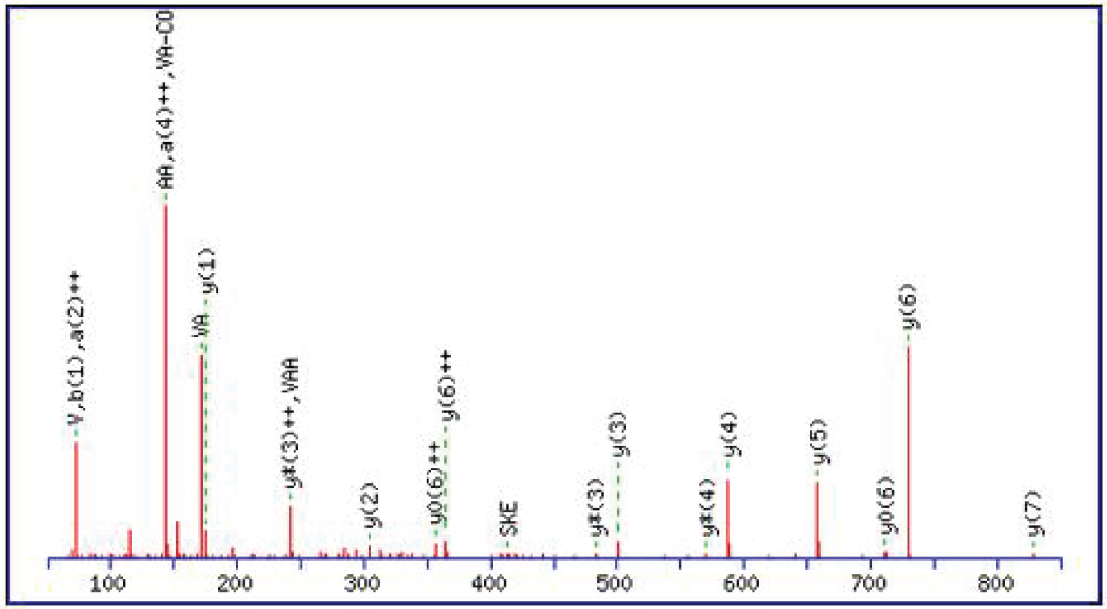

H1K51ma

MS/MS Fragmentation of AVAASKER
Found in P10412, Histone H1.4

Match to Query 194: 898.486870 from(450.250711,2+)

Monoisotopic mass of neutral peptide Mr(calc): 898.49
Variable modifications:
K6 : Methacryl (K)
Ions Score: 60 **Expect:** 0.00038
Matches (Bold Red): 25/126 fragment ions using 24 most intense peaks

#	Immon.	a	a^{++}	a^{*}	a^{*++}	a^{0}	a^{0++}	b	b^{++}	b^{*}	b^{*++}	b^{0}	b^{0++}	Seq.	y	y^{++}	y^{*}	y^{*++}	y^{0}	y^{0++}	#
1	44.05	44.05	22.53					**72.04**	36.53					A							8
2	**72.08**	**143.12**	**72.06**					**171.11**	86.06					V	**828.46**	414.73	811.43	406.22	810.45	405.73	7
3	44.05	214.15	107.58					**242.15**	121.58					A	**729.39**	**365.20**	712.36	356.68	**711.38**	**356.19**	6
4	44.05	285.19	**143.10**					313.19	157.10					A	**658.35**	329.68	641.33	321.17	640.34	320.67	5
5	60.04	372.22	186.62			354.21	177.61	400.22	200.61			382.21	191.61	S	**587.31**	294.16	**570.29**	285.65	569.30	285.16	4
6	169.13	568.35	284.68	551.32	276.16	550.33	275.67	596.34	298.67	579.31	290.16	578.33	289.67	K	**500.28**	250.64	**483.26**	**242.13**	482.27	241.64	3
7	102.05	697.39	349.20	680.36	340.68	679.38	340.19	725.38	363.20	708.36	354.68	707.37	354.19	E	**304.16**	152.58	287.13	144.07	286.15	143.58	2
8	129.11													R	**175.12**	88.06	158.09	79.55			1

H1K62ma

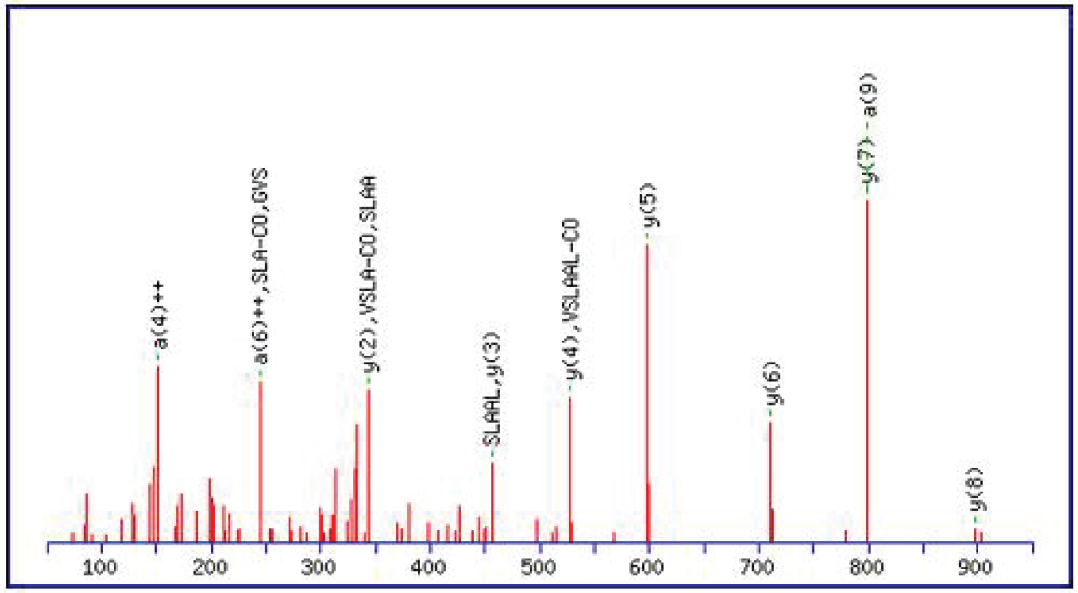

MS/MS Fragmentation of **SGVSLAALKK**
Found in **P10412**, Histone H1.4

Match to Query 496: 1040.622854 from(521.318703,2+)

Monoisotopic mass of neutral peptide Mr(calc): 1040.62
Variable modifications:
K10 : Methacryl (K)
Ions Score: 78 **Expect:** 7.2e-006
Matches (Bold Red): 17/182 fragment ions using 10 most intense peaks

Should be K9

#	Immon.	a	a^{++}	a^{*}	a^{*++}	a^{0}	a^{0++}	b	b^{++}	b^{*}	b^{*++}	b^{0}	b^{0++}	Seq.	y	y^{++}	y^{*}	y^{*++}	y^{0}	y^{0++}	#
1	60.04	60.04	30.53			42.03	21.52	88.04	44.52			70.03	35.52	S							10
2	30.03	117.07	59.04			99.06	50.03	145.06	73.03			127.05	64.03	G	954.60	477.80	937.57	469.29	936.59	468.80	9
3	72.08	216.13	108.57			198.12	99.57	**244.13**	122.57			226.12	113.56	V	**897.58**	449.29	880.55	440.78	879.57	440.29	8
4	60.04	303.17	**152.09**			285.16	143.08	331.16	166.08			313.15	157.08	S	**798.51**	399.76	781.48	391.24	780.50	390.75	7
5	86.10	416.25	208.63			398.24	199.62	444.25	222.63			426.23	213.62	L	**711.48**	356.24	694.45	347.73			6
6	44.05	487.29	**244.15**			469.28	235.14	515.28	258.14			497.27	249.14	A	**598.39**	299.70	581.37	291.19			5
7	44.05	558.32	279.67			540.31	270.66	586.32	293.66			568.31	284.66	A	**527.36**	264.18	510.33	255.67			4
8	86.10	671.41	336.21			653.40	327.20	699.40	350.21			681.39	341.20	L	**456.32**	228.66	439.29	220.15			3
9	101.11	**799.50**	400.26	782.48	391.74	781.49	391.25	827.50	414.25	810.47	405.74	809.49	405.25	K	**343.23**	172.12	326.21	163.61			2
10	169.13													K	215.14	108.07	198.11	99.56			1

H1K63ma

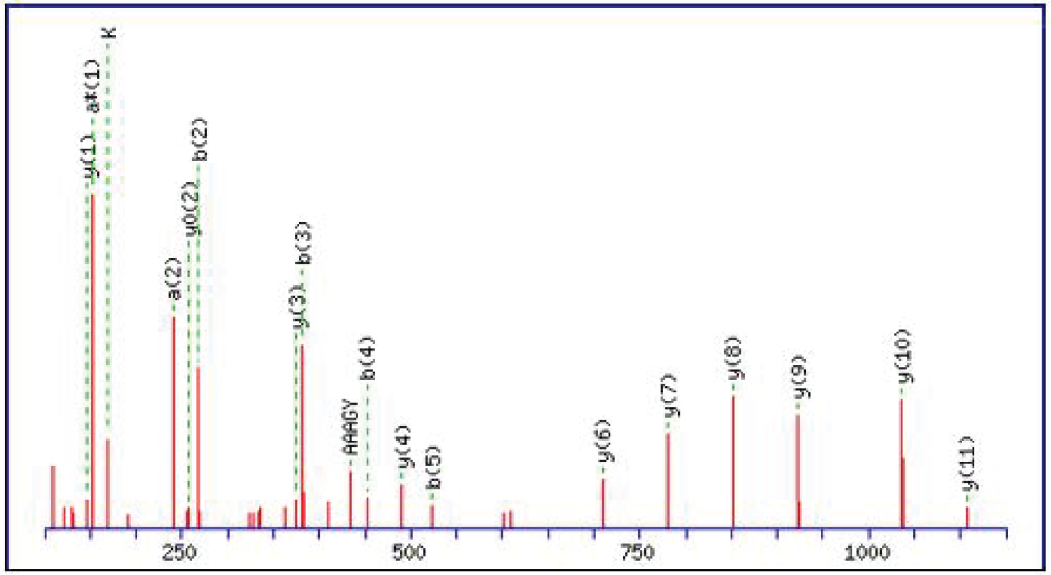

MS/MS Fragmentation of **KALAAAGYDVEK**
Found in **P10412**, Histone H1.4

Match to Query 944: 1302.681970 from(652.348261,2+)

Monoisotopic mass of neutral peptide Mr(calc): 1302.68
Variable modifications:
K1 : Methacryl (K)
Ions Score: 70 **Expect:** 7.3e-005
Matches (Bold Red): 19/253 fragment ions using 28 most intense peaks

#	Immon.	a	a^{++}	a^{*}	a^{*++}	a^{0}	a^{0++}	b	b^{++}	b^{*}	b^{*++}	b^{0}	b^{0++}	Seq.	y	y^{++}	y^{*}	y^{*++}	y^{0}	y^{0++}	#
1	**169.13**	**169.13**	85.07	**152.11**	76.56			197.13	99.07	180.10	90.55			K							12
2	44.05	**240.17**	120.59	223.14	112.08			**268.17**	134.59	251.14	126.07			A	**1107.57**	554.29	1090.54	545.77	1089.56	545.28	11
3	86.10	353.25	177.13	336.23	168.62			**381.25**	191.13	364.22	182.62			L	**1036.53**	518.77	1019.50	510.26	1018.52	509.76	10
4	44.05	424.29	212.65	407.27	204.14			**452.29**	226.65	435.26	218.13			A	**923.45**	462.23	906.42	453.71	905.44	453.22	9
5	44.05	495.33	248.17	478.30	239.65			**523.32**	262.17	506.30	253.65			A	**852.41**	426.71	835.38	418.20	834.40	417.70	8
6	44.05	566.37	283.69	549.34	275.17			594.36	297.68	577.33	289.17			A	**781.37**	391.19	764.35	382.68	763.36	382.18	7
7	30.03	623.39	312.20	606.36	303.68			651.38	326.19	634.36	317.68			G	**710.34**	355.67	693.31	347.16	692.32	346.67	6
8	136.08	786.45	393.73	769.42	385.22			814.45	407.73	797.42	399.21			Y	653.31	327.16	636.29	318.65	635.30	318.16	5
9	88.04	901.48	451.24	884.45	442.73	883.47	442.24	929.47	465.24	912.45	456.73	911.46	456.23	D	**490.25**	245.63	473.22	237.12	472.24	236.62	4
10	72.08	1000.55	500.78	983.52	492.26	982.54	491.77	1028.54	514.77	1011.51	506.26	1010.53	505.77	V	**375.22**	188.12	358.20	179.60	357.21	179.11	3
11	102.05	1129.59	565.30	1112.56	556.78	1111.58	556.29	1157.58	579.30	1140.56	570.78	1139.57	570.29	E	276.16	138.58	259.13	130.07	**258.14**	129.58	2
12	101.11													K	**147.11**	74.06	130.09	65.55			1

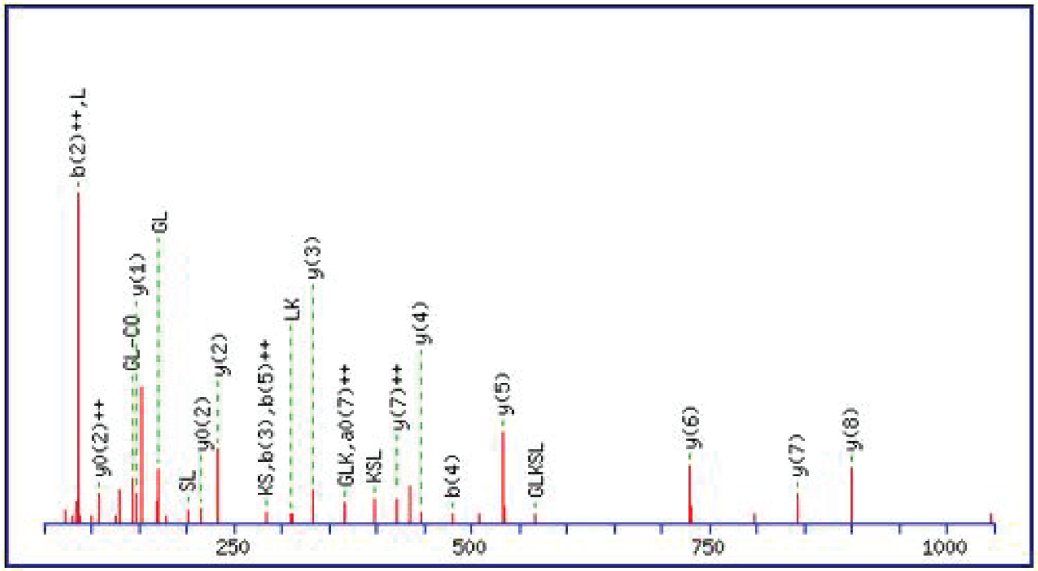

H1K84ma

MS/MS Fragmentation of **LGLKSLVSK**
Found in **P10412**, Histone H1.4

Match to Query 432: 1011.631672 from(506.823112,2+)

Monoisotopic mass of neutral peptide Mr(calc): 1011.63
Variable modifications:
K4 : Methacryl (K)
Ions Score: 59 **Expect:** 0.00045
Matches (Bold Red): 32/163 fragment ions using 32 most intense peaks

#	Immon.	a	a^{++}	a^{*}	a^{*++}	a^{0}	a^{0++}	b	b^{++}	b^{*}	b^{*++}	b^{0}	b^{0++}	Seq.	y	y^{++}	y^{*}	y^{*++}	y^{0}	y^{0++}	#
1	**86.10**	**86.10**	43.55					114.09	57.55					L							9
2	30.03	**143.12**	72.06					**171.11**	**86.06**					G	**899.56**	450.28	882.53	441.77	881.55	441.28	8
3	**86.10**	256.20	128.60					**284.20**	142.60					L	**842.53**	**421.77**	825.51	413.26	824.52	412.77	7
4	169.13	452.32	226.67	435.30	218.15			**480.32**	240.66	463.29	232.15			K	**729.45**	365.23	712.42	356.72	711.44	356.22	6
5	60.04	539.36	270.18	522.33	261.67	521.34	261.18	**567.35**	**284.18**	550.32	275.67	549.34	275.17	S	**533.33**	267.17	516.30	258.66	515.32	258.16	5
6	**86.10**	652.44	326.72	635.41	318.21	634.43	317.72	680.43	340.72	663.41	332.21	662.42	331.72	L	**446.30**	223.65	429.27	215.14	428.29	214.65	4
7	72.08	751.51	376.26	734.48	367.74	733.50	**367.25**	779.50	390.25	762.48	381.74	761.49	381.25	V	**333.21**	167.11	316.19	158.60	315.20	158.10	3
8	60.04	838.54	419.77	821.51	411.26	820.53	410.77	866.53	433.77	849.51	425.26	848.52	424.77	S	**234.14**	117.58	217.12	109.06	**216.13**	**108.57**	2
9	101.11													K	**147.11**	74.06	130.09	65.55			1

H1K89ma

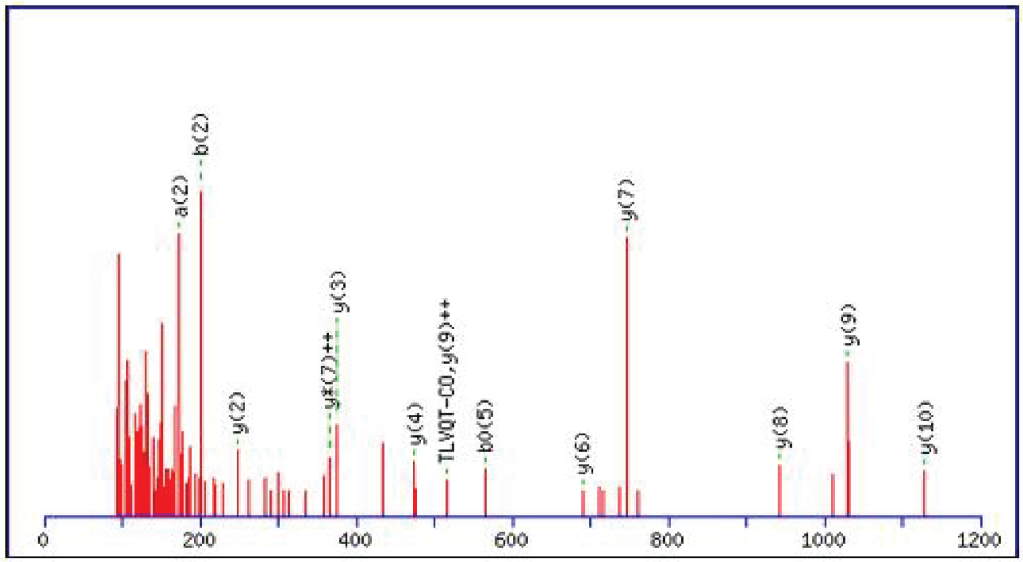

MS/MS Fragmentation of **SLVSKGTLVQTK**
Found in **P10412**, Histone H1.4

Match to Query 990: 1327.769796 from(664.892174,2+)

Monoisotopic mass of neutral peptide Mr(calc): 1327.77
Variable modifications:
K5 : Methacryl (K)
Ions Score: 70 **Expect:** 9.7e-005
Matches (Bold Red): 14/262 fragment ions using 19 most intense peaks

#	Immon.	a	a^{++}	a^*	a^{*++}	a^0	a^{0++}	b	b^{++}	b^*	b^{*++}	b^0	b^{0++}	Seq.	y	y^{++}	y^*	y^{*++}	y^0	y^{0++}	#
1	60.04	60.04	30.53			42.03	21.52	88.04	44.52			70.03	35.52	S							12
2	86.10	**173.13**	87.07			155.12	78.06	**201.12**	101.07			183.11	92.06	L	1241.75	621.38	1224.72	612.86	1223.74	612.37	11
3	72.08	272.20	136.60			254.19	127.60	300.19	150.60			282.18	141.59	V	**1128.66**	564.83	1111.64	556.32	1110.65	555.83	10
4	60.04	359.23	180.12			341.22	171.11	387.22	194.12			369.21	185.11	S	**1029.59**	**515.30**	1012.57	506.79	1011.58	506.30	9
5	169.13	555.35	278.18	538.32	269.67	537.34	269.17	583.34	292.18	566.32	283.66	**565.33**	283.17	K	**942.56**	471.78	925.54	463.27	924.55	462.78	8
6	30.03	612.37	306.69	595.34	298.18	594.36	297.68	640.37	320.69	623.34	312.17	622.36	311.68	G	**746.44**	373.72	729.41	**365.21**	728.43	364.72	7
7	74.06	713.42	357.21	696.39	348.70	695.41	348.21	741.41	371.21	724.39	362.70	723.40	362.21	T	**689.42**	345.21	672.39	336.70	671.41	336.21	6
8	86.10	826.50	413.76	809.48	405.24	808.49	404.75	854.50	427.75	837.47	419.24	836.49	418.75	L	588.37	294.69	571.34	286.18	570.36	285.68	5
9	72.08	925.57	463.29	908.55	454.78	907.56	454.28	953.57	477.29	936.54	468.77	935.56	468.28	V	**475.29**	238.15	458.26	229.63	457.28	229.14	4
10	101.07	1053.63	527.32	1036.60	518.81	1035.62	518.31	1081.63	541.32	1064.60	532.80	1063.61	532.31	Q	**376.22**	188.61	359.19	180.10	358.21	179.61	3
11	74.06	1154.68	577.84	1137.65	569.33	1136.67	568.84	1182.67	591.84	1165.65	583.33	1164.66	582.83	T	**248.16**	124.58	231.13	116.07	230.15	115.58	2
12	101.11													K	147.11	74.06	130.09	65.55			1

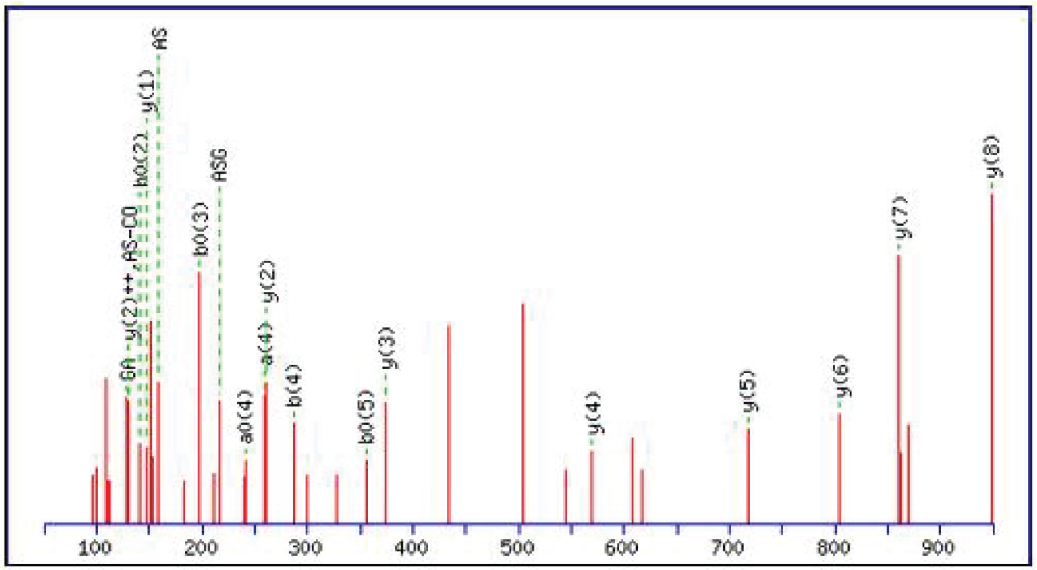

H1K105ma

MS/MS Fragmentation of **GTGASGSFKLNK**
Found in **P10412**, Histone H1.4

Match to Query 802: 1233.635636 from(617.825094,2+)

Monoisotopic mass of neutral peptide Mr(calc): 1233.64
Variable modifications:
K9 : Methacryl (K)
Ions Score: 56 **Expect:** 0.0017
Matches (Bold Red): 26/236 fragment ions using 30 most intense peaks

#	Immon.	a	a^{++}	a^{*}	a^{*++}	a^{0}	a^{0++}	b	b^{++}	b^{*}	b^{*++}	b^{0}	b^{0++}	Seq.	y	y^{++}	y^{*}	y^{*++}	y^{0}	y^{0++}	#
1	30.03	30.03	15.52					58.03	29.52					G							12
2	74.06	**131.08**	66.04			113.07	57.04	**159.08**	80.04			**141.07**	71.04	T	1177.62	589.31	1160.59	580.80	1159.61	580.31	11
3	30.03	188.10	94.56			170.09	85.55	**216.10**	108.55			**198.09**	99.55	G	1076.57	538.79	1059.55	530.28	1058.56	529.79	10
4	44.05	**259.14**	130.07			**241.13**	121.07	**287.13**	144.07			269.12	135.07	A	1019.55	510.28	1002.53	501.77	1001.54	501.27	9
5	60.04	346.17	173.59			328.16	164.58	374.17	187.59			**356.16**	178.58	S	**948.51**	474.76	931.49	466.25	930.50	465.76	8
6	30.03	403.19	202.10			385.18	193.10	431.19	**216.10**			413.18	207.09	G	**861.48**	431.25	844.46	422.73	843.47	422.24	7
7	60.04	490.23	245.62			472.22	236.61	518.22	259.61			500.21	250.61	S	**804.46**	402.73	787.43	394.22	786.45	393.73	6
8	120.08	637.29	319.15			619.28	310.15	665.29	333.15			647.28	324.14	F	**717.43**	359.22	700.40	350.71			5
9	169.13	833.42	417.21	816.39	408.70	815.40	408.21	861.41	431.21	844.38	422.70	843.40	422.20	K	**570.36**	285.68	553.33	277.17			4
10	86.10	946.50	473.75	929.47	465.24	928.49	464.75	974.49	487.75	957.47	479.24	956.48	478.75	L	**374.24**	187.62	357.21	179.11			3
11	87.06	1060.54	530.77	1043.52	522.26	1042.53	521.77	1088.54	544.77	1071.51	536.26	1070.53	535.77	N	**261.16**	**131.08**	244.13	122.57			2
12	101.11													K	**147.11**	74.06	130.09	65.55			1

H2AK4ma

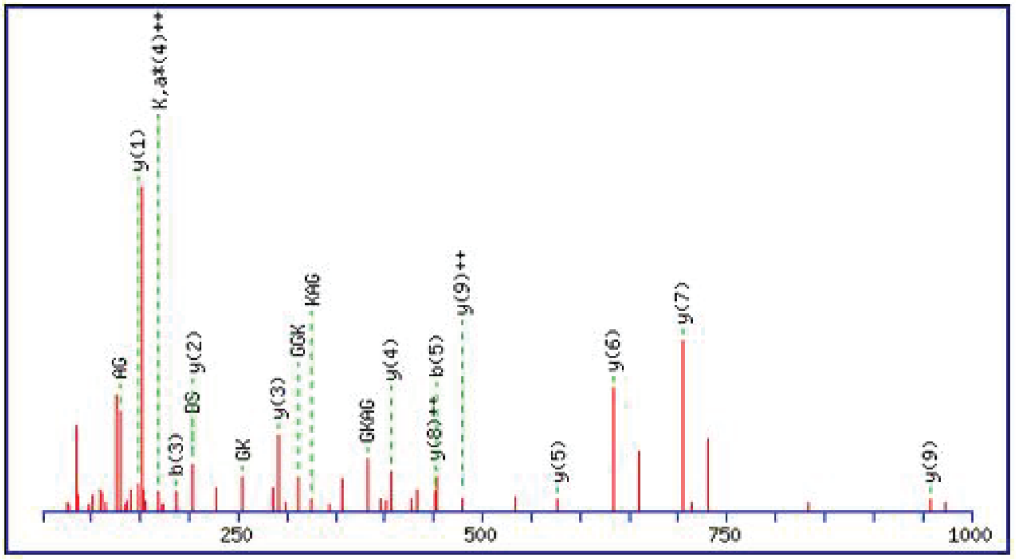

MS/MS Fragmentation of **AGGKAGKDSGK**
Found in **P0C0S5**, Histone H2A.Z

Match to Query 562: 1084.551322 from(543.282937,2+)

Monoisotopic mass of neutral peptide Mr(calc): 1084.55
Variable modifications:
K4 : Methacryl (K)
K7 : Acetyl (K)
Ions Score: 45 **Expect:** 0.011
Matches (Bold Red): 25/208 fragment ions using 38 most intense peaks

#	Immon.	a	a^{++}	a^*	a^{*++}	a^0	a^{0++}	b	b^{++}	b^*	b^{*++}	b^0	b^{0++}	Seq.	y	y^{++}	y^*	y^{*++}	y^0	y^{0++}	#
1	44.05	44.05	22.53					72.04	36.53					A							11
2	30.03	101.07	51.04					**129.07**	65.04					G	1014.52	507.76	997.49	499.25	996.51	498.76	10
3	30.03	158.09	79.55					**186.09**	93.55					G	**957.50**	**479.25**	940.47	470.74	939.49	470.25	9
4	**169.13**	354.21	177.61	337.19	**169.10**			**382.21**	191.61	365.18	183.09			K	900.48	**450.74**	883.45	442.23	882.47	441.74	8
5	44.05	425.25	213.13	408.22	204.62			**453.25**	227.13	436.22	218.61			A	**704.36**	352.68	687.33	344.17	686.35	343.68	7
6	30.03	482.27	241.64	465.25	233.13			510.27	255.64	493.24	247.12			G	**633.32**	317.16	616.29	308.65	615.31	308.16	6
7	143.12	652.38	326.69	635.35	318.18			680.37	340.69	663.35	332.18			K	**576.30**	288.65	559.27	280.14	558.29	279.65	5
8	88.04	767.40	384.21	750.38	375.69	749.39	375.20	795.40	398.20	778.37	389.69	777.39	389.20	D	**406.19**	203.60	389.17	195.09	388.18	194.59	4
9	60.04	854.44	427.72	837.41	419.21	836.43	418.72	882.43	441.72	865.40	433.21	864.42	432.71	S	**291.17**	146.09	274.14	137.57	273.16	137.08	3
10	30.03	911.46	456.23	894.43	447.72	893.45	447.23	939.45	470.23	922.43	461.72	921.44	461.22	G	**204.13**	102.57	187.11	94.06			2
11	101.11													K	**147.11**	74.06	130.09	65.55			1

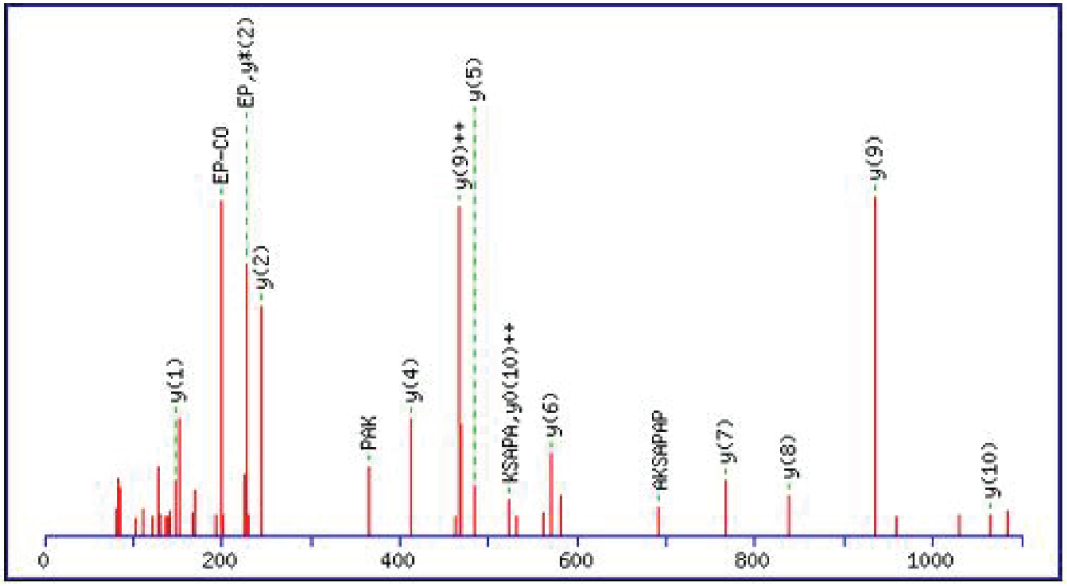

H2BK5ma

MS/MS Fragmentation of **PEPAKSAPAPK**
Found in **P06899**, Histone H2B type 1-J

Match to Query 685: 1159.623604 from(580.819078,2+)

Monoisotopic mass of neutral peptide Mr(calc): 1159.62
Variable modifications:
K5 : Methacryl (K)
Ions Score: 65 **Expect:** 0.00027
Matches (Bold Red): 22/225 fragment ions using 27 most intense peaks

#	Immon.	a	a^{++}	a^*	a^{*++}	a^0	a^{0++}	b	b^{++}	b^*	b^{*++}	b^0	b^{0++}	Seq.	y	y^{++}	y^*	y^{*++}	y^0	y^{0++}	#
1	70.07	70.07	35.54					98.06	49.53					P							11
2	102.05	**199.11**	100.06			181.10	91.05	**227.10**	114.05			209.09	105.05	E	**1063.58**	532.29	1046.55	523.78	1045.57	**523.29**	10
3	70.07	296.16	148.58			278.15	139.58	324.16	162.58			306.14	153.58	P	**934.54**	**467.77**	917.51	459.26	916.52	458.77	9
4	44.05	367.20	184.10			349.19	175.10	395.19	198.10			377.18	189.09	A	**837.48**	419.25	820.46	410.73	819.47	410.24	8
5	169.13	563.32	282.16	546.29	273.65	545.31	273.16	591.31	296.16	574.29	287.65	573.30	287.16	K	**766.45**	383.73	749.42	375.21	748.44	374.72	7
6	60.04	650.35	325.68	633.32	317.17	632.34	316.67	678.35	339.68	661.32	331.16	660.34	330.67	S	**570.32**	285.67	553.30	277.15	552.31	276.66	6
7	44.05	721.39	361.20	704.36	352.68	703.38	352.19	749.38	375.20	732.36	366.68	731.37	366.19	A	**483.29**	242.15	466.27	233.64			5
8	70.07	818.44	409.72	801.41	401.21	800.43	400.72	846.44	423.72	829.41	415.21	828.42	414.72	P	**412.26**	206.63	395.23	198.12			4
9	44.05	889.48	445.24	872.45	436.73	871.47	436.24	917.47	459.24	900.45	450.73	899.46	450.23	A	315.20	158.10	298.18	149.59			3
10	70.07	986.53	493.77	969.50	485.26	968.52	484.76	1014.53	507.77	997.50	499.25	996.51	498.76	P	**244.17**	122.59	**227.14**	114.07			2
11	101.11													K	**147.11**	74.06	130.09	65.55			1

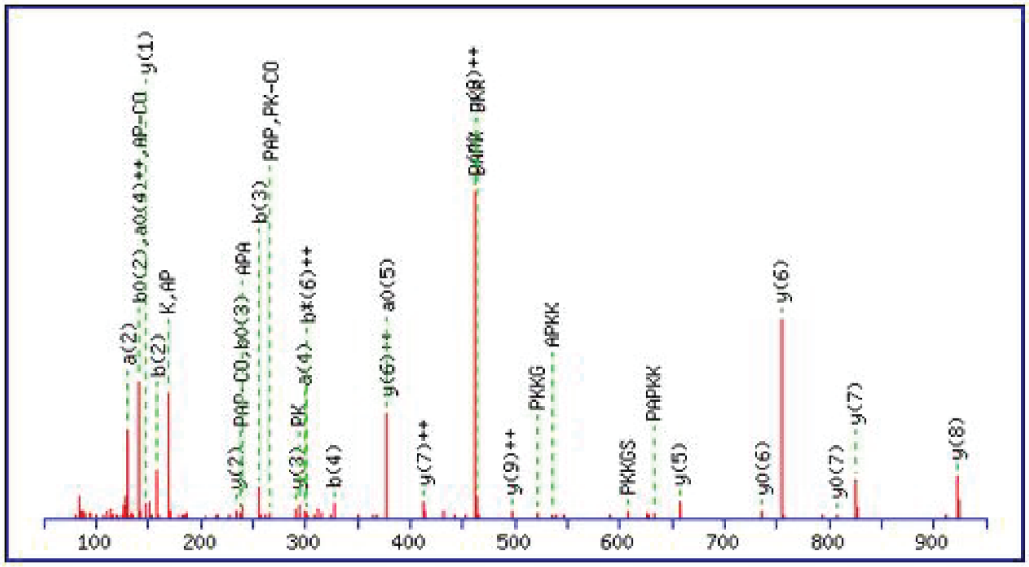

H2BK11ma

MS/MS Fragmentation of **SAPAPKKGSK**
Found in **P06899**, Histone H2B type 1-J

Match to Query 555: 1079.596942 from(540.805747,2+)

Monoisotopic mass of neutral peptide Mr(calc): 1079.60
Variable modifications:
K6 : Methacryl (K)
K7 : Acetyl (K)
Ions Score: 44 **Expect:** 0.019
Matches (Bold Red): 42/199 fragment ions using 57 most intense peaks

#	Immon.	a	a^{++}	a*	a^{*++}	a^{0}	a^{0++}	b	b^{++}	b*	b^{*++}	b^{0}	b^{0++}	Seq.	y	y^{++}	y*	y^{*++}	y^{0}	y^{0++}	#
1	60.04	60.04	30.53			42.03	21.52	88.04	44.52			70.03	35.52	S							10
2	44.05	**131.08**	66.04			113.07	57.04	**159.08**	80.04			**141.07**	71.04	A	993.57	**497.29**	976.55	488.78	975.56	488.28	9
3	70.07	228.13	114.57			210.12	105.57	**256.13**	128.57			**238.12**	119.56	P	**922.54**	**461.77**	905.51	453.26	904.52	452.77	8
4	44.05	**299.17**	150.09			281.16	**141.08**	**327.17**	164.09			309.16	155.08	A	**825.48**	**413.25**	808.46	404.73	**807.47**	404.24	7
5	70.07	396.22	198.62			**378.21**	189.61	424.22	212.61			406.21	203.61	P	**754.45**	**377.73**	737.42	369.21	**736.44**	368.72	6
6	**169.13**	592.35	296.68	575.32	288.16	574.33	287.67	620.34	310.67	603.31	**302.16**	602.33	301.67	K	**657.39**	329.20	640.37	320.69	639.38	320.19	5
7	143.12	762.45	381.73	745.42	373.22	744.44	372.72	790.45	395.73	773.42	387.21	772.44	386.72	K	**461.27**	231.14	444.25	222.63	443.26	222.13	4
8	30.03	819.47	410.24	802.45	401.73	801.46	401.23	847.47	424.24	830.44	415.72	829.46	415.23	G	**291.17**	146.09	274.14	137.57	273.16	137.08	3
9	60.04	906.50	453.76	889.48	445.24	888.49	444.75	934.50	467.75	917.47	459.24	916.49	458.75	S	**234.14**	117.58	217.12	109.06	216.13	108.57	2
10	101.11													K	**147.11**	74.06	130.09	65.55			1

H2BK85ma

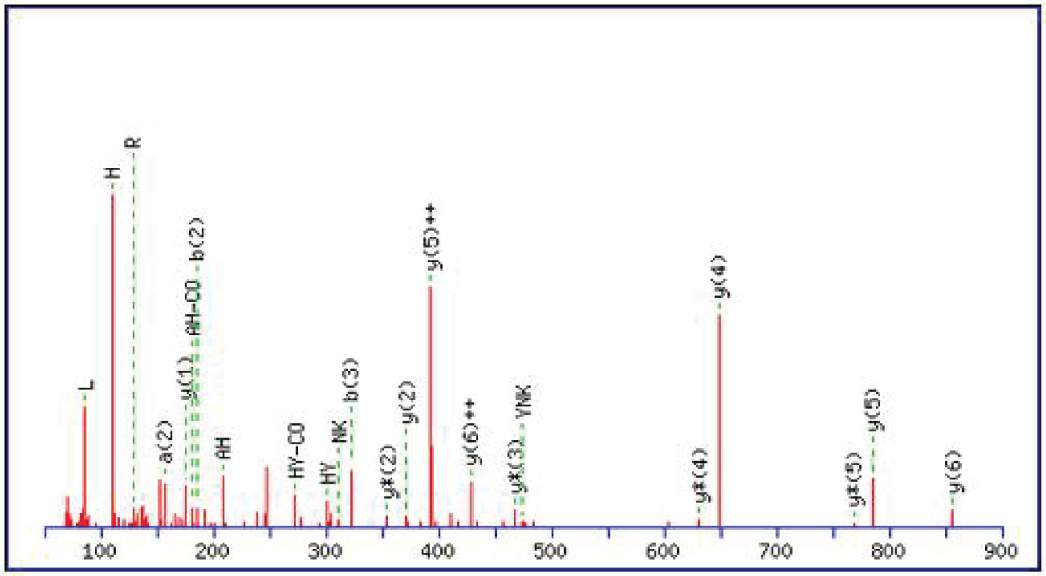

MS/MS Fragmentation of **LAHYNKR**
Found in **P06899**, Histone H2B type 1-J

Match to Query 370: 968.519236 from(485.266894,2+)

Monoisotopic mass of neutral peptide Mr(calc): 968.52
Variable modifications:
K6 : Methacryl (K)
Ions Score: 21 **Expect:** 2.5
Matches (Bold Red): 24/83 fragment ions using 44 most intense peaks

#	Immon.	a	a^{++}	a^*	a^{*++}	b	b^{++}	b^*	b^{*++}	Seq.	y	y^{++}	y^*	y^{*++}	#
1	**86.10**	**86.10**	43.55			114.09	57.55			L					7
2	44.05	**157.13**	79.07			**185.13**	93.07			A	**856.44**	**428.72**	839.42	420.21	6
3	**110.07**	294.19	147.60			**322.19**	161.60			H	**785.41**	**393.21**	**768.38**	384.69	5
4	136.08	457.26	229.13			485.25	243.13			Y	**648.35**	324.68	**631.32**	316.16	4
5	87.06	571.30	286.15	554.27	277.64	599.29	300.15	582.27	291.64	N	485.28	243.15	**468.26**	234.63	3
6	169.13	767.42	384.21	750.39	375.70	795.41	398.21	778.39	389.70	K	**371.24**	186.12	**354.21**	177.61	2
7	**129.11**									R	**175.12**	88.06	158.09	79.55	1

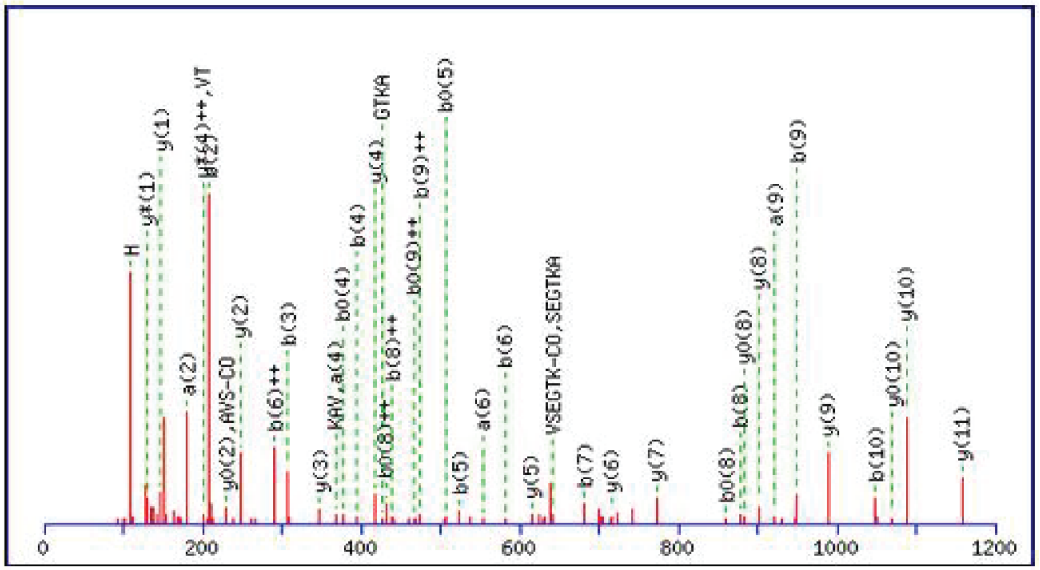

H2BK116ma

MS/MS Fragmentation of **HAVSEGTKAVTK**
Found in **P06899**, Histone H2B type 1-J

Match to Query 934: 1294.687784 from(648.351168,2+)

Monoisotopic mass of neutral peptide Mr(calc): 1294.69
Variable modifications:
K8 : Methacryl (K)
Ions Score: 85 **Expect:** 2.1e-006
Matches (Bold Red): 45/238 fragment ions using 64 most intense peaks

#	Immon.	a	a^{++}	a*	a^{*++}	a^{0}	a^{0++}	b	b^{++}	b*	b^{*++}	b^{0}	b^{0++}	Seq.	y	y^{++}	y*	y^{*++}	y^{0}	y^{0++}	#
1	**110.07**	**110.07**	55.54					138.07	69.54					H							12
2	44.05	**181.11**	91.06					**209.10**	105.06					A	**1158.64**	579.82	1141.61	571.31	1140.63	570.82	11
3	72.08	280.18	140.59					**308.17**	154.59					V	**1087.60**	544.30	1070.57	535.79	**1069.59**	535.30	10
4	60.04	**367.21**	184.11			349.20	175.10	**395.20**	198.11			**377.19**	189.10	S	**988.53**	494.77	971.50	486.26	970.52	485.76	9
5	102.05	496.25	248.63			478.24	239.62	**524.25**	262.63			**506.24**	253.62	E	**901.50**	451.25	884.47	442.74	**883.49**	442.25	8
6	30.03	**553.27**	277.14			535.26	268.13	**581.27**	**291.14**			563.26	282.13	G	**772.46**	386.73	755.43	378.22	754.45	377.73	7
7	74.06	654.32	327.66			636.31	318.66	**682.32**	341.66			664.30	332.66	T	**715.43**	358.22	698.41	349.71	697.42	349.22	6
8	169.13	850.44	425.72	833.42	417.21	832.43	416.72	**878.44**	**439.72**	861.41	431.21	**860.43**	**430.72**	K	**614.39**	307.70	597.36	299.18	596.38	298.69	5
9	44.05	**921.48**	461.24	904.45	452.73	903.47	452.24	**949.47**	**475.24**	932.45	466.73	931.46	**466.24**	A	**418.27**	209.64	401.24	**201.12**	400.26	200.63	4
10	72.08	1020.55	510.78	1003.52	502.26	1002.54	501.77	**1048.54**	524.77	1031.52	516.26	1030.53	515.77	V	**347.23**	174.12	330.20	165.60	329.22	165.11	3
11	74.06	1121.59	561.30	1104.57	552.79	1103.58	552.30	1149.59	575.30	1132.56	566.79	1131.58	566.29	T	**248.16**	124.58	231.13	116.07	**230.15**	115.58	2
12	101.11													K	**147.11**	74.06	**130.09**	65.55			1

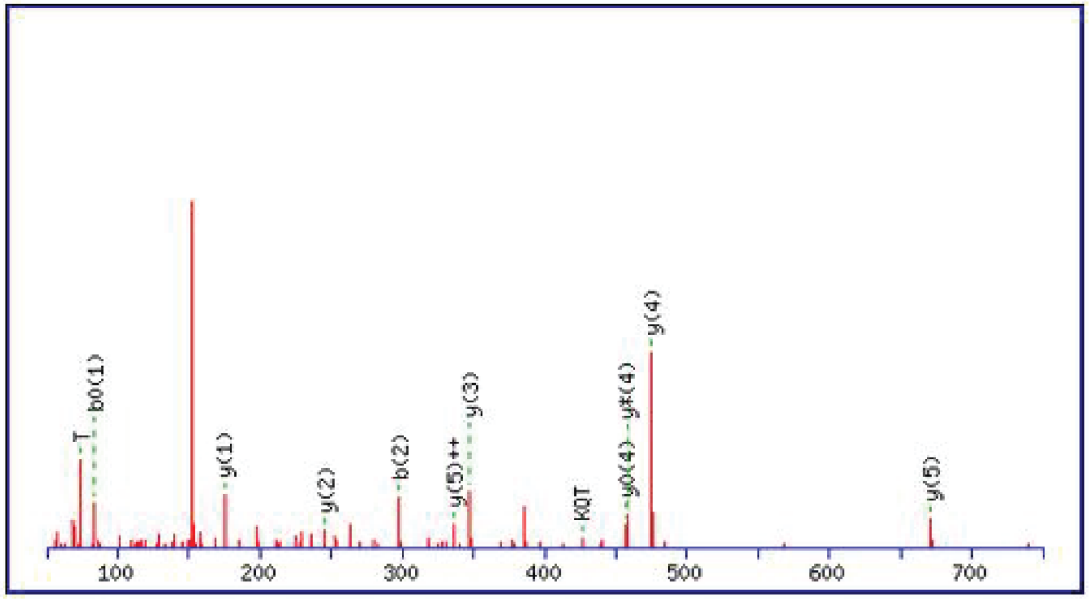

H3K4ma

MS/MS Fragmentation of **TKQTAR**
Found in **Q71DI3**, Histone H3.2

Match to Query 17: 771.423906 from(386.719229,2+)

Monoisotopic mass of neutral peptide Mr(calc): 771.42
Variable modifications:
K2 : Methacryl (K)
Ions Score: 37 **Expect:** 0.091
Matches (Bold Red): 15/100 fragment ions using 23 most intense peaks

#	Immon.	a	a^{++}	a^{*}	a^{*++}	a^{0}	a^{0++}	b	b^{++}	b^{*}	b^{*++}	b^{0}	b^{0++}	Seq.	y	y^{++}	y^{*}	y^{*++}	y^{0}	y^{0++}	#
1	**74.06**	**74.06**	37.53			56.05	28.53	102.05	51.53			**84.04**	42.53	T							6
2	169.13	270.18	135.59	253.15	127.08	252.17	126.59	**298.18**	149.59	281.15	141.08	280.17	140.59	K	**671.38**	**336.20**	654.36	327.68	653.37	327.19	5
3	101.07	398.24	199.62	381.21	191.11	380.23	190.62	**426.23**	213.62	409.21	205.11	408.22	204.62	Q	**475.26**	238.13	**458.24**	229.62	**457.25**	229.13	4
4	**74.06**	499.29	250.15	482.26	241.63	481.28	241.14	527.28	264.14	510.26	255.63	509.27	255.14	T	**347.20**	174.11	330.18	165.59	329.19	165.10	3
5	44.05	570.32	285.67	553.30	277.15	552.31	276.66	598.32	299.66	581.29	291.15	580.31	290.66	A	**246.16**	123.58	229.13	115.07			2
6	129.11													R	**175.12**	88.06	158.09	79.55			1

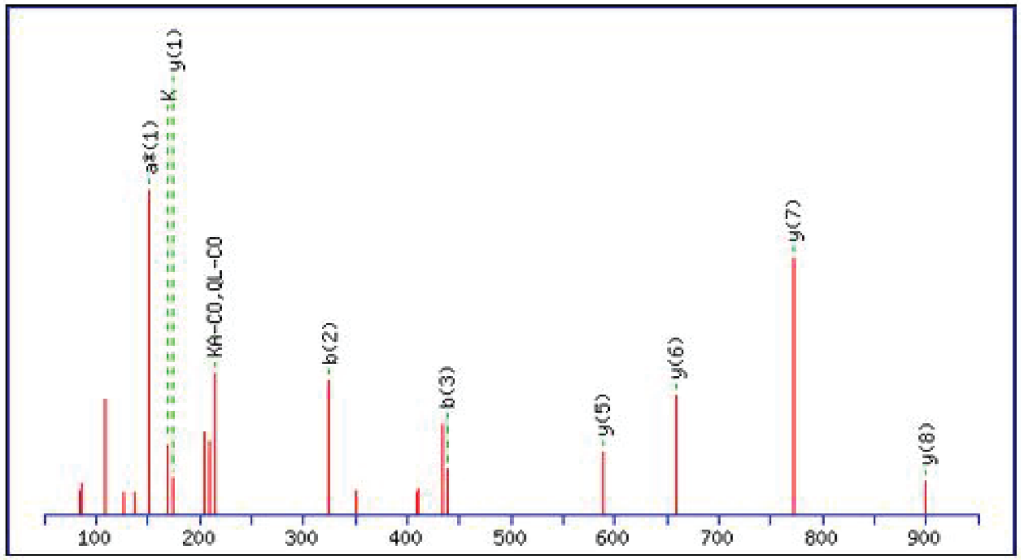

H3K18ma

MS/MS Fragmentation of **KQLATKAAR**
Found in **Q71DI3**, Histone H3.2

Match to Query 582: 1095.639848 from(548.827200,2+)

Monoisotopic mass of neutral peptide Mr(calc): 1095.64
Variable modifications:
K1 : Methacryl (K)
K6 : Acetyl (K)
Ions Score: 28 **Expect:** 0.72
Matches (Bold Red): 12/170 fragment ions using 19 most intense peaks

#	Immon.	a	a^{++}	a^{*}	a^{*++}	a^{0}	a^{0++}	b	b^{++}	b^{*}	b^{*++}	b^{0}	b^{0++}	Seq.	y	y^{++}	y^{*}	y^{*++}	y^{0}	y^{0++}	#
1	**169.13**	**169.13**	85.07	**152.11**	76.56			197.13	99.07	180.10	90.55			K							9
2	101.07	297.19	149.10	280.17	140.59			**325.19**	163.10	308.16	154.58			Q	**900.53**	450.77	883.50	442.25	882.52	441.76	8
3	86.10	410.28	205.64	393.25	197.13			**438.27**	219.64	421.24	211.13			L	**772.47**	386.74	755.44	378.22	754.46	377.73	7
4	44.05	481.31	241.16	464.29	232.65			509.31	255.16	492.28	246.64			A	**659.38**	330.20	642.36	321.68	641.37	321.19	6
5	74.06	582.36	291.68	565.33	283.17	564.35	282.68	610.36	305.68	593.33	297.17	592.35	296.68	T	**588.35**	294.68	571.32	286.16	570.34	285.67	5
6	143.12	752.47	376.74	735.44	368.22	734.46	367.73	780.46	390.73	763.43	382.22	762.45	381.73	K	487.30	244.15	470.27	235.64			4
7	44.05	823.50	412.26	806.48	403.74	805.49	403.25	851.50	426.25	834.47	417.74	833.49	417.25	A	317.19	159.10	300.17	150.59			3
8	44.05	894.54	447.77	877.51	439.26	876.53	438.77	922.54	461.77	905.51	453.26	904.52	452.77	A	246.16	123.58	229.13	115.07			2
9	129.11													R	**175.12**	88.06	158.09	79.55			1

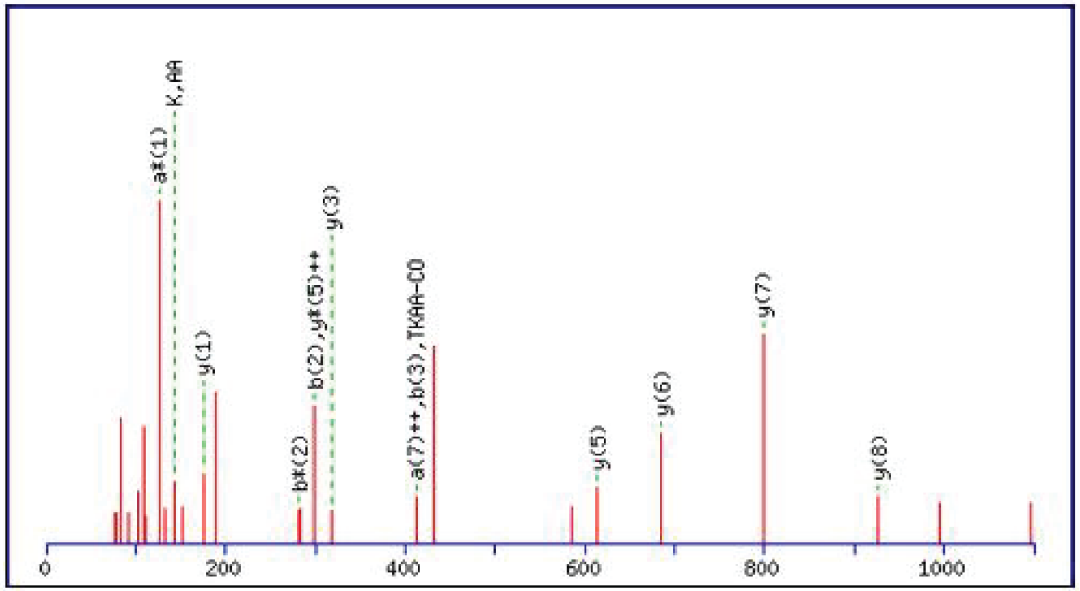

H3K23ma

MS/MS Fragmentation of KQLATKAAR
Found in Q71DI3, Histone H3.2

Match to Query 580: 1095.639692 from(548.827122,2+)

Monoisotopic mass of neutral peptide Mr(calc): 1095.64
Variable modifications:
K1 : Acetyl (K)
K6 : Methacryl (K)
Ions Score: 41 **Expect:** 0.041
Matches (Bold Red): 17/169 fragment ions using 19 most intense peaks

#	Immon.	a	a^{++}	a^{*}	a^{*++}	a^{0}	a^{0++}	b	b^{++}	b^{*}	b^{*++}	b^{0}	b^{0++}	Seq.	y	y^{++}	y^{*}	y^{*++}	y^{0}	y^{0++}	#
1	**143.12**	**143.12**	72.06	**126.09**	63.55			171.11	86.06	154.09	77.55			K							9
2	101.07	271.18	136.09	254.15	127.58			**299.17**	150.09	**282.14**	141.58			Q	**926.54**	463.77	909.52	455.26	908.53	454.77	8
3	86.10	384.26	192.63	367.23	184.12			**412.26**	206.63	395.23	198.12			L	**798.48**	399.75	781.46	391.23	780.47	390.74	7
4	44.05	455.30	228.15	438.27	219.64			483.29	242.15	466.27	233.64			A	**685.40**	343.20	668.37	334.69	667.39	334.20	6
5	74.06	556.35	278.68	539.32	270.16	538.33	269.67	584.34	292.67	567.31	284.16	566.33	283.67	T	**614.36**	307.68	597.34	**299.17**	596.35	298.68	5
6	169.13	752.47	376.74	735.44	368.22	734.46	367.73	780.46	390.73	763.43	382.22	762.45	381.73	K	513.31	257.16	496.29	248.65			4
7	44.05	823.50	**412.26**	806.48	403.74	805.49	403.25	851.50	426.25	834.47	417.74	833.49	417.25	A	**317.19**	159.10	300.17	150.59			3
8	44.05	894.54	447.77	877.51	439.26	876.53	438.77	922.54	461.77	905.51	453.26	904.52	452.77	A	246.16	123.58	229.13	115.07			2
9	129.11													R	**175.12**	88.06	158.09	79.55			1

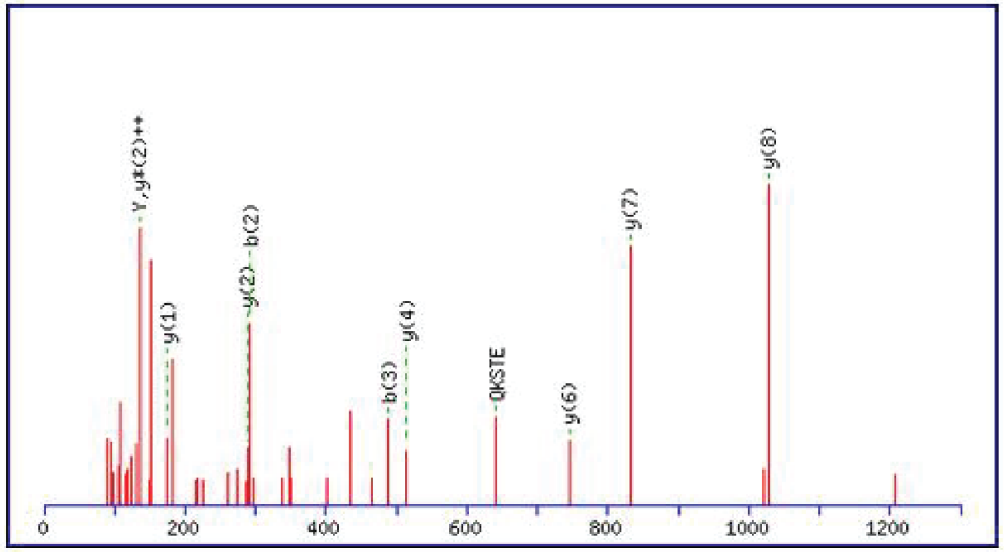

H3K56ma

MS/MS Fragmentation of YQKSTELLIR
Found in Q71DI3, Histone H3.2

Match to Query 962: 1317.730428 from(659.872490,2+)

Monoisotopic mass of neutral peptide Mr(calc): 1317.73
Variable modifications:
K3 : Methacryl (K)
Ions Score: 39 **Expect:** 0.11
Matches (Bold Red): 12/194 fragment ions using 15 most intense peaks

#	Immon.	a	a^{++}	a^{*}	a^{*++}	a^{0}	a^{0++}	b	b^{++}	b^{*}	b^{*++}	b^{0}	b^{0++}	Seq.	y	y^{++}	y^{*}	y^{*++}	y^{0}	y^{0++}	#
1	**136.08**	**136.08**	68.54					164.07	82.54					Y							10
2	101.07	264.13	132.57	247.11	124.06			**292.13**	146.57	275.10	138.05			Q	1155.67	578.34	1138.65	569.83	1137.66	569.33	9
3	169.13	460.26	230.63	443.23	222.12			**488.25**	244.63	471.22	236.12			K	**1027.61**	514.31	1010.59	505.80	1009.60	505.31	8
4	60.04	547.29	274.15	530.26	265.63	529.28	265.14	575.28	288.14	558.26	279.63	557.27	279.14	S	**831.49**	416.25	814.47	407.74	813.48	407.25	7
5	74.06	648.34	324.67	631.31	316.16	630.32	315.67	676.33	338.67	659.30	330.16	658.32	329.66	T	**744.46**	372.73	727.43	364.22	726.45	363.73	6
6	102.05	777.38	389.19	760.35	380.68	759.37	380.19	805.37	403.19	788.35	394.68	787.36	394.18	E	643.41	322.21	626.39	313.70	625.40	313.21	5
7	86.10	890.46	445.73	873.44	437.22	872.45	436.73	918.46	459.73	901.43	451.22	900.45	450.73	L	**514.37**	257.69	497.34	249.18			4
8	86.10	1003.55	502.28	986.52	493.76	985.54	493.27	1031.54	516.27	1014.51	507.76	1013.53	507.27	L	401.29	201.15	384.26	192.63			3
9	86.10	1116.63	558.82	1099.60	550.31	1098.62	549.81	1144.62	572.82	1127.60	564.30	1126.61	563.81	I	**288.20**	144.61	271.18	**136.09**			2
10	129.11													R	**175.12**	88.06	158.09	79.55			1

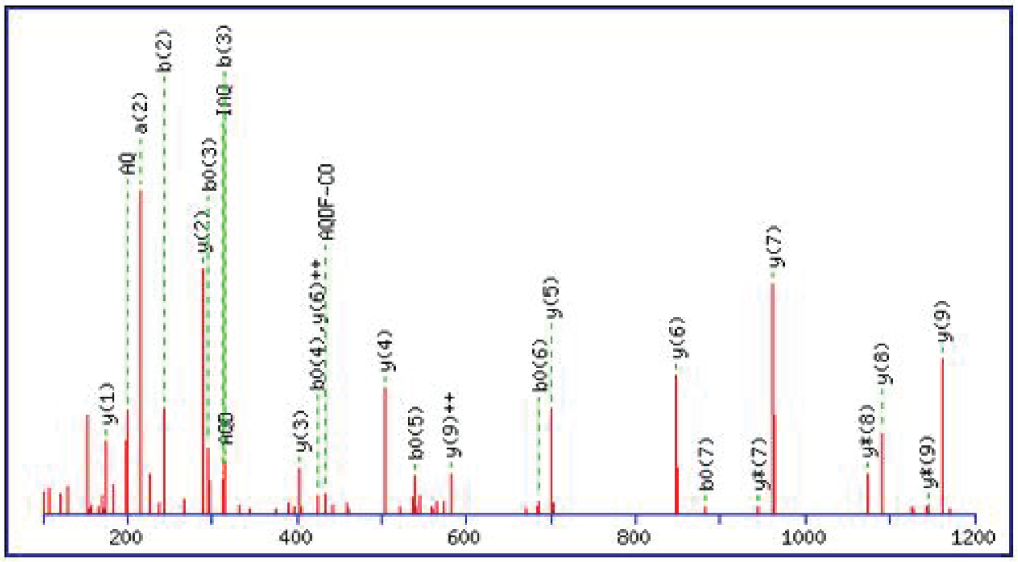

H3K79ma

MS/MS Fragmentation of EIAQDFKTDLR
Found in Q71DI3, Histone H3.2

Match to Query 1092: 1402.709062 from(702.361807,2+)

Monoisotopic mass of neutral peptide Mr(calc): 1402.71
Variable modifications:
K7 : Methacryl (K)
Ions Score: 69 **Expect:** 8.7e-005
Matches (Bold Red): 26/227 fragment ions using 34 most intense peaks

#	Immon.	a	a^{++}	a*	a^{*++}	a^0	a^{0++}	b	b^{++}	b*	b^{*++}	b^0	b^{0++}	Seq.	y	y^{++}	y*	y^{*++}	y^0	y^{0++}	#
1	102.05	102.05	51.53			84.04	42.53	130.05	65.53			112.04	56.52	E							11
2	86.10	**215.14**	108.07			197.13	99.07	**243.13**	122.07			225.12	113.07	I	1274.67	637.84	1257.65	629.33	1256.66	628.84	10
3	44.05	286.18	143.59			268.17	134.59	**314.17**	157.59			**296.16**	148.58	A	**1161.59**	**581.30**	**1144.56**	572.79	1143.58	572.29	9
4	101.07	414.23	207.62	397.21	199.11	396.22	198.62	442.23	221.62	425.20	213.11	**424.22**	212.61	Q	**1090.55**	545.78	**1073.53**	537.27	1072.54	536.77	8
5	88.04	529.26	265.13	512.24	256.62	511.25	256.13	557.26	279.13	540.23	270.62	**539.25**	270.13	D	**962.49**	481.75	**945.47**	473.24	944.48	472.75	7
6	120.08	676.33	338.67	659.30	330.16	658.32	329.66	704.32	352.67	687.30	344.15	**686.31**	343.66	F	**847.47**	**424.24**	830.44	415.72	829.46	415.23	6
7	169.13	872.45	436.73	855.42	428.22	854.44	427.72	900.45	450.73	883.42	442.21	**882.44**	441.72	K	**700.40**	350.70	683.37	342.19	682.39	341.70	5
8	74.06	973.50	487.25	956.47	478.74	955.49	478.25	1001.49	501.25	984.47	492.74	983.48	492.25	T	**504.28**	252.64	487.25	244.13	486.27	243.64	4
9	88.04	1088.53	544.77	1071.50	536.25	1070.52	535.76	1116.52	558.76	1099.49	550.25	1098.51	549.76	D	**403.23**	202.12	386.20	193.61	385.22	193.11	3
10	86.10	1201.61	601.31	1184.58	592.80	1183.60	592.30	1229.60	615.31	1212.58	606.79	1211.59	606.30	L	**288.20**	144.61	271.18	136.09			2
11	129.11													R	**175.12**	88.06	158.09	79.55			1

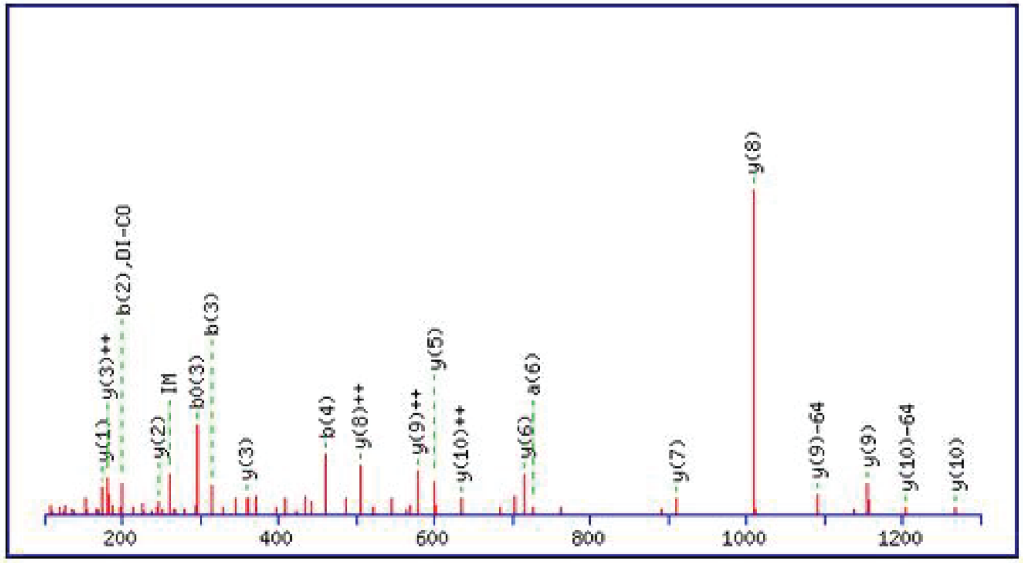

H3K122ma

MS/MS Fragmentation of VTIMPKDIQLAR
Found in Q71DI3, Histone H3.2

Match to Query 1183: 1467.810982 from(734.912767,2+)

Monoisotopic mass of neutral peptide Mr(calc): 1467.81
Variable modifications:
M4 : Oxidation (M), with neutral losses 0.00(shown in table), 64.00
K6 : Methacryl (K)
Ions Score: 68 **Expect:** 0.00013
Matches (Bold Red): 22/365 fragment ions using 31 most intense peaks

#	Immon.	a	a^{++}	a^*	a^{*++}	a^0	a^{0++}	b	b^{++}	b^*	b^{*++}	b^0	b^{0++}	Seq.	y	y^{++}	y^*	y^{*++}	y^0	y^{0++}	#
1	72.08	72.08	36.54					100.08	50.54					V							12
2	74.06	173.13	87.07			155.12	78.06	**201.12**	101.07			183.11	92.06	T	1369.75	685.38	1352.72	676.87	1351.74	676.37	11
3	86.10	286.21	143.61			268.20	134.60	**314.21**	157.61			**296.20**	148.60	I	**1268.70**	**634.86**	1251.68	626.34	1250.69	625.85	10
4	120.05	433.25	217.13			415.24	208.12	**461.24**	231.13			443.23	222.12	M	**1155.62**	**578.31**	1138.59	569.80	1137.61	569.31	9
5	70.07	530.30	265.65			512.29	256.65	558.30	279.65			540.29	270.65	P	**1008.58**	**504.80**	991.56	496.28	990.57	495.79	8
6	169.13	**726.42**	363.71	709.40	355.20	708.41	354.71	754.42	377.71	737.39	369.20	736.41	368.71	K	**911.53**	456.27	894.50	447.76	893.52	447.26	7
7	88.04	841.45	421.23	824.42	412.71	823.44	412.22	869.44	435.23	852.42	426.71	851.43	426.22	D	**715.41**	358.21	698.38	349.70	697.40	349.20	6
8	86.10	954.53	477.77	937.51	469.26	936.52	468.76	982.53	491.77	965.50	483.25	964.52	482.76	I	**600.38**	300.70	583.36	292.18			5
9	101.07	1082.59	541.80	1065.56	533.29	1064.58	532.79	1110.59	555.80	1093.56	547.28	1092.58	546.79	Q	487.30	244.15	470.27	235.64			4
10	86.10	1195.68	598.34	1178.65	589.83	1177.66	589.34	1223.67	612.34	1206.64	603.83	1205.66	603.33	L	**359.24**	**180.12**	342.21	171.61			3
11	44.05	1266.71	633.86	1249.69	625.35	1248.70	624.85	1294.71	647.86	1277.68	639.34	1276.70	638.85	A	**246.16**	123.58	229.13	115.07			2
12	129.11													R	**175.12**	88.06	158.09	79.55			1

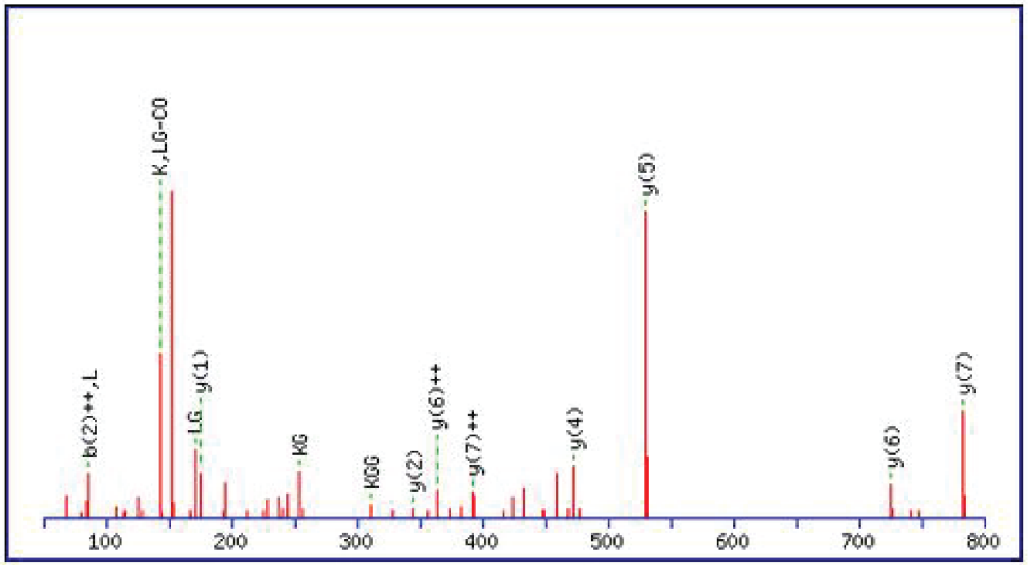

H4K12ma

MS/MS Fragmentation of GLGKGGAKR
Found in P62805, Histone H4

Match to Query 323: 952.545324 from(477.279938,2+)

Monoisotopic mass of neutral peptide Mr(calc): 952.55
Variable modifications:
K4 : Methacryl (K)
K8 : Acetyl (K)
Ions Score: 43 **Expect:** 0.016
Matches (Bold Red): 19/134 fragment ions using 20 most intense peaks

#	Immon.	a	a^{++}	a^{*}	a^{*++}	b	b^{++}	b^{*}	b^{*++}	Seq.	y	y^{++}	y^{*}	y^{*++}	#
1	30.03	30.03	15.52			58.03	29.52			G					9
2	**86.10**	**143.12**	72.06			**171.11**	**86.06**			L	896.53	448.77	879.50	440.26	8
3	30.03	200.14	100.57			228.13	114.57			G	**783.45**	**392.23**	766.42	383.71	7
4	169.13	396.26	198.63	379.23	190.12	424.26	212.63	407.23	204.12	K	**726.43**	**363.72**	709.40	355.20	6
5	30.03	453.28	227.14	436.26	218.63	481.28	241.14	464.25	232.63	G	**530.30**	265.66	513.28	257.14	5
6	30.03	510.30	255.66	493.28	247.14	538.30	269.65	521.27	261.14	G	**473.28**	237.15	456.26	228.63	4
7	44.05	581.34	291.17	564.31	282.66	609.34	305.17	592.31	296.66	A	416.26	208.63	399.24	200.12	3
8	**143.12**	751.45	376.23	734.42	367.71	779.44	390.22	762.41	381.71	K	**345.22**	173.12	328.20	164.60	2
9	129.11									R	**175.12**	88.06	158.09	79.55	1

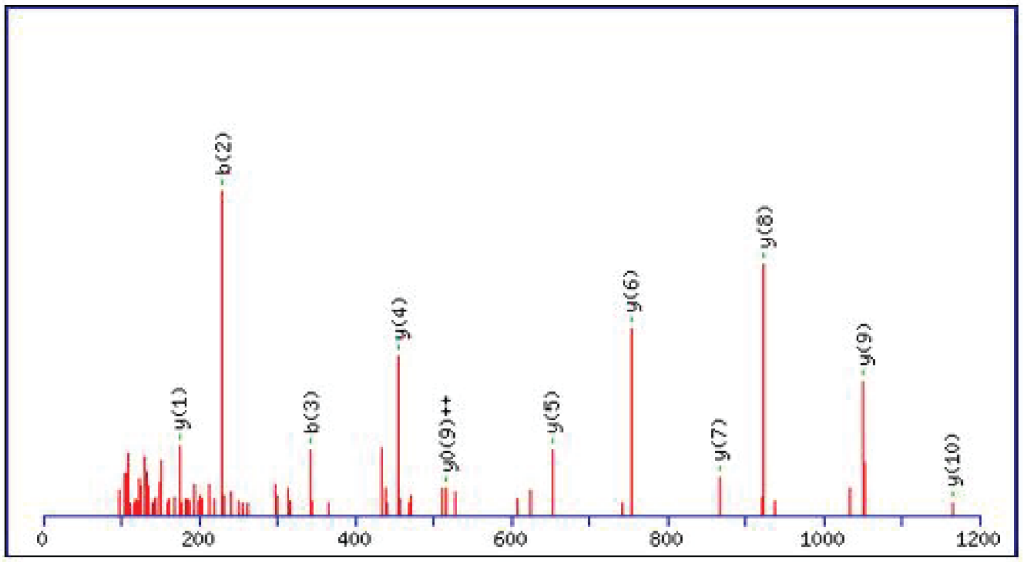

H4K31ma

MS/MS Fragmentation of **DNIQGITKPAIR**
Found in **P62805**, Histone H4

Match to Query 1078: 1392.771922 from(697.393237,2+)

Monoisotopic mass of neutral peptide Mr(calc): 1392.77
Variable modifications:
K8 : Methacryl (K)
Ions Score: 86 **Expect:** 1.8e-006
Matches (Bold Red): 11/265 fragment ions using 14 most intense peaks

#	Immon.	a	a^{++}	a^{*}	a^{*++}	a^{0}	a^{0++}	b	b^{++}	b^{*}	b^{*++}	b^{0}	b^{0++}	Seq.	y	y^{++}	y^{*}	y^{*++}	y^{0}	y^{0++}	#
1	88.04	88.04	44.52			70.03	35.52	116.03	58.52			98.02	49.52	D							12
2	87.06	202.08	101.54	185.06	93.03	184.07	92.54	**230.08**	115.54	213.05	107.03	212.07	106.54	N	1278.75	639.88	1261.73	631.37	1260.74	630.87	11
3	86.10	315.17	158.09	298.14	149.57	297.16	149.08	**343.16**	172.08	326.13	163.57	325.15	163.08	I	**1164.71**	582.86	1147.68	574.35	1146.70	573.85	10
4	101.07	443.22	222.12	426.20	213.60	425.21	213.11	471.22	236.11	454.19	227.60	453.21	227.11	Q	**1051.63**	526.32	1034.60	517.80	1033.62	**517.31**	9
5	30.03	500.25	250.63	483.22	242.11	482.24	241.62	528.24	264.62	511.21	256.11	510.23	255.62	G	**923.57**	462.29	906.54	453.77	905.56	453.28	8
6	86.10	613.33	307.17	596.30	298.66	595.32	298.16	641.33	321.17	624.30	312.65	623.31	312.16	I	**866.55**	433.78	849.52	425.26	848.54	424.77	7
7	74.06	714.38	357.69	697.35	349.18	696.37	348.69	742.37	371.69	725.35	363.18	724.36	362.68	T	**753.46**	377.23	736.44	368.72	735.45	368.23	6
8	169.13	910.50	455.75	893.47	447.24	892.49	446.75	938.49	469.75	921.47	461.24	920.48	460.75	K	**652.41**	326.71	635.39	318.20			5
9	70.07	1007.55	504.28	990.53	495.77	989.54	495.27	1035.55	518.28	1018.52	509.76	1017.54	509.27	P	**456.29**	228.65	439.27	220.14			4
10	44.05	1078.59	539.80	1061.56	531.28	1060.58	530.79	1106.58	553.80	1089.56	545.28	1088.57	544.79	A	359.24	180.12	342.21	171.61			3
11	86.10	1191.67	596.34	1174.65	587.83	1173.66	587.33	1219.67	610.34	1202.64	601.82	1201.66	601.33	I	288.20	144.61	271.18	136.09			2
12	129.11													R	**175.12**	88.06	158.09	79.55			1

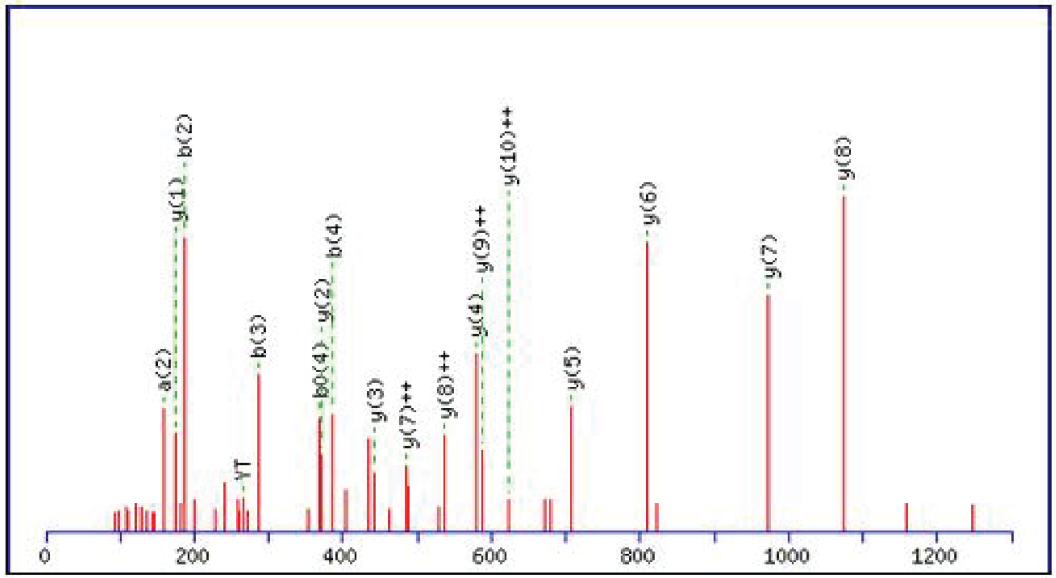

H4K77ma

MS/MS Fragmentation of **DAVTYTEHAKR**
Found in **P62805**, Histone H4

Match to Query 1027: 1357.662022 from(679.838287,2+)

Monoisotopic mass of neutral peptide Mr(calc): 1357.66
Variable modifications:
K10 : Methacryl (K)
Ions Score: 58 **Expect:** 0.00056
Matches (Bold Red): 19/202 fragment ions using 29 most intense peaks

#	Immon.	a	a^{++}	a^*	a^{*++}	a^0	a^{0++}	b	b^{++}	b^*	b^{*++}	b^0	b^{0++}	Seq.	y	y^{++}	y^*	y^{*++}	y^0	y^{0++}	#
1	88.04	88.04	44.52			70.03	35.52	116.03	58.52			98.02	49.52	D							11
2	44.05	**159.08**	80.04			141.07	71.04	**187.07**	94.04			169.06	85.03	A	1243.64	**622.33**	1226.62	613.81	1225.63	613.32	10
3	72.08	258.14	129.58			240.13	120.57	**286.14**	143.57			268.13	134.57	V	1172.61	**586.81**	1155.58	578.29	1154.60	577.80	9
4	74.06	359.19	180.10			341.18	171.09	**387.19**	194.10			**369.18**	185.09	T	**1073.54**	**537.27**	1056.51	528.76	1055.53	528.27	8
5	136.08	522.26	261.63			504.25	252.63	550.25	275.63			532.24	266.62	Y	**972.49**	**486.75**	955.46	478.24	954.48	477.74	7
6	74.06	623.30	312.16			605.29	303.15	651.30	326.15			633.29	317.15	T	**809.43**	405.22	792.40	396.70	791.42	396.21	6
7	102.05	752.35	376.68			734.34	367.67	780.34	390.67			762.33	381.67	E	**708.38**	354.69	691.35	346.18	690.37	345.69	5
8	110.07	889.41	445.21			871.39	436.20	917.40	459.20			899.39	450.20	H	**579.34**	290.17	562.31	281.66			4
9	44.05	960.44	480.72			942.43	471.72	988.44	494.72			970.43	485.72	A	**442.28**	221.64	425.25	213.13			3
10	169.13	1156.56	578.79	1139.54	570.27	1138.55	569.78	1184.56	592.78	1167.53	584.27	1166.55	583.78	K	**371.24**	186.12	354.21	177.61			2
11	129.11													R	**175.12**	88.06	158.09	79.55			1

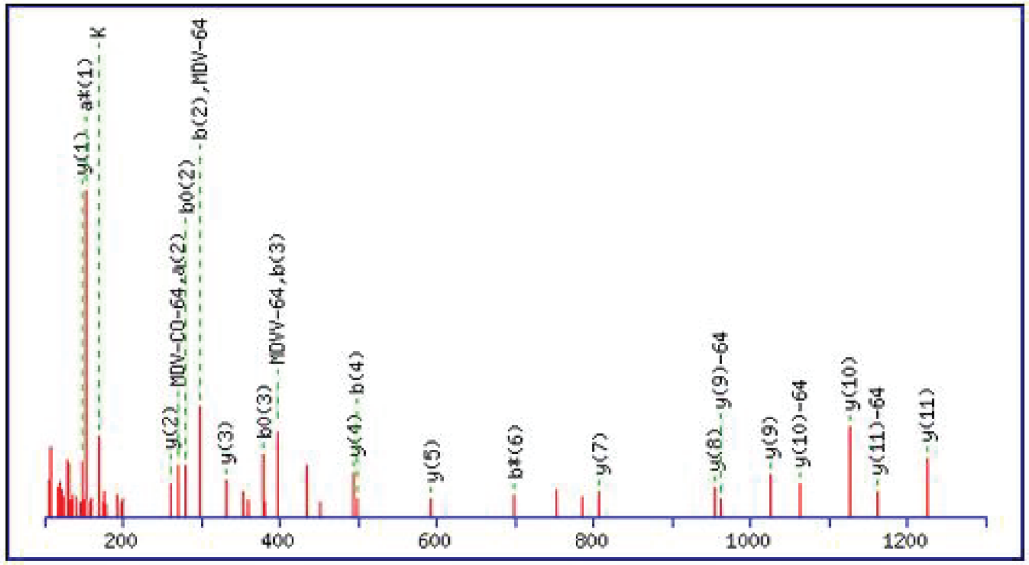

H4K79ma

MS/MS Fragmentation of **KTVTAMDVVYALK**
Found in **P62805**, Histone H4

Match to Query 1237: 1521.810238 from(761.912395,2+)

Monoisotopic mass of neutral peptide Mr(calc): 1521.81
Variable modifications:
K1 : Methacryl (K)
M6 : Oxidation (M), with neutral losses 0.00(shown in table), 64.00
Ions Score: 75 **Expect:** 2.9e-005
Matches (Bold Red): 26/446 fragment ions using 34 most intense peaks

#	Immon.	a	a^{++}	a*	a^{*++}	a^{0}	a^{0++}	b	b^{++}	b*	b^{*++}	b^{0}	b^{0++}	Seq.	y	y^{++}	y*	y^{*++}	y^{0}	y^{0++}	#
1	**169.13**	**169.13**	85.07	**152.11**	76.56			197.13	99.07	180.10	90.55			K							13
2	74.06	**270.18**	135.59	253.15	127.08	252.17	126.59	**298.18**	149.59	281.15	141.08	**280.17**	140.59	T	1326.70	663.85	1309.67	655.34	1308.69	654.85	12
3	72.08	369.25	185.13	352.22	176.62	351.24	176.12	**397.24**	199.13	380.22	190.61	**379.23**	190.12	V	**1225.65**	613.33	1208.62	604.82	1207.64	604.32	11
4	74.06	470.30	235.65	453.27	227.14	452.29	226.65	**498.29**	249.65	481.27	241.14	480.28	240.64	T	**1126.58**	563.79	1109.55	555.28	1108.57	554.79	10
5	44.05	541.33	271.17	524.31	262.66	523.32	262.17	569.33	285.17	552.30	276.65	551.32	276.16	A	**1025.53**	513.27	1008.51	504.76	1007.52	504.27	9
6	120.05	688.37	344.69	671.34	336.18	670.36	335.68	716.36	358.69	**699.34**	350.17	698.35	349.68	M	**954.50**	477.75	937.47	469.24	936.49	468.75	8
7	88.04	803.40	402.20	786.37	393.69	785.39	393.20	831.39	416.20	814.37	407.69	813.38	407.19	D	**807.46**	404.23	790.43	395.72	789.45	395.23	7
8	72.08	902.47	451.74	885.44	443.22	884.45	442.73	930.46	465.73	913.43	457.22	912.45	456.73	V	692.43	346.72	675.41	338.21			6
9	72.08	1001.53	501.27	984.51	492.76	983.52	492.27	1029.53	515.27	1012.50	506.75	1011.52	506.26	V	**593.37**	297.19	576.34	288.67			5
10	136.08	1164.60	582.80	1147.57	574.29	1146.59	573.80	1192.59	596.80	1175.57	588.29	1174.58	587.79	Y	**494.30**	247.65	477.27	239.14			4
11	44.05	1235.63	618.32	1218.61	609.81	1217.62	609.32	1263.63	632.32	1246.60	623.80	1245.62	623.31	A	**331.23**	166.12	314.21	157.61			3
12	86.10	1348.72	674.86	1331.69	666.35	1330.71	665.86	1376.71	688.86	1359.69	680.35	1358.70	679.85	L	**260.20**	130.60	243.17	122.09			2
13	101.11													K	**147.11**	74.06	130.09	65.55			1